

10526 487 NT ACAN



0066889

NATIONAL ADVISORY COMMITTEE FOR AERONAUTICS

TECHNICAL NOTE 4187

HIGH-SPEED HYDRODYNAMIC CHARACTERISTICS OF A
FLAT PLATE AND 20° DEAD-RISE SURFACE IN
UNSYMMETRICAL PLANING CONDITIONS

By Daniel Savitsky, R. E. Prowse, and D. H. Lueders

Stevens Institute of Technology



Washington

June 1958

AFMDC
TECHNICAL LIBRARY



0066889

NATIONAL ADVISORY COMMITTEE FOR AERONAUTICS

TECHNICAL NOTE 4187

HIGH-SPEED HYDRODYNAMIC CHARACTERISTICS OF A
FLAT PLATE AND 20° DEAD-RISE SURFACE IN
UNSYMMETRICAL PLANING CONDITIONS

By Daniel Savitsky, R. E. Prowse, and D. H. Lueders

SUMMARY

The results of an investigation made to obtain the wetted areas, the three components of planing forces, and the three components of moments acting on a 0° and a 20° dead-rise surface in high-speed, unsymmetrical planing conditions are presented. Hydrodynamic data were obtained for trim angles between 6° and 30°, roll angles between -15° and 15°, yaw angles between 0° and 20°, mean wetted-length-beam ratios up to 7.7, load coefficients up to 49.0, and speed coefficients up to 18.0.

The collected test data are presented in summary plots which are readily applicable for use in determining the lift, drag, side force, pitching moment, rolling moment, and yawing moment. An analysis is presented of the variation of these quantities with unsymmetrical planing parameters.

It was found that the wave rise at the leading edge of the tested planing surfaces was independent of yaw angle for all test conditions. The wave rise at the leading edge of an unrolled flat plate was equal to that of the symmetrical planing flat plate. For the rolled flat plate, the angle of inclination of the spray root line to the keel was identical to that of a wedge whose dead-rise angle is equal to the roll angle. In the case of the tested 20° dead-rise wedge, the spray root angle at the leading edge of the rolled-down side was equal to that of a hypothetical wedge whose dead rise is equal to 20° less the roll angle. The angle of the spray root line relative to the keel for the rolled-up side of the 20° deadrise surface was essentially constant and independent of roll angle.

There was a pronounced effect of finite chine-edge thickness on the hydrodynamic forces, moments, and spray formation at certain unsymmetrical planing conditions for a flat plate. Depending upon particular combinations of planing parameters large negative or positive pressures were developed along the length of the chine with finite thickness and noticeable

changes were observed in the spray formation associated with the affected chine edge. Summary plots are presented which define the inception of the chine-edge effects in terms of unsymmetrical planing conditions.

INTRODUCTION

In recent years various research studies have been made at the Experimental Towing Tank, by the National Advisory Committee for Aeronautics, and at the David Taylor Model Basin with the intent of providing fundamental hydrodynamic planing data for planing surfaces of simple prismatic form. Most of these investigations have been concerned with symmetrical planing conditions and have resulted in the publication of much data for the unyawed, unrolled case (refs. 1 to 7). Present developments in water-based aircraft have demonstrated the need for information on the hydrodynamic forces and moments on surfaces in unsymmetrical planing conditions. The existing literature, however, contains very little experimental or analytical work on this subject (ref. 8).

The present paper presents the results of an experimental study of the hydrodynamic forces and moments acting on 0° (flat bottom) and 20° dead-rise prismatic surfaces when operating in unsymmetrical, high-speed planing conditions. The investigation was carried out at the Experimental Towing Tank, Stevens Institute of Technology, Hoboken, New Jersey, under the sponsorship and with the financial assistance of the NACA.

Planing tests were made for beam loadings up to 49.0, wetted lengths up to 7.7 beams, trim angles up to 30° , yaw angles up to 20° , roll angles up to 15° , and at speed coefficients between 7 and 18.0. The planing characteristics determined were wetted area; resistance; side force; pitching, rolling, and yawing moments; and draft for various combinations of load, speed, trim, yaw, and roll. An investigation was also made of the effect of finite chine-edge thickness on the forces and moments on the planing flat plate.

SYMBOLS

A	area of wetted chine, sq ft
b	beam of planing surface, ft
C	side force, lb
C_{C_b}	side-force coefficient (positive to starboard), $\frac{C}{\frac{\rho}{2} V^2 b^2}$

C_{D_b}	drag coefficient (positive aft), $\frac{D}{\frac{\rho}{2} v^2 b^2}$
C_d	draft coefficient, d/b
C_e'	normal-chine-force coefficient (positive to starboard), $\frac{E}{\frac{\rho}{2} v^2 A}$
C_k	rolling-moment coefficient (positive to starboard), $\frac{K}{\frac{\rho}{2} v^2 b^3}$
C_{L_b}	lift coefficient (positive upward), $\frac{L}{\frac{\rho}{2} v^2 b^2} = \frac{2C_{\Delta}}{C_v^2}$
C_v	speed coefficient, $\frac{V}{\sqrt{gb}}$
C_m	pitching-moment coefficient (positive bow up), $\frac{M}{\frac{\rho}{2} v^2 b^3}$
C_n	yawing-moment coefficient (positive to starboard), $\frac{N}{\frac{\rho}{2} v^2 b^3}$
C_{p_e}'	coefficient of longitudinal center of normal chine force, $\frac{P_e}{L_c b}$
C_p'	longitudinal center-of-pressure coefficient in body axis, $\frac{p}{\lambda b}$
C_y'	lateral center-of-pressure coefficient in body axis, y/b
C_{Δ}	load coefficient, $\frac{\Delta}{wb^3}$
D	drag force, lb
d	draft of model center line at trailing edge (measured vertically from undisturbed water surface), ft
E	incremental force due to chine thickness, normal to chine, lb
g	acceleration due to gravity, 32.2 ft/sec ²
K	rolling moment, ft-lb

4

L lift force, lb

$$L_c = \frac{\text{Wetted length of port or starboard chine}}{\text{Beam}}$$

$$L_k = \frac{\text{Wetted length of keel}}{\text{Beam}}$$

$$L_l = \frac{\text{Wetted length of port chine}}{\text{Beam}}$$

$$L_r = \frac{\text{Wetted length of starboard chine}}{\text{Beam}}$$

M pitching moment, ft-lb

N yawing moment, ft-lb

p distance from center of pressure to ski trailing edge, ft

p_e distance from center of pressure on wetted chine to ski trailing edge, ft

t thickness of chine edge of flat plate, ft

V horizontal velocity, ft/sec

w specific weight of water, lb/cu ft

y lateral distance from center of pressure to ski center line in body axis, ft

β angle of dead rise, deg

β_e effective angle of deadrise, $\beta \pm \phi$, deg

Δ vertical load on water, lb

λ mean wetted-length—beam ratio, $\frac{L_r + L_l}{4} + \frac{L_k}{2}$

ρ density of water, slugs/cu ft

τ trim angle (as defined in appendix A, positive bow up), deg

ϕ roll angle (as defined in appendix A, positive to starboard), deg

ψ yaw angle (as defined in appendix A, positive to starboard),
deg

Subscripts:

- 1 in regard to moment coefficients refers to trailing edge of ski. All moment coefficients without this subscript have their origins at a point on the ski-bottom center line 3 beams forward of the trailing edge. Moment coefficients with this subscript have their origins on the ski-bottom center line at the trailing edge. With regard to wetted-length-beam ratio, subscript signifies distance from ski trailing edge to still water surface, taken along ski, as computed from draft and trim.

A prime indicates coefficient in body axis.

DESCRIPTION OF MODELS

A sketch and pertinent dimensions of the four planing models used in this investigation are shown in figure 1. The models, made of brass, had a length of 18 inches and a beam of 2 inches. The planing bottom of each model was machined to a high polish and all edges, including the trailing edge, were machined knife sharp. A series of lines, spaced at intervals of 0.10 beam, were painted across the keel and chines in order to obtain measurements of the wetted lengths. These painted stripes were then buffed in order to provide for a smooth finish of the planing bottom.

It will be noted that there are three flat-plate models having chine-edge thicknesses of 0.000, 0.182, and 0.364 inch. Three flat-plate models were constructed in order to investigate the effect of finite chine-edge thickness on the hydrodynamic forces and moments.

APPARATUS AND PROCEDURES

Towing Equipment

All tests were run in Tank No. 3 of the Experimental Towing Tank (designated ETT herein) using a towing apparatus which permitted the model to be towed at a fixed trim, roll, and yaw, and with freedom in heave. A photograph of the test setup is given in figure 2. The towing carriage is equipped with a loading and counterbalancing beam so that a specified load on the water can be obtained. For each test run, the model was set at a specified trim, roll, and yaw, loaded to the desired

load, and towed at a constant speed. The model was free to rise and seek the position of equilibrium at which the bottom area was sufficient to support the load. No devices for inducing turbulence into the boundary layer were used.

Force and Moment Dynamometer

Instrumentation was provided to measure the six components of force and moment acting on the planing surface. The horizontal drag force and the vertical load on the water were obtained from the standard instrumentation provided on the towing carriage. The side force and the three components of moment were measured by a specially constructed four-component electronic balance mounted between the towing carriage and the planing surface. Since the existing apparatus on the towing carriage provided for force measurements in a fixed-axis system oriented in the direction of the horizontal planing velocity, the four-component balance was constructed so as to measure forces and moments in this same fixed-axis system. Hence, regardless of the orientation of the planing body, the test forces and moments were always measured in the fixed-wind-axes system. The origins of both the fixed-axes and body-axes systems coincided and were located on the bottom surface of the model, a distance 6 inches (3 beams) forward of the trailing edge measured along the longitudinal center-line axis of the model (see fig. 1). The orientation of the model axes relative to the fixed axes in terms of trim, roll, and yaw is described in appendix A and illustrated in figure 3. The sign convention for the forces and moments is that adopted by the American Towing Tank Conference (ref. 9) and is described in appendix A.

The drag-force dynamometer used in these tests can be seen in figure 2. Under the action of a drag force, a portion of the towing carriage that was restrained by horizontal springs moved aft and, in the process, activated the core of a Schaevitz linear variable differential transformer. The signal from this unit was transmitted through an overhead shielded cable to stationary amplifying and recording equipment. The overhead cable was supported along the entire length of the tank and moved with the carriage, thus providing a continuous circuit with no sliding contacts.

The four-component balance used to measure side force, yawing, rolling, and pitching moment is shown in figure 4. As in the drag-force dynamometer, Schaevitz units are used as the sensitive elements and their signal is transmitted to the recording equipment through the system of overhead cables.

The action of the four-component balance is as follows. Four separate spring systems, marked (a), (b), (c), and (d), in figure 4 compose the dynamometer and each is sensitive to only one component of force or moment. Spring system (a), which is sensitive to pitching moment, can be considered

as being a section of the lower part of an A-frame whose apex is located on the bottom of the test model at the origin of the axes system previously described. The small, necked-down links to which the arrow (a) is directed in figure 4 are parts of the equal legs of the A-frame. If the resultant hydrodynamic force is applied at the apex of the A-frame, it is resolved into axial loads in each of the links which are designed so as to be considered infinitely rigid under the action of an axial force. If the resultant force is applied away from the apex this results in a moment being applied to the A-frame at the apex. The necked-down section of the links causes them to bend under the action of a moment and, hence, to actuate the core of the Schaevitz unit. The spring system (b) works on the same principle as (a) and measures the rolling moment. The yawing moment is measured by the system of four vertically positioned torsion springs (c) whose axis passes through the origin point on the bottom of the planing surface. The side force is measured by the spring system (d) which acts as fixed-end cantilever beams. A thorough calibration of the balance indicated insignificant interaction effects between the various spring systems over the range of test measurements.

The adjustments and scales for setting the yaw, pitch, and roll angles are located between the four-component balance and the planing model and are marked (e), (f), and (g), respectively, in figure 4.

Wetted Length and Area

The wetted bottom area of the model was obtained from underwater photographs taken with a 70-millimeter camera. The apparatus used to obtain the photographs is shown in figure 5. The camera and lights were located in watertight glass-top boxes submerged in the center of the tank and 3 feet (18 model beams) under the level water surface. As the model passed over the camera, the shutter was actuated by a photocell unit which also flashed two high-speed, electroflash lights. The actuating mechanism in the camera automatically cocked the shutter and wound the film between test runs. Figure 6 is an enlargement of a typical underwater photograph of the bottom. The wetted lengths are measured from the trailing edge to the intersection of the spray root line with the keel and chines. The mean wetted-length--beam ratio is taken to be the area defined by wetted keel and chine lengths divided by the square of the beam.

Draft

Measurements of the model draft were made during each run by visual observation of a heave scale attached to the carriage as shown in figure 2. The running draft is defined as the depth to the bottom of the center of the trailing edge below the level water surface.

Aerodynamic Tares

The aerodynamic forces and moments acting on the model and apparatus were determined by towing the model in air, over the test range of yaw, roll, trim, and speed with the trailing edge of the model 1/2 inch above the level water surface. For the most part, the aerodynamic forces were only of moderate value, while the aerodynamic moments were insignificant. The force coefficients given in table I have been corrected for the aerodynamic tares.

PRECISION

The quantities measured are believed to be within the following limits of precision:

Resistance, lb	±0.163
Side force, lb	±0.125
Pitching moment, ft-lb	±0.150
Yawing moment, ft-lb	±0.041
Rolling moment, ft-lb	±0.042
Wetted length, ft	±0.021
Draft, ft	±0.0082
Trim, roll, yaw, deg	±0.20
Speed, ft/sec	±0.05

These limits were obtained from a statistical analysis of reruns made during the tests. They are the values obtained for a confidence level of 95 percent.

TEST PROGRAM

An outline of the basic planing test program is presented in figure 7. This outline is mainly intended to indicate the range of test parameters and hence it is not to be concluded that each load-speed combination plotted in figure 7(a) was tested at each yaw-roll combination given in figure 7(b). The tabulation of test data in table I indicates the specific combinations of yaw, roll, load, and speed considered in these tests. The major portion of the investigation was conducted at trim angles of 6° and 30° with a moderate number of tests being made at intermediate trim angles of 12°, 18°, and 24°.

In the initial stages of the program it had been planned to make an extensive study of the planing forces and moments at speed coefficients of 10 and 14. In the early stages of testing it was found that, for the

given test parameters, there was no noticeable gravity effect at these speed coefficients and hence the bulk of the test conditions at $C_v = 10$ was omitted.

TEST RESULTS

The experimental data obtained for each of the tested planing surfaces, together with a tabulation of the test conditions, are given in tables I and II. The data in table I are for the flat plate with chine edges of zero thickness and for the 20° dead-rise surface. Table II presents supplementary data obtained for flat plates having chine edges 0.091b and 0.182b thick in order to demonstrate the effect of finite chine thickness on the basic planing forces and moments. All data are tabulated in the form of nondimensional coefficients of load, resistance, side force, pitching moment, yawing moment, rolling moment, wetted length, draft, and center of pressure. The six components of force and moment coefficients are presented in both the wind- and body-axes system. The reference point for the tabulated moment coefficients C_m , C_n , C_k , C_m' , C_n' , and C_k' is located on the bottom surface of the model a distance 3 beams forward of the trailing edge, measured along the longitudinal center-line axis of the model. For the 20° dead-rise surface two additional moment coefficients C_{m_1}' and C_{n_1}' are tabulated in the body axis. The reference point for these coefficients is at the trailing edge of the model. For the flat plate, the longitudinal and lateral locations of the resultant hydrodynamic force are tabulated in the form of coefficients C_p' and C_y' . The sign conventions for the force and moment coefficients are those presented in reference 9 and are described in appendix A. The test data are tabulated in order of increasing values of C_v , τ , ψ , ϕ , and C_Δ .

The lift-coefficient data obtained herein, with 2-inch-beam models, are compared with corresponding data obtained at the NACA with 4-inch-beam models (refs. 4 and 5) in figures 8 and 9. Plots of the lift, drag, side-force, and center-of-pressure coefficients, in both the wind and body axes, are presented in figures 10 to 14 for the flat plate of zero chine-edge thickness. The lift, drag, side-force, and moment coefficients for the 20° dead-rise surface are presented in figures 15 to 20.

Figures 21 to 23 indicate the wave rise at the leading edge of a flat plate in both symmetrical and unsymmetrical planing conditions. Figures 24 and 25 show the wave rise for the 20° dead-rise surface.

The boundaries of inception and the magnitude of the finite-thickness chine-edge effect on the hydrodynamic forces acting on a flat plate in unsymmetrical planing conditions are given in figures 26 to 28.

ANALYSIS AND DISCUSSION

An analysis of the present test data has been made for the purposes of determining the effect of unsymmetrical planing conditions on (a) the hydrodynamic lift, side force, and drag, (b) the three components of moment and the center of pressure, (c) the wave rise at the leading edge of the wetted area, and (d) the effect of finite chine thickness on the hydrodynamic forces on a flat planing surface. A discussion of each of these phases of the analysis is given separately in the following sections.

The discussions of the effects of roll and yaw on the dependent variables are based on analyses of the data and of crossplots of these data. These discussions are intended to be qualitative rather than quantitative, since a quantitative analysis would be extremely lengthy and would require the presentation of a very large number of crossplots. These additional complications are felt to be unwarranted at this time.

Hydrodynamic Scale Effect

In order to determine whether any hydrodynamic scale effect was introduced by the use of the 2-inch-beam model, the lift-coefficient data for the symmetrical planing conditions of the flat plates having zero and 0.182b chine-edge thickness are compared with data obtained by the NACA in symmetrical planing tests of a 4-inch-beam flat plate (ref. 4). Figure 8 presents this comparison of test results and indicates good agreement between the 2-inch-beam lift data obtained at ETT and the 4-inch-beam data obtained by the NACA. The differences between the ETT data and the NACA curves are well within the experimental scatter of test data from which the NACA curves were established (ref. 4).

Figure 9 presents a similar comparison for the 20° dead-rise data. Good agreement exists between the ETT 2-inch-beam lift data and the 4-inch-beam data obtained by the NACA (ref. 5).

The agreement between the ETT data for 2-inch-beam models and the NACA data for 4-inch-beam models indicates that no hydrodynamic scale effect was introduced by using 2-inch-beam models.

Lift of Planing Surfaces

Lift of flat plate.- In figures 10 to 12 the tabulated lift coefficients for the tested flat planing surfaces of zero chine-edge thickness are plotted against the mean wetted-length-beam ratio for each of the test trim angles. To expedite the usefulness of the test data, the plots are arranged in order of increasing yaw angle and, at each test yaw angle, in the order of increasing roll angle.

It will be noted from the data tabulations that all flat-plate tests were at $C_v = 14.00$. It was found from the tests of the 20° dead-rise surface that, for the test range of wetted lengths, the lift coefficient was essentially independent of speed coefficient for $C_v > 10$. Since it was the intent of this investigation to provide planing data in the range where gravity and buoyant effects are insignificant, it was decided to conduct all flat-plate planing tests at $C_v = 14.00$.

The effect of specific combinations of unsymmetrical planing conditions on the variation of C_{L_b} against λ at any trim can be directly evaluated from the plots in figures 10 to 12. Certain generalizations concerning the effect of unsymmetrical planing parameters can be established from an examination of these plots. For the unyawed condition, an increase in roll angle reduces C_{L_b} at given values of λ and τ . This follows from the fact that the effective deadrise of the surface is increased and the effective beam decreased with increasing roll angle. For the unrolled surface, the effect of increasing the yaw angle, up to 20° , is to increase C_{L_b} at given values of λ and τ . This yaw-angle effect is most pronounced at large values of λ and for $\tau < 18^\circ$. For small values of λ and for $\tau > 18^\circ$, there is only a small increase in C_{L_b} with increasing yaw angle. A possible explanation for this increase in C_{L_b} is that there is an increase in effective aspect ratio with increasing yaw angle and consequently there is an increase in pressure in the vicinity of the leading chine edge of the yawed, unrolled, flat plate. As evidence of these larger pressures the spray along the leading chine edge was observed to be more severe for the yawed than the unyawed planing case. Since at the longer wetted lengths and low trim angles there is more chine length exposed to larger pressures than at the shorter wetted lengths, the longer wetted lengths should have a substantial load increase with an increase in yaw angle.

For the positive rolled surface there is a substantial increase in lift coefficient as the positive yaw angle is increased at given values of λ and τ . This follows from the fact that the effective trim angle of the positive rolled surface is increased as the yaw angle increases. Conversely, for the negative rolled surface, there is a reduction in effective trim angle with increasing positive yaw angle and consequently

a reduction in lift coefficient at a given combination of λ and τ . There was a complete breakdown in lift at low trim angles for certain conditions of negative roll angle and positive yaw angle, with the model submerged. No attempt was made to define experimentally the lowest trim or load at which the test model would develop a supporting lift force for a given value of λ at a given combination of negative roll angle and positive yaw angle. However, it can be seen from the plots that for $\psi = 10^\circ$ there are no lift data for the combination $\tau = 6^\circ$ and $\phi = -15^\circ$; at $\psi = 20^\circ$ there are no lift data for the combinations $\tau = 6^\circ$ and $\phi = -10^\circ$, $\tau = 6^\circ$ and $\phi = -15^\circ$, and $\tau = 12^\circ$ and $\phi = -15^\circ$. It is seen that, with increasing positive yaw angle and increasing negative roll angle, it is necessary to increase the trim angle in order to continue to generate dynamic lift.

At a given positive yaw angle, the effect of increasing positive roll angle is to increase the flat-plate lift coefficient for given values of λ and τ . Increasing the negative roll angle decreases the lift coefficient. This behavior again follows from the fact that the effective trim angle of the bottom of a yawed flat planing surface increases with increasing positive roll angle and decreases with increasing negative roll angle.

The most pronounced effects of roll-angle and yaw-angle combinations occur at the small test trims (figs. 10 to 12). At the largest test trim angle (30°) there is only a small change in the curves of C_{L_b} against λ for the investigated range of roll- and yaw-angle settings.

Lift of 20° dead-rise surface.— The tabulated lift coefficients for the 20° dead-rise surface are plotted against the mean wetted-length—beam ratio for each of the test trims (figs. 15 to 17).

An analysis of the plots in figures 15 to 17 indicates that, for the yawed surface, at given values of τ and λ , the effect of rolling the surface 15° is to decrease the lift coefficient. This indicates that the gain in lift on the rolled-down side of the surface (because of decreased effective dead rise) is not so great as the loss in lift on the rolled-up side of the surface (because of increased effective dead rise). One possible explanation for this decrease in total lift is that the rolled-up side of the surface provides a pressure relief to the rolled-down side and hence the larger pressures on the rolled-down side cannot be fully developed. Another possible explanation is that, considering a transverse plane through the planing surface, if the dividing crossflow streamline is displaced laterally from the keel, a high-velocity flow across the keel will result which in turn will develop low pressures in the keel area and hence reduce the total lift for given values of λ and τ .

The effect of yaw angle on the lift coefficient at zero roll angle can be determined from figures 15(a), 16(a), and 17(a). It is seen that

for increasing yaw angle, C_{L_b} decreases for given values of λ and τ . This decrease is especially pronounced at the low trim angles; for a trim angle of 6° and a yaw angle of 20° , it is seen in figure 17(a), that the tested surface could not support the minimum test load. A probable explanation for this behavior can be established from the following combination of effects. For positive yaw angles, the effective trim of the port side of the surface is increased, while that of the starboard side is decreased. Further, the starboard side is no longer planing in an undisturbed flow but rather is partially in the wake generated by the port side. Hence, although the port-side load is increased by the yaw angle, the load reduction on the starboard side is such as to cause a reduction in total lift coefficient.

For the 20° dead-rise surface at positive roll angles, the lift coefficient is increased as the surface is yawed from 0° to 15° at fixed values of λ and τ . The port side achieves an increased effective trim and, consequently, an increase in C_{L_b} as the surface is yawed. The starboard side, which has been reduced in effective deadrise with positive roll angle, is probably not so extensively shielded by the port side as it is for the unrolled case and hence does not experience as serious a loss in lift as does the unrolled surface. The combined effect of port- and starboard-side flows is to cause an increase in lift for a given yaw angle.

For the negative rolled surface, there is a decrease in lift coefficient as the positive yaw angle is increased from 0° to 15° . In this case the starboard side, which has been increased in effective deadrise with negative roll angle, is more completely shielded by the port side and hence experiences a significant loss in lift as the yaw angle is increased.

In summary then, for given values of ψ , τ , and λ , the lift coefficient of a 20° dead-rise surface increases with increasing positive roll angle and decreases with increasing negative roll angle. These lift effects increase in severity with increasing yaw angle.

Side Forces on Unsymmetrical Planing Surfaces

In the following analysis the side-force coefficients in the wind axis are discussed.

Side forces on flat plate.- In figures 10 to 12 the tabulated side-force coefficients C_{C_b} for the tested flat planing surface of zero chine-edge thickness are plotted against the lift coefficient C_{L_b} for each of the test trim angles.

The side-force coefficient should be proportional to the lift-force coefficient since the side force is primarily due to pressure forces on the wetted bottom area. An analytical expression can be derived for the relation between C_{C_b} and C_{L_b} in terms of the unsymmetrical planing parameters. This relation is expressed as follows:

$$C_{C_b} = C_{L_b} \left(\frac{\tan \phi \cos \psi}{\cos \tau} - \tan \tau \sin \psi \right) \quad (1)$$

Equation (1) has been compared with the experimental data of figures 10 to 12 with resulting good agreement. The trends of side-force-coefficient variation with planing parameters can be established from an examination of equation (1) and from the discussion of flat-plate lift coefficient given in the section "Lift of Planing Surface."

The side-force coefficient in the body axis is nearly zero for all test combinations of planing parameters. Since the body-axis side-force coefficient is representative of the viscous friction, it is apparent that the velocity component transverse to the bottom is very small.

Side forces on 20° dead-rise surface.- In figures 15 to 17 the side-force coefficients for the tested 20° dead-rise surfaces are plotted against the lift coefficient for each of the test trim angles. Since the side-force coefficient for a deadrise surface is composed of two components, one on each side of the bottom, and since the division of total load between each side has not been established, a relation similar to equation (1) cannot be formed. Certain generalizations concerning the variation of the side-force coefficient with unsymmetrical planing conditions can be established from an examination of the plotted data.

For the unyawed deadrise surface, rolled 15°, the side force is very small, being of the order of magnitude of 10 percent of the lift force. These small side forces compare with the precision of the side-force dynamometer (± 0.125 pound) and hence there is considerable scatter in these test data. The change in direction of the side-force coefficient between the wind- and body-axes systems (fig. 15(b)) is a further indication of the small side forces since, in the conversion process, the wind-axis lift component predominates and results in a negative side component in the body-axis system.

The effect of increasing positive yaw angle at zero roll angle is a continuous increase in the side-force coefficient for a given lift coefficient. This effect of course follows from the sideward inclination of the resultant force vector as the yaw angle is increased. An examination of figures 16(a) and 17(a) shows that, for a given lift coefficient, the side-force component is reduced with increasing trim and becomes negative

for trim angles of 24° and 30° . The reason for this behavior is that the effective yaw angle of the port side is reduced with increasing trim angle while that of the starboard side is increased with increasing trim angle. The net result of these changes is to cause the starboard side force (which is negative in direction) to become increasingly pronounced in its effect on the total side force as the trim is increased. This change in direction of the side force may be of concern in the overall behavior of hydro-ski configurations if they experience large trim changes during an unsymmetrical landing.

For a positive roll angle of 15° the effect of increasing the positive yaw angle up to 20° (figs. 15(b), 16(b), and 17(b)) is to increase the positive side-force coefficient, especially at low trim angles. The port side is contributing most to the generation of the side force and since, with increasing yaw angle the hydrodynamic loads on the port side are increased, the positive side-force component is increased. For the yawed and rolled case, the side-force coefficients become appreciable, being almost 50 percent of the lift coefficient for a trim of 6° and a yaw angle of 20° (fig. 17(b)). An increase in trim angle reduces the positive side-force coefficient because, as discussed in the previous paragraph, the effectiveness of the starboard side is increased with increasing trim angle. Since the starboard side produces a negative side-force component, the net effect of trim angle is to reduce the side-force coefficient.

For a negative roll angle of 15° , the side-force coefficient is negative and there is only a small variation of C_{C_b} with increasing positive yaw angle. Because of the small variations of C_{C_b} with ψ it is not feasible to derive general conclusions concerning the behavior of C_{C_b} with ψ . One interesting observation which is evident from figures 16(b) and 17(b) is that, for negative roll angles, C_{C_b} becomes more negative with increasing values of τ and, for positive roll angles, C_{C_b} becomes less positive with increasing values of τ . For the negative-roll-angle condition, the starboard side of the bottom contributes most to the hydrodynamic side force. With increasing trim angle, the effectiveness of the starboard side is continuously increased and there is an overall increase in the negative value of C_{C_b} with increasing trim angle.

Drag of Planing Surfaces

Drag of flat plate.- In figures 10 to 12 the tabulated drag coefficients C_{D_b} for the flat plate of zero chine-edge thickness are plotted against lift coefficient C_{L_b} for each of the test trim angles. In

general, there is a small variation in C_{D_b} (at a given value of C_{L_b}) with a change in unsymmetrical planing conditions. These variations are discussed as follows.

For the case of zero yaw angle and increasing roll angle (fig. 10) there is a slight increase in C_{D_b} for given values of τ and C_{L_b} . This result follows from the fact that, with increasing roll angle, the effective dead rise of the flat plate is increased; consequently, its wetted length is increased for a given value of C_{L_b} and hence the friction drag component is increased.

When the yaw angle of the flat plate is increased at zero roll angle (figs. 10(a), 11(a), and 12(a)) there is a reduction in C_{D_b} for given values of C_{L_b} and τ . Two factors contribute to the drag-coefficient reduction. One is that, because of the increased effective aspect ratio of the yawed surface, there is a decrease in wetted area with increasing yaw angle for given values of C_{L_b} and τ . This area reduction would naturally reduce the friction drag component. The second factor which contributes to a drag reduction is that, with increasing yaw angle, the resultant hydrodynamic force is rotated towards the starboard direction and its drag component in the wind axis is reduced.

For the case of a positive roll angle, the effect of positive yaw angle is to cause a slight increase in C_{D_b} for given values of C_{L_b} and τ . The dynamic component of drag is increased because of the increase of effective trim of the rolled flat plate with an increase in positive yaw angle. The friction drag component, however, is reduced since there is a large reduction in wetted area as the yaw angle is increased at given values of C_{L_b} and τ . The net effect of increasing the dynamic drag component and decreasing the viscous component is to cause a slight increase in the drag coefficient.

With the flat plate at a negative roll angle there is a reduction in C_{D_b} as the positive yaw angle is increased. The effects are opposite from those for the positive rolled case; that is, the effective trim of the bottom surface is decreased which decreases the dynamic drag component and the wetted area, for given values of C_{L_b} and τ , is increased which increases the viscous drag component. The dynamic drag component predominates and there is a net decrease in drag with increasing positive yaw angle.

Drag of 20° dead-rise surface.— The tabulated drag coefficients for the 20° dead-rise surface are plotted against lift coefficient in figures 15 to 17.

For the case of zero yaw angle, there is no significant change in C_{D_b} with roll angle. This effect is consistent with the slight variation in lift with increasing roll angle.

The effect of increasing positive yaw angle for the zero-roll case is to cause a slight increase in C_{D_b} at a given value of C_{L_b} . Since a major portion of the planing load is carried by the port side, an increase in C_{D_b} with yaw angle must occur because the wind-axis drag component of the port side force increases with yaw angle. When the 20° dead-rise surface is at a positive roll angle, the effect of the positive yaw angle is again to cause an increase in C_{D_b} .

For the negative-roll-angle condition, there is little change in C_{D_b} for increasing positive yaw angle. This is similar to the side-force behavior with yaw angle as discussed previously.

Center of Pressure of Planing Surfaces

Center of pressure of flat plate.— The test pitching-, yawing-, and rolling-moment coefficients, C_m' , C_n' , and C_k' , respectively, are listed in table I for each of the flat-plate test conditions. These moment coefficients are measured about a point on the longitudinal center line of the bottom a distance of 3 beams forward of the trailing edge.

In order to simplify the presentation of the voluminous amount of flat-plate moment data, the longitudinal and lateral positions of the center of pressure of the resultant force were calculated and their variations with unsymmetrical planing conditions are discussed. The longitudinal center of pressure C_p' obtained from the pitching moment C_m' is measured in the body axis and is expressed as a percentage of the mean wetted length forward of the trailing edge. The lateral center of pressure C_y' obtained from the rolling moment C_k' is measured in the body axis and is expressed as a percentage of the beam outboard of the longitudinal center line.

Figure 13 presents the variation of C_p' with λ for each of the flat-plate test trim conditions. It was found that both the yaw angle and roll angle had no discernible effect on C_p' ; therefore, all test data were plotted without separately identifying the test yaw and roll angles. Some scatter of the computed values of C_p' appears in the plots, particularly at small values of λ . It will be remembered, however, that at short wetted lengths the measured values of C_m' , C_{L_b}' ,

and λ (all three of which are used to calculate C_p') are small and consequently are more affected by experimental accuracy than at large values of λ . In general, it is seen that C_p' is essentially constant and, for the test conditions, varies between 0.69 and 0.80. The effect of increasing trim is to reduce the value of C_p' . The effect of λ on C_p' is very small.

The variation of lateral center-of-pressure position C_y' with ϕ is presented in figure 14. It will be noted that the test results are separately plotted for various test values of yaw angle and each value of C_y' is identified as to test trim. No attempt was made to identify each test wetted length. Because the measured rolling moments were very small, a considerable scatter in C_y' appears in figure 14 and hence it is not possible to separate the effects of planing variables on C_y' .

The body-axis yawing moment for a flat plate is developed by the viscous forces acting on the planing bottom. Since the viscous forces are very small, relative to the dynamic forces, the yawing moments were very small and consequently were not analyzed. Table I presents the test values of C_n' .

Moment coefficients for 20° dead-rise planing surfaces.- The test values of C_m' , C_n' , and C_k' for the 20° dead-rise surface, measured about a point on the keel 3 beams forward of the step, are presented in table I. The pitching- and yawing-moment coefficients (C_{m_1}' and C_{n_1}') are also presented in table I in the body-axis system relative to the point of keel intersection with the trailing edge.

Because of the fact that the resultant load on a deadrise surface is made up of unknown port and starboard components, the conversion of the measured moments into longitudinal and lateral center-of-pressure positions was not considered to be a useful way of presenting the test results. With the possible existence of negative pressures around the keel area (as discussed in the sections on lift) centers of pressures could be calculated to be outside the wetted areas. Hence, it was decided to plot the body-axis moment data in coefficient form and to discuss their variation with unsymmetrical planing conditions. The moment coefficients for the 20° dead-rise surface, taken about the trailing-edge reference point, are plotted against lift coefficient in figures 18 to 20.

Pitching-moment coefficient.- For the unyawed surface, at given values of C_{L_b} and τ , there is a small increase in C_{m_1}' with increasing roll angle. This result follows from the fact that there is a small increase in wetted length, for a given value of C_{L_b} , as roll angle is increased.

At zero roll angle and with increasing yaw angle there is an increase in C_{m_1}' at a given C_{L_b} . The wetted length is increased with increasing yaw angle for a given C_{L_b} and hence the longitudinal center of pressure is moved forward with a consequent increase in pitching moment.

For the case of positive roll angle there is a decrease in C_{m_1}' with increase in positive yaw angle. Again this result follows from the previously discussed result that there is a decrease in λ for a given value of C_{L_b} and a consequent reduction in moment arm about the trailing edge. When the 20° surface is at a negative roll angle and is given a positive yaw angle, there is an increase in C_{m_1}' , at a given value of C_{L_b} , because of a corresponding increase in λ .

Yawing-moment coefficient.- For the unyawed surface, the effect of positive roll angle is to produce a negative side force in the body-axis system and consequently to develop a negative yawing moment about the trailing edge. With negative roll angle, a positive side force is developed with a corresponding generation of positive yawing moment.

For the unrolled surface, the effect of increasing positive yaw angle, for a given value of C_{L_b} , is to increase the positive yawing-moment coefficient C_{n_1}' . For these conditions both the side force and wetted length forward of the trailing edge are increased with increasing values of ψ . Since the increasing value of λ increases the side-force moment arm about the trailing edge, an increase in C_{n_1}' is expected.

For the positive rolled surface, the effect of positive yaw angle is to develop a very slight positive yawing moment. Both the port and starboard sides of the dead-rise bottom are contributing to the lift and, consequently, the resultant side force in the body axis is small. Further, for a given value of C_{L_b} the mean wetted-length-beam ratio is reduced with increasing ψ . The combination of small side force and small moment arm results in a small value of C_{n_1}' for the positive rolled and positive yawed dead-rise surface.

When the dead-rise surface is at a negative roll angle the effect of positive yaw angle is to increase the positive yawing-moment coefficient at given values of C_{L_b} and τ . The port side of the bottom carries a major portion of the total load, and consequently both the positive side-force component and the mean wetted length are increased with increasing yaw angle. These conditions result in an increasing yawing moment with increasing values of ψ .

Rolling-moment coefficient.- The rolling-moment coefficient is dependent on the distribution of load between the two halves of the planing bottom. Since the side force is also dependent on this distribution the variation in the rolling-moment coefficient with ψ and ϕ corresponds to the side-force-coefficient variation. A positive roll angle generates a negative side force for the unyawed surface (in the body axis) and consequently develops a negative rolling moment. When the dead-rise surface is at zero roll angle and at positive yaw angle a large positive side force is developed which results in large positive rolling moments. For a positive roll angle and positive yaw angle, the side force has been shown to be small and consequently the rolling moments are small. For a negative roll angle at a positive yaw angle, there is a large positive side force developed with a resulting large positive rolling moment.

Wetted Areas of Planing Surfaces

Wave rise for unrolled flat plate.- A comparison of the measured wetted-length-beam ratio λ with that computed from the running draft $d/b \sin \tau$ is presented in figure 21 where λ_1 is plotted against λ . The test wetted length is measured from the trailing edge of the model to the intersection of the spray root line with the bottom and was obtained from underwater photographs. The purpose of this plot is to examine the magnitude of the wave rise which occurs at the intersection of the planing plate with the free water surface.

Figure 21 presents the test data for all test yaw angles for the 0° roll case. It was found that, for the unrolled case, yaw angle had no effect on the shape of the leading edge of the wetted area and that, practically, the wave-rise behavior at the leading edge was similar to that for the symmetrical planing condition. An examination of the running wetted lengths presented in table I indicates almost the same port and starboard chine lengths for the unrolled yawed flat plate. Hence, in figure 21, the test points are not identified as to test yaw but only as to test trim.

The present wave-rise data are compared in figure 21 with the empirical relation for flat-plate wave rise developed in reference 1. The data analyzed in reference 1 included all available published flat-plate wave-rise data through the year 1955. It will be noted that, except for the 6° trim data, there is fairly good agreement between the present data and the empirical relation. At 6° trim the present data indicate a negative wave rise. This same result was obtained by the NACA in high-speed flat-plate planing tests described in reference 4. At present, no complete explanation has been developed for this unexpected result.

Wave rise for rolled flat plate.— When a flat plate is set at a roll angle its physical appearance is that of one-half of a dead-rise surface having a dead-rise angle equal to the roll angle. The shape of the wetted leading edge of the rolled flat plate was examined to determine whether the usual dead-rise—wave-rise relations hold for this flat-plate case.

A comparison is made between the measured wetted length of the rolled-down chine edge (L_r for positive ϕ , L_l for negative ϕ) and that computed from the running draft (L_{r1} , L_{l1}) (fig. 22). This rolled-down chine edge would correspond to the keel line of the equivalent half-dead-rise surface. The computed chine length is $d/b \sin \tau$. The data for all test yaw-angle and roll-angle conditions are presented in one plot since their separate effects were not discernible in the collected test data. This plot is analyzed to determine whether any water pileup exists at the forward extremity of the rolled-down edge of the flat plate.

It is seen in figure 22 that the measured wetted chine length for the 6° trim tests is less than the calculated values. This result, which is contrary to expectation, is similar to that observed in the unrolled case. As stated previously, no satisfactory explanation has been established for this result. The remaining data indicate a slight increase in water pileup as the trim angle is increased.

The spray root line for the rolled flat plate is inclined aft relative to the longitudinal axis of the model and intersects each chine line at different distances forward of the trailing edge. To determine whether the wave rise in the spray root area of a rolled flat plate corresponds to that for an equivalent half-dead-rise surface having a dead-rise angle equal to roll angle, the difference between the wetted chine lengths was compared, in figure 23, with the expression

$$L_r - L_l = \frac{2 \cos \phi \tan \beta_e}{\pi \tan \tau} \quad (2)$$

which is derived from Wagner's work (ref. 10) and where β_e is taken to be equal to the roll angle ϕ . Equation (2) has been shown in reference 1 to be applicable to the symmetrically planing dead-rise surface.

It is seen in figure 23 that there is good agreement between the wave rise at the leading edge of a rolled flat plate and equation (2) indicating the apparent correspondence between rolled flat plate and an equivalent dead-rise surface. The test data in figure 23 are for all test combinations of yaw angle and roll angle. There was no discernible yaw-angle effect on the plotted results and agreement with equation (2) existed whether the roll angle was positive or negative.

Wave rise for 20° dead-rise surface.— In figure 24 the running draft coefficient C_d is plotted against the computed draft $L_k \sin \tau$ where L_k is the wetted-keel-length—beam ratio obtained from the underwater photographs. The purpose of this plot is to indicate the magnitude of the water pileup at the keel. The yaw- and roll-angle test conditions are not separately identified in figure 24 since there was no apparent effect of these variables on the curve of C_d against $L_k \sin \tau$. It will be noted that at a test trim of 6° there is a depression of the water surface at the keel. With increasing trim angle, there is a gradual rise of the water surface at the keel so that at $\tau = 30^\circ$ there is a substantial water pileup at the keel. These results are in general agreement with those found in reference 5.

For the rolled dead-rise surface, the rolled-up side of the bottom may be considered to be increased in effective dead rise while the rolled-down side may be considered as being decreased in effective dead rise. In order to determine whether the wave rise in the spray root area of each bottom side of a rolled dead-rise surface corresponds to the usual $\pi/2$ factor developed by Wagner (ref. 10) for two-dimensional wedges, the experimental values of $L_k - L_r$ and $L_k - L_l$ are plotted in figure 25 and compared with the following equation:

$$L_k - L_c = \frac{\tan \beta_e}{\pi \tan \tau} \quad (3)$$

where $\beta_e = 20^\circ \pm \phi$ and $L_c = L_l$ or L_r , whichever is appropriate. Equation (3) is derivable from Wagner's $\pi/2$ wave-rise relation.

In figure 25 it is seen that the data for the rolled-up and rolled-down chines are presented in separate plots. Further, since it was found that yaw angle had no effect on these results, the data are not identified as to their yaw-angle test conditions. Examining the data for the rolled-down side of the surface ($\beta_e \leq 20^\circ$) it is seen that the experimental values of $L_k - L_c$ are in agreement with the results obtained from equation (3) when β_e is taken to be the geometric dead rise less the absolute value of the roll angle. For the rolled-up side of the surface ($\beta_e > 20^\circ$) there is no agreement between the experimental values $L_k - L_c$ and those predicted by equation (3). For this rolled-up side it appears that the wave rise is much larger than the theoretical value $\pi/2$ and that beyond a roll angle of 5° the values of $L_k - L_c$ are essentially constant. The above results were independent of the sign of the roll angle.

Hydrodynamic Effect of Finite Chine Thickness on a Flat Plate

At the inception of the flat-plate planing tests, the test model was of constant thickness equal to 0.182b. During unsymmetrical tests of this flat-plate model, large sudden changes in both the hydrodynamic forces and the spray formation were observed when particular combinations of unsymmetrical planing conditions were tested. An analysis of the test results indicated that chine-edge wetting was responsible for the sudden changes in hydrodynamic behavior. In order to present flat-plate planing data which are independent of chine-edge-thickness effects, tests on the 0.182b-thick-chine model were curtailed and a zero-thick-chine-edge model was constructed and tested. The data for the zero-edge-thickness flat plate are plotted herein and have been discussed in the previous sections of this report.

To explore further the effect of chine-edge thickness on the hydrodynamic behavior of flat plates, an additional model of 0.091b-chine-edge thickness was briefly tested. The data for the 0.182b- and 0.091b-thick models are presented in table II. In this tabulation yaw- and roll-angle test conditions appear which were not considered in the basic planing program described in figure 7. These additional unsymmetrical planing conditions were necessary to define more thoroughly the boundaries of inception of the chine-edge effects.

The effect of chine-edge wetting was to generate either negative or positive pressures on the chine edges depending upon the combination of unsymmetrical test planing conditions. The development of chine-edge pressure in turn altered the geometry of the spray across the length of the model. The chine-edge pressures were established as being positive or negative by comparing the resultant hydrodynamic loads with those obtained from tests of the flat plate with zero chine-edge thickness. In the case of the unyawed flat plate at moderate positive roll angles, the resultant force is essentially normal to the bottom (except for viscous effects) and the ratio of side force to lift force is as given by equation (1). The flow breaks clear at the chines and the lateral spray formation is displaced outboard of both chines. As the positive roll angle is increased, a critical angle is reached at which the fluid flow at the starboard side clings to the rolled-down chine edge. When this happens, there is a large increase in side force, for a given lift, and the spray on the starboard side is reduced in height and is moved inboard towards the model by a significant amount. The fluid-flow pattern along the port chine edge is not noticeably affected by the increased roll angle. It is concluded that, since the crossflow component of the bottom velocity cannot separate from the rolled-down edge, it creates large negative pressures on the finite-thick chine in flowing around the sharp corner of the chine. This action develops very suddenly - where at one roll angle there

is a clean separation of the flow from the rolled-down edge, at a slightly larger roll angle there is complete attachment of the flow to the chine with attendant very large increases in side force. When the positive yaw angle was increased to a certain value, the fluid flow would again separate from the starboard chine; the ratio of side force to lift force would be given by equation (1) and the lateral sprays would take on their normal appearance.

For the negative rolled surface at zero yaw angle, negative side pressures are developed along the port chine and the fluid-flow action is of course identical to that for the positive roll angle. As the positive yaw angle is increased, for the negative roll angle, the suction forces on the port chine are maintained until a yaw angle is reached at which the port chine edge is exposed to the free-stream velocity and positive pressures are developed on this edge. In this case of positive pressures on the chine, the side forces were less than those predicted by equation (1). Increasing yaw angle increased the port-chine-edge pressures and consequently decreased the resultant side-force coefficient.

By comparing the measured side forces with those predicted by equation (1) and also by observing the running spray patterns, it was possible to establish the boundaries of chine-edge interference for unsymmetrical planing conditions of a flat plate. These boundaries are summarized in the plots of figure 26. A separate boundary plot is presented for each test trim. The data used to establish these plots were for the tested flat plates of 0.182b and 0.091b edge thickness. It was found that both models had the same interference boundaries. The nature of the interference effects for various combinations of unsymmetrical planing conditions is identified in these plots. The areas marked "no chine-edge effects" indicate an agreement in measured hydrodynamic forces between the flat plates of finite edge thickness and those for zero chine-edge thickness. It will be noted that, for increasing trim angle, the areas of chine-edge interference are reduced.

The magnitude of the chine-edge effects was established by determining the resultant normal force on the chine edge and its point of application forward of the trailing edge. The absolute magnitude of the chine force was obtained by noting the difference between the side forces, in the body axis, for the flat plates having finite and zero chine-edge thicknesses. The point of application of the force was determined by the difference in yawing moment, in the body axis, between the flat plates having finite and zero chine-edge thicknesses.

Figure 27 presents the force on the chine edge as a normal-force coefficient C_e' on the leading chine edge. Data for both models (0.182b and 0.091b chine-edge thicknesses) are presented together since it was found that expressing the chine force as the coefficient C_e' collapsed.

the data very satisfactorily. In figure 27, C_e' is plotted against ϕ for various test trims. Separate plots are prepared for each test ψ . Only the data for positive pressure development on the chine edge are plotted and analyzed herein. Where negative chine-edge pressures were developed, the conversion of the data into a negative normal-force coefficient resulted in very large negative coefficients having no consistent variation with planing parameters.

It is seen in figure 27 that C_e' increases with increasing negative roll angle and that, at large angles of negative roll, the value of C_e' lies between 1.0 and 1.3 for the yaw-angle range from 10° to 20° for all trims.

The longitudinal center of pressure of the resultant positive chine force C_{pe}' as a percentage of wetted chine length forward of the trailing edge is presented in figure 28 as a function of chine wetted length. Separate plots are presented for each yaw angle and the code system of test data identifies the test trim. No distinction in data is made for the separate test roll angles since no roll-angle effect was discernible. Because of the scatter of center-of-pressure data in figure 28 no single summary curve could be drawn through the data. The data appear to be more consistent at $\psi = 20^\circ$ and indicate an aft motion of the resultant chine force with increasing chine wetted length. On the average, the center of pressure of the positive chine force appears to be at approximately 65 percent of the chine wetted length.

The effect of positive chine-edge pressures on the lift, drag, pitching moment, and rolling moment was small and hence is not discussed herein.

In the course of the tests it was determined that the roll-yaw combinations for which chine-edge wetting began were not dependent on speed, for speeds in the range corresponding to a value of C_v between 14 and 20. This was found in the following manner. At $C_v = 14$, the roll and yaw were adjusted to values which just caused chine-edge wetting. The speed was then increased to give $C_v = 20$. At this higher speed the chine edge remained wet, and the direction of the spray leaving the model and the value of C_e' remained the same as at $C_v = 14$, indicating no dependence on speed over this range. Consideration of the general shape of the separated flow past the edge of a plate indicates that this is to be expected. In this case there is a separation at the edge of the plate which gives rise to a free streamline which forms a cavity between the body and the fluid. Theoretically it can be shown that the shape of this free streamline is independent of speed (ref. 11). Therefore, the conditions at which the fluid flowing past the plate will wet the chine edge

should be determined only by the geometry of the plate relative to the direction of motion and not by the speed.

SUMMARY OF RESULTS

An experimental investigation was conducted to obtain the wetted areas and six components of forces and moments acting on a 0° and 20° dead-rise surface in high-speed unsymmetrical planing conditions. The analysis of the collected test data has led to a general qualitative evaluation of the effects of yaw and roll angle upon the hydrodynamic behavior of a planing surface and these effects have been summarized in table IV.

Effect of Yaw and Roll Angle on Leading-Edge Wave Rise

1. For all test conditions of $\beta = 0^\circ$ and $\beta = 20^\circ$ models, yaw angle had no effect on the leading-chine-edge wave rise.
2. For a flat plate at zero roll angle the leading-edge wave rise is equal to that of a flat plate in symmetrical planing conditions.
3. For the rolled flat plate, the angle of the spray root line relative to the keel is identical to that of a wedge whose dead rise is equal to the roll angle.
4. For the rolled-down side of the 20° dead-rise surface the angle of the spray root line relative to the keel is equal to that of a wedge whose dead rise is equal to 20° less the roll angle. In the rolled-up side of the 20° dead-rise surface, the angle of the spray root line is essentially constant and independent of roll angle.

Hydrodynamic Effect of Finite Chine-Edge Thickness

on a Flat Plate

1. At small angles of yaw and large positive roll angles the cross-flow does not separate from the chine and negative pressures are generated along the rolled-down chine edge of a flat plate with finite thickness. As the yaw angle is increased, the flow will separate cleanly from the chines.
2. At large yaw angles and negative roll angles, positive pressures are developed along the leading chine edge.

3. With the development of negative pressures along the chine of finite thickness the lateral spray is moved inboard and somewhat reduced in height.

4. The boundaries of inception of chine interference, in terms of unsymmetrical planing conditions, are independent of chine-edge thickness.

5. The normal-force coefficient on the positive-pressure edge of the wetted chines approaches a value of approximately 1.3 at large angles of yaw and negative roll.

6. Chine-edge interference effects are reduced with increasing trim angle.

Stevens Institute of Technology,
Hoboken, N. J., March 13, 1957.

APPENDIX A

ORIENTATION OF PLANING BODY AXES RELATIVE
 TO FIXED WIND AXES

The following discussion of axes systems follows the procedures established by the American Towing Tank Conference in 1949 (ref. 9). There are two coordinate-axes systems which must be considered in this study. Both are right-handed, orthogonal axes and have the same origin. One is a set of fixed axes (also referred to as wind axes) with x , y , and z fixed relative to the earth, so that the x - and y -axes are in a horizontal plane with the positive x -axis directed in the direction of the horizontal planing velocity and the positive z -axis vertical and directed downwards, as shown in figure 3. The origin of this axes system is located on the center line planing bottom 3 beams forward of the trailing edge. Linear displacements are taken as positive in the positive direction of the coordinate axes. Angular displacements are taken as positive in the sense of rotation of a right-hand screw advancing in the positive direction of the axis of rotation.

The orientation of the right-handed, orthogonal set of body axes, x' , y' , and z' , relative to the fixed axes is described in terms of the angle of trim τ , the angle of yaw ψ , and the angle of roll ϕ . It will be recalled that the origins of both axes systems coincide. The space orientation of both axes systems may be described by the following procedure (see fig. 3). First, suppose that the body axes x' , y' , and z' coincide with the wind axes x , y , and z . Rotate the body about z through an angle of yaw ψ so that the axes x, y assume the intermediate positions x_1, y_1 ; then rotate the body about the new position of the y -axis through an angle of trim τ , so that z moves to z_1 and x_1 moves to x' ; finally, rotate the body about the new position of the x -axis through an angle of roll ϕ so that the axes y_1, z_1 assume their final positions y', z' .

The direction cosines of the body axes (x' , y' , and z') relative to the fixed wind axes (x , y , and z) are as follows:

	x'	y'	z'
x	$\cos \tau \cos \psi$	$-\cos \phi \sin \psi + \sin \tau \sin \phi \cos \psi$	$\sin \phi \sin \psi + \sin \tau \cos \phi \cos \psi$
y	$\cos \tau \sin \psi$	$\cos \phi \cos \psi + \sin \tau \sin \phi \sin \psi$	$-\sin \phi \cos \psi + \sin \tau \cos \phi \sin \psi$
z	$-\sin \tau$	$\cos \tau \sin \phi$	$\cos \tau \cos \phi$

Moments are taken as positive when they tend to make the associated angle more positive. Therefore, to convert moments from the wind-axis system to the body-axis system make the following substitutions in the above set of direction cosines:

Roll K for x
 Pitch M for y
 Yaw N for z

The positive directions of the hydrodynamic lift and drag forces are opposite to the positive direction of the coordinates. As pointed out above the coordinate directions are taken as

x positive forward
 y positive to starboard
 z positive downward

The hydrodynamic forces are taken as

Drag D positive aft
 Side force C positive to starboard
 Lift L positive upward

Therefore, a new set of direction cosines is required for the conversion of forces from the wind axes to the body axes. They are

	D'	C'	L'
D	$\cos \tau \cos \psi$	$\cos \phi \sin \psi - \sin \tau \sin \phi \cos \psi$	$\sin \phi \sin \psi + \sin \tau \cos \phi \cos \psi$
C	$-\cos \tau \sin \psi$	$\cos \phi \cos \psi + \sin \tau \sin \phi \sin \psi$	$\sin \phi \cos \psi - \sin \tau \cos \phi \sin \psi$
L	$-\sin \tau$	$-\cos \tau \sin \phi$	$\cos \tau \cos \phi$

REFERENCES

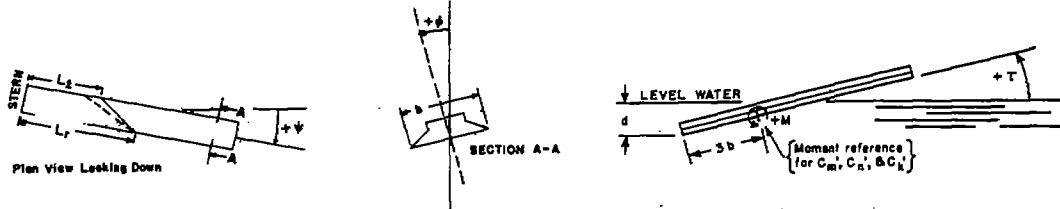
1. Savitsky, Daniel, and Neidinger, Joseph W.: Wetted Area and Center of Pressure of Planing Surfaces at Very Low Speed Coefficients. S.M.F. Fund Paper No. FF-11, Inst. Aero. Sci. (Rep. No. 493, Contract No. N6onr-24704, Project No. NR 062-012, Office of Naval Res., Exp. Towing Tank, Stevens Inst. Tech.), Sept. 1954.
2. Kapryan, Walter J., and Weinstein, Irving: The Planing Characteristics of a Surface Having a Basic Angle of Dead Rise of 20° and Horizontal Chine Flare. NACA TN 2804, 1952.
3. Blanchard, Ulysse J.: The Planing Characteristics of a Surface Having a Basic Angle of Dead Rise of 40° and Horizontal Chine Flare. NACA TN 2842, 1952.
4. Weinstein, Irving, and Kapryan, Walter J.: The High-Speed Planing Characteristics of a Rectangular Flat Plate Over a Wide Range of Trim and Wetted Length. NACA TN 2981, 1953.
5. Chambliss, Derrill B., and Boyd, George M., Jr.: The Planing Characteristics of Two V-Shaped Prismatic Surfaces Having Angles of Dead Rise of 20° and 40° . NACA TN 2876, 1953.
6. Kapryan, Walter J., and Boyd, George M., Jr.: The Effect of Vertical Chine Strips on the Planing Characteristics of V-Shaped Prismatic Surfaces Having Angles of Dead Rise of 20° and 40° . NACA TN 3052, 1953.
7. Springston, George B., Jr., and Sayre, Clifford L., Jr.: The Planing Characteristics of a V-Shaped Prismatic Surface With 50 Degrees Dead Rise. Rep. 920, David W. Taylor Model Basin, Navy Dept., Feb. 1955.
8. Smiley, Robert F.: A Theoretical and Experimental Investigation of the Effects of Yaw on Pressures, Forces, and Moments During Seaplane Landings and Planing. NACA TN 2817, 1952.
9. Anon.: Nomenclature for Treating the Motion of a Submerged Body Through a Fluid. Tech. and Res. Bull. No. 1-5, Soc. of Naval Arch. and Marine Eng., Apr. 1950.
10. Pierson, John D.: On the Pressure Distribution for a Wedge Penetrating a Fluid Surface. Preprint No. 167, S.M.F. Fund Paper, Inst. Aero. Sci. (Rep. No. 336, Project No. NR 062-012, Office of Naval Res., Exp. Towing Tank, Stevens Inst. Tech.), June 1948.

11. Korvin-Kroukovsky, B. V., and Chabrow, Faye R.: The Discontinuous Fluid Flow Past an Immersed Wedge. Preprint No. 169, S.M.F. Fund Paper, Inst. Aero. Sci. (Rep. No. 334, Project No. NR 062-012, Office of Naval Res., Exp. Towing Tank, Stevens Inst. Tech.), Oct. 1948.

TABLE I

TABULATION OF TEST DATA AND RESULTS

(a) $\beta = 0^\circ$; $\tau = 6^\circ$



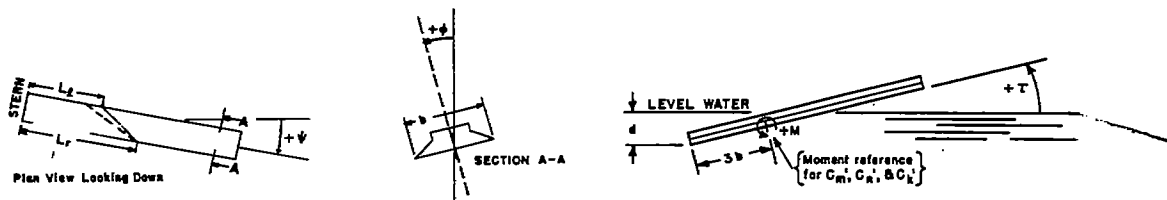
$C_v = 14.00$

TEST PARAMETERS			WIND AXIS										BODY AXIS									
ψ	ϕ	C_A	C_{L_1}	C_{D_1}	C_{C_1}	C_m	C_n	C_k	d/b	L_1	L_2	λ	C_{L_1}'	C_{D_1}'	C_{C_1}'	C_m'	C_n'	C_k'	C_p'	C_y'		
0	0	7.80	.08	.0098	.0088	-.1683	.0165	-.0083	.128	0.80	.90	.90	-.0806	.0014	-.0085	-.1683	.0110	-.0086	1.171	-.0794		
0	12.25	.125	.0215	-.0095	-.1894	.0070	-.0009	.800	1.83	1.83	1.83	-.1286	-.0083	-.0035	-.1894	-.0069	-.0015	.856	-.0188			
0	17.61	.18	.0872	-.0035	-.0560	.0105	-.0083	.480	4.00	4.00	4.00	-.1829	.0182	-.0035	-.0560	-.0110	-.0048	.658	-.0250			
0	23.93	.245	.0809	0	-.8548	.0193	-.0035	.775	7.15	7.15	7.15	-.2490	.0260	0	-.8548	.0196	-.0015	.731	-.0080			
5	23.93	.245	.0442	.0124	-.6548	.0378	-.0035	.775	7.20	6.75	6.98	-.2494	.0184	-.0090	-.5877	.0063	-.0028	.761	-.0101			
-5	7.80	.08	.0109	.0070	-.1330	0	-.0035	0	.125	.90	.30	.0810	.0024	0	-.1328	.0021	-.0004	1.887	.0049			
-5	12.25	.125	.0284	-.0212	-.1443	.0284	-.0004	.225	1.80	2.15	1.88	-.1280	.0084	-.0101	-.1461	.0135	-.0032	.989	-.0280			
-5	17.61	.18	.0518	-.0124	-.0787	.0123	-.0018	.475	4.00	4.88	4.88	-.1827	.0188	-.0035	-.0743	.0190	-.0031	.796	-.0170			
-5	23.93	.245	.0219	-.0247	-.1247	-.0184	-.0080	.300	2.60	1.60	2.10	-.1290	.0087	-.0035	-.1293	-.0021	-.0028	.858	-.0287			
-10	7.80	.08	.0158	-.0105	-.1248	.0388	-.0080	.180	.40	1.45	.93	-.0818	.0073	-.0035	-.1294	.0170	.0048	1.254	-.0287			
-10	12.25	.125	.0285	-.0088	-.0158	0	-.825	6.00	4.00	4.80	-.1848	.0174	-.0087	.0912	-.0002	-.0117	.776	-.0092				
-10	17.61	.18	.0527	-.0467	-.6598	-.0788	-.0035	.825	7.08	6.15	7.62	-.2355	.0268	-.0027	-.8334	.0378	.0117	.737	-.0462			
-10	23.93	.245	.0293	.0141	.2517	-.0211	-.0176	.300	3.25	1.80	2.55	-.1287	.0180	-.0194	-.2373	-.0872	-.0163	1.826	-.1208			
-15	7.80	.08	.0147	-.0175	-.1138	.0360	.0105	.160	.40	2.08	1.23	-.0889	.0062	-.0070	-.1198	.0078	-.0008	1.887	.0796			
-15	12.25	.125	.0409	.0406	.1890	-.0387	-.0288	.878	8.70	4.18	4.93	-.1876	.0219	-.0082	-.1730	-.0078	-.0129	.794	-.0688			
-15	17.61	.18	.0574	.0413	.0433	-.0188	-.0087	.425	3.80	3.85	3.89	-.1828	.0181	-.0035	-.0284	-.0154	.0107	.844	-.0287			
-15	23.93	.245	.0169	-.0169	0	-.0142	-.360	3.25	8.00	3.05	3.05	-.1828	.0084	-.0025	-.0483	-.0053	-.0099	.903	-.0542			
-8	17.61	.18	.0318	-.0177	.1584	.0035	-.0147	.425	4.60	5.10	4.85	-.1797	.0142	.0011	.1554	-.0104	.0373	.797	.1819			
-7	17.61	.18	.0360	-.0247	.2200	-.0070	.0123	.550	4.95	6.00	5.28	-.1778	.0190	.0010	.2160	-.0345	.0320	.789	.1800			
-10	17.61	.18	.0434	-.0408	.2200	-.0158	.0141	.075	5.00	6.15	5.68	-.1787	.0277	-.0048	.2168	-.0843	.0348	.798	.2018			
-12	17.61	.18	.0518	-.0489	.2484	-.0387	.0141	.625	5.30	6.80	5.95	-.1695	.0382	-.0019	.2461	-.0897	.0394	.784	.2324			
-10	17.61	.18	.0904	-.0800	.4400	-.1182	-.0183	.790	8.90	8.90	7.95	-.1840	.0780	-.0898	.4536	-.2280	.0861	.794	.3323			
0	7.80	.08	.0105	-.0088	-.1330	.0105	-.0184	.125	1.80	1.80	1.80	-.0806	.0014	-.0035	-.1294	.0110	-.0048	1.858	-.0178			
0	12.25	.125	.0204	-.0035	-.1894	.0080	-.0458	.225	1.85	1.80	1.53	-.1285	.0078	-.0001	-.1928	.0100	-.0104	.935	-.0034			
0	17.61	.18	.0238	-.0035	-.0848	.0088	-.0352	.375	3.18	3.18	3.18	-.1825	.0139	-.0022	-.0893	.0208	.0080	.797	.1140			
0	23.93	.245	.0446	-.0035	.1998	.0105	-.0035	.875	6.10	5.10	5.10	-.2483	.0186	.0042	.1959	.0144	-.0322	.743	-.1297			
5	7.80	.08	.0083	.0070	-.1683	-.0018	.0815	.100	.80	.25	.53	.0804	-.0044	-.0009	-.1882	.0123	.0008	2.019	.0897			
5	12.25	.125	.0206	.0070	-.2283	-.0088	.0493	.175	1.25	.75	1.80	-.1267	.0068	-.0005	-.2306	.0124	.0103	.879	.0813			
5	17.61	.18	.0278	.0124	-.1864	-.0088	.0899	.275	2.80	1.95	2.23	-.1824	.0080	.0011	-.1893	.0074	-.0020	.787	.0110			
5	23.93	.245	.0372	.0140	-.0283	-.0075	.0210	.475	4.70	2.95	3.85	-.1824	.0084	-.0012	-.0289	-.0058	.0148	.754	.0988			
10	7.80	.08	.0068	.0070	-.1313	-.0193	.0420	.125	.85	--	.40	.0805	-.0010	-.0056	-.1378	.0087	.0004	3.235	.8431			
10	12.25	.125	.0187	-.0184	-.0344	.0440	.228	1.30	.70	.75	.1879	.0018	-.0002	-.2214	.0080	.0005	1.692	.0743				
10	17.61	.18	.0321	.0300	-.2887	-.0422	.0475	.260	2.30	1.30	1.80	-.1861	.0074	.0030	-.2863	-.0048	.0052	.867	.0358			
10	23.93	.245	.0366	.0381	-.0878	-.0228	.0438	.375	3.80	2.70	3.18	-.2800	.0031	-.0027	-.0958	-.0032	.0305	.831	.1220			
15	7.80	.08	.0147	-.0176	-.1290	-.0315	.0175	.150	1.40	--	.70	.0832	.0030	-.0017	-.1310	.0022	-.0013	2.037	-.0184			
15	12.25	.125	.0237	.0247	-.2308	-.0388	.0317	.200	1.90	.08	.88	-.1894	.0089	-.0038	-.2394	.0025	-.0029	1.868	-.0254			
15	17.61	.18	.0319	.0404	-.2800	-.0759	.0818	.200	2.40	.98	1.98	-.1871	.0064	-.0032	-.2348	.0048	.0159	.847	.0880			
15	23.93	.245	.0440	.0357	-.1784	-.0438	.0315	.325	3.40	2.18	2.78	-.2848	.0101	-.0022	-.1884	.0048	.0048	.816	.0181			
-5	7.80	.08	.0130	-.0035	-.1018	.0228	.0388	.180	.80	1.38	1.08	.0808	.0080	.0059	-.1081	.0185	.0161	1.840	.1993			
-5	12.25	.125	.0240	-.0141	-.0827	.0264	-.0176	.250	2.40	2.90	2.65	-.1274	.0129	.0014	-.0866	.0191	.0002	.876	.0016			
-5	17.61	.18	.0362	-.0211	.0700	.0088	.0185	.825	4.20	4.80	4.50	-.1837	.0203	.0015	.0849	.0174	.0266	.745	.1448			
-5	23.93	.245	.0744	-.0281	.3985	-.0193	-.0176	.725	6.35	6.85	6.80	-.2882	.0221	.0073	.3889	.0208	.0832	.688	.3108			
-10	7.80	.08	.0176	-.0105	-.0890	.0193	.0298	.200	1.38	2.85	1.98	.0816	.0107	.0070	-.0631	.0104	.0175	1.142	.1148			
-10	12.25	.125	.0349	-.0108	.0440	-.0108	.0083	.600	3.80	5.00	4.40	-.1869	.0289	.0179	.0434	-.0017	.0139	.789	.1085			
-10	17.61	.18	.0516	-.0123	.4488	-.0648	-.0360	.800	6.80	7.95	7.58	-.1843	.0080	.0478	.4489	.0177	.0490	.754	.2813			
-10	23.93	.245	.0581	-.0140	.0595	-.0360	.058	3.80	6.75	6.75	.0793	.0432	.0468	.0633	-.0168	.0842	1.004	.3052				
20	0	7.80	.08	.0141	0	-.1232	.0106	.0757	.125	--	--	.0810	.0048	.0048	-.1417	.0136	.0277	--	.3420			
20	0	12.25	.125	.0233	-.0035	-.1619	.0070	.0988	.200	1.38	1.28	-.1287	.0089	.0047	-.1853	.0107	.0347	.480	.2739			
20	0	17.61	.18	.0281	-.0083	-.1663	.0019	.0988	.275	2.45	2.38	2.40	-.1820	.0092	.0046	-.1904	.0066	.0365	.814	.2005		
20	0	23.93	.245	.0491	.0140	0	-.0485	.0700	.450	3.90	3.90	-.2480	.0186	.0030	-.0239	-.0384	.0702	.754	.2381			
5	7.80	.08	.0111	.0070	-.1265	0	-.0388	.0440	.450	4.18	4.08	4.10	-.2490	.0268	.0078	.0380	-.0498	.0182	.748	.2537		
5	12.25	.125	.0206	.0083	-.2484	-.0080	.0288	.288	.98	.30	.63	-.1827	.0043	.0010	-.2611	.0174	-.0010	1.490	-.0079			
5	17.61	.18	.0318	.0070	-.2590	-.0193	-.1225	.288	1.60	1.00	1.80	-.1827	.0083	.0018	-.2884	.0088	.0284	.888	.1554			
5	23.93	.245	.0372	.0140	-.2433	-.0188	.1050	.275	2.70	2.15	2.43	-.2481	.0044	.0043	-.2648	.0090	.0170	.798	.0688			
10	7.80	.08	.0208	.0134	-.1408	-.0141	.0616	.080	.90	--	.45	.0833	.0068	-.0053	-.1853	.0138	.0112	2.877	.1345			
10	12.25	.125	.0264	.0154	-.2464	-.0317	.0845	.200	1.15	--	.70	-.1282	.0058	-.0003	-.2480	.0137	-.0012	1.365	-.0117			
10	17.61	.18	.0351	.0228	-.2273	-.0225	.1295	.180	1.80	.40	.95	-.1847	.0082	.0014	-.3856	.0107	.0128	1.133	.0823			
10	23.93	.245	.0361	.0305	-.2850	-.0856	.1348	.225	2.20	1.20	1.70	-.2485	-.0052	-.0030								

TABLE I.- Continued

TABULATION OF TEST DATA AND RESULTS

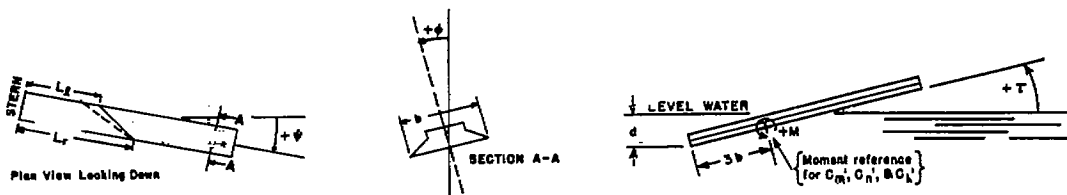
(b) $\beta = 0^\circ$; $\tau = 12^\circ$



TEST PARAMETERS		WIND AXIS										BODY AXIS																	
ψ	ϕ	C_{L_0}	C_{D_0}	C_{L_1}	C_{D_1}	C_{L_2}	C_{D_2}	C_{L_3}	C_{D_3}	C_{L_4}	C_{D_4}	d/b	L_T	L_Z	λ	$C_{L_b}^1$	$C_{D_b}^1$	$C_{L_b}^2$	$C_{D_b}^2$	$C_{L_b}^3$	$C_{D_b}^3$	$C_{L_b}^4$	$C_{D_b}^4$	$C_{L_b}^5$	$C_{D_b}^5$	$C_{L_b}^6$	$C_{D_b}^6$		
0	0	12.25	.0246	-.0070	-.2992	.0123	-.0018	.125	0.40	0.40	0.40	.1274	-.0019	-.0070	-.2992	.0117	-.0043	1.627	-.0338										
	0	31.36	.32	.0702	-.0035	-.3190	.0166	-.0123	.450	2.20	2.20	2.20	.3276	.0021	-.0035	-.3190	.0153	-.0029	1.629	-.0467									
	0	48.89	.60	.1221	-.0105	-.2608	.0210	0	.900	4.80	4.80	4.80	.6145	.0165	-.0105	-.2608	.0208	-.0044	1.730	-.0066									
	5	12.25	.125	.0511	.0127	-.3582	-.0141	-.0088	.125	.60	3.0	4.8	.1294	.0244	.0014	-.3582	.0137	-.0057	1.801	-.0440									
	5	31.36	.32	.0819	.0200	-.2850	-.0210	-.0210	.450	2.38	2.20	2.29	.3242	.0188	-.0035	-.3242	.0088	-.0162	1.751	-.0500									
	5	48.89	.60	.1137	.0351	.2825	.0816	-.0193	.900	4.80	4.60	4.70	.6136	.0273	-.0097	-.2825	.0056	-.0284	1.747	-.0494									
	-10	12.25	.125	.0297	-.0233	-.2816	.0616	.0141	.125	.20	.80	.80	.1305	.0031	-.0007	-.2816	.0031	-.0007	1.582	-.0077									
	-10	31.36	.32	.0754	-.0578	-.3000	.0808	.0178	.500	2.15	2.80	2.38	.3333	.0053	-.0008	-.3330	.0203	.0004	1.808	-.0012									
	-10	48.89	.60	.1185	-.0954	-.3225	.0355	1.000	4.80	5.40	5.15	.6217	.0100	-.0028	-.3330	.0204	.0103	1.706	-.0197										
	-15	12.25	.125	.0339	-.0300	-.2640	-.0933	.0248	.150	1.00	1.00	.80	.1287	.0072	.0043	-.1327	-.1316	.0438	1.295	-.3354									
	-15	31.36	.32	.0772	-.0920	-.2900	.0945	.0088	.580	2.35	3.05	2.70	.3325	.0090	-.0037	-.2949	.0186	-.0130	1.783	-.0351									
	-15	48.89	.60	.1306	-.1418	-.4900	-.0910	0	1.125	5.30	6.05	5.68	.6212	.0238	-.0024	-.4964	.0408	-.0188	1.866	-.0363									
10	0	12.25	.125	.0255	-.0053	-.2816	.0106	.0659	.125	.40	.40	.40	.1277	.0004	-.0006	-.2869	.0139	.0144	1.845	-.1128									
	0	31.36	.32	.0698	-.0140	-.4288	.0123	.0675	.450	2.20	2.20	2.20	.3273	.0031	-.0017	-.4575	.0146	.0069	1.766	-.0272									
	0	48.89	.60	.1183	-.0038	-.4728	-.0106	.0088	.880	4.40	4.35	4.38	.6133	.0106	.0172	-.4638	.0086	.0909	1.991	-.1771									
	5	12.25	.125	.0307	.0080	-.4798	-.0106	.0332	.100	.40	.40	.30	.1288	.0026	0	-.2817	.0113	-.0114	1.710	-.0886									
	5	31.36	.32	.0716	.0140	-.4813	-.0300	.0770	.375	2.00	1.75	1.88	.3282	.0001	-.0034	-.4868	.0068	-.0003	1.804	-.0009									
	5	48.89	.60	.1221	.0232	-.0910	-.0053	.0385	.600	4.15	3.95	4.05	.6121	.0097	-.0008	-.0950	.0078	-.0227	1.894	-.0341									
	10	12.25	.125	.0250	.0142	-.2974	-.0407	.125	.60	1.15	1.00	.90	.1300	.0034	-.0029	-.3021	.0112	-.0038	1.853	-.0277									
	10	31.36	.32	.0797	.0453	-.6250	-.0658	.0898	.300	1.95	1.45	1.70	.3330	.0024	.0018	-.6387	.0084	-.0113	1.813	-.0339									
	10	48.89	.60	.1243	.0832	-.2288	-.0315	.0263	.700	3.70	3.20	3.45	.6190	.0050	-.0084	-.2293	.0064	-.0186	1.741	-.0318									
	15	12.25	.125	.0303	.0267	-.2388	-.0648	.0296	.075	.80	1.28	1.25	1.25	.3390	.0053	-.0070	-.2397	.0063	-.0058	1.848	-.0104								
	15	31.36	.32	.0853	.0667	-.5478	-.1400	.0700	.300	1.88	1.25	1.65	.6284	.0071	-.0087	-.2728	-.0049	-.0081	1.750	-.0133									
	15	48.89	.60	.1341	.1067	-.2555	-.0700	.0288	-.650	3.70	3.10	3.40	.6284	.0071	-.0087	-.2728	-.0049	-.0081	1.647	-.0396									
20	0	12.25	.125	.0232	-.0178	-.2748	.0350	.0615	.125	.35	.60	.45	.1263	.0007	-.0001	-.2854	.0182	.0061	1.847	-.0766									
	5	12.25	.125	.0232	-.0178	-.2748	.0350	.0615	.125	.35	.60	.45	.1263	.0007	-.0001	-.2854	.0182	.0061	1.847	-.0766									
	5	31.36	.32	.0691	-.0379	-.3290	.0403	.0963	.500	2.40	2.60	2.50	.3293	.0058	-.0032	-.3436	.0174	-.0255	1.782	-.0865									
	5	48.89	.60	.1186	-.0632	-.2345	-.0140	.0123	.980	4.66	4.90	4.78	.6166	.0183	.0029	-.2282	.0172	.0546	1.780	-.1057									
	-10	12.25	.125	.0283	-.0391	-.2637	.0620	.0802	.175	.46	1.00	.73	.1319	.0067	-.0037	-.2771	.0156	.0003	1.231	-.0023									
	-10	31.36	.32	.0674	-.0684	-.1903	.0808	.0683	.800	3.00	3.40	3.20	.3339	.0100	.0024	-.1965	.0234	.0246	1.754	-.0737									
	-10	48.89	.60	.1397	-.1071	-.4388	-.0770	-.0403	1.125	5.40	6.85	5.63	.6277	.0436	.0106	-.3020	.0820	.0619	1.702	-.1173									
	-15	12.25	.125	.0318	-.0353	-.2112	.0862	.0810	.225	.78	1.56	1.15	.1316	.0007	.0032	-.3366	.0266	-.0042	1.571	-.1839									
	-15	31.36	.32	.0776	-.0961	-.0280	.0193	.0678	.800	3.55	4.35	3.95	.3416	.0244	.0086	-.0440	.0190	.0499	1.724	-.1372									
	-15	48.89	.60	.1285	-.0035	-.2805	.0123	.1285	.125	.40	.35	.38	.1269	.0041	.0044	-.2887	.0186	-.0284	1.807	-.2258									
	0	31.36	.32	.0683	-.0211	-.4820	.0053	.2065	.375	2.00	1.95	1.98	.3275	.0015	.0029	-.8048	.0127	.0342	1.726	-.1044									
	0	48.89	.60	.1025	-.0386	-.1400	.0035	.0175	.675	3.40	3.20	3.30	.6219	.0032	-.0012	-.1376	-.0031	-.0315	1.825	-.0615									
5	12.25	.125	.0283	0	-.2728	-.0106	.1302	.100	.60	.20	.40	.1284	.0009	-.0012	-.3001	.0219	.0806	1.656	-.2363										
5	31.36	.32	.0741	.0070	-.4648	-.0485	.3013	.325	1.80	2.26	1.45	.3285	.0006	-.0033	-.6915	.0070	.0069	1.837	-.0271										
5	48.89	.60	.1181	.0038	-.3885	-.0403	.1908	.560	3.35	3.00	3.18	.6131	.0007	-.0021	-.4313	.0079	.0058	1.679	-.0498										
10	12.25	.125	.0297	.0106	-.2693	-.0362	.1144	.075	.68	1.50	1.28	.1288	.0022	-.0023	-.2932	.0200	.0224	1.738	-.0541										
10	31.36	.32	.0846	.0898	-.6125	-.1050	.1925	.280	1.80	1.00	1.25	.3383	.0013	-.0008	-.6505	.0044	-.0061	1.834	-.0184										
10	48.89	.60	.1318	.0439	-.5585	-.1120	.2100	.800	2.60	2.05	2.33	.6189	.0023	-.0039	-.8045	-.0032	.0301	1.788	-.0580										
15	12.25	.125	.0417	.0212	-.2540	-.0563	.0880	.080	.75	1.40	1.33	.1334	.0033	-.0004	-.4824	.0173	.0045	1.900	-.0222										
15	31.36	.32	.0979	.0807	-.6335	-.1698	.2048	.200	2.40	1.78	2.06	.6287	.0039	-.0056	-.6870	.0089	.0116	1.853	-.0341										
15	48.89	.60	.1502	.0842	-.6650	-.1785	.2206	.425	1.85	.78	.87	.6283	.0018	-.0006	-.7227	.0085	.0173	1.786	-.0327										
-5	12.25	.125	.0315																										

TABLE I.- Continued
 TABULATION OF TEST DATA AND RESULTS

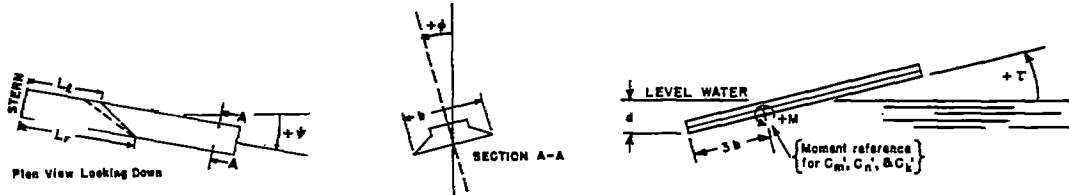
(c) $\beta = 0^\circ$; $\tau = 18^\circ$



TEST PARAMETERS		WIND AXIS										BODY AXIS													
ψ	ϕ	C_x	C_{x_b}	C_{x_b}	C_{x_b}	C_m	C_n	C_z	d/h	L_r	L_f	λ	$C_{L'}$	$C_{D'}$	$C_{Q'}$	$C_{L'}$	$C_{D'}$	$C_{Q'}$	$C_{L'}$	$C_{D'}$	$C_{Q'}$	$C_{L'}$	$C_{D'}$	$C_{Q'}$	
$C_p = 14.00$																									
0	0	12.28	.128	.0319	0	-.3168	.0123	0	.080	0.28	0.33	0.31	.1287	-.0083	0	-.3168	.0117	-.0038	1.758	-.0295					
0	0	31.36	.32	.0911	-.0071	-.7928	.0123	-.0229	.250	1.00	1.05	1.03	.3325	-.0123	-.0071	-.7928	.0046	-.0256	.595	-.0770					
0	0	48.89	.800	.1647	-.0083	-.7890	-.0133	-.0263	.576	2.05	2.05	2.05	.5433	-.0074	-.0083	-.7890	.0038	-.0288	.778	-.0860					
5	12.25	.125	.0485	.0105	-.0160	-.0141	-.0317	.0560	.40	.40	.20	.50	.1334	.0046	-.0010	-.3158	.0045	-.0258	1.110	-.1254					
5	31.36	.32	.0280	.0282	-.7834	-.0493	-.0440	.250	1.05	1.05	.90	1.00	.3325	-.0074	-.0010	-.7258	.0028	-.0266	.824	-.0784					
5	48.89	.800	.1806	.0481	-.7458	-.0680	-.0580	.550	2.28	2.18	2.20	2.28	.8238	-.0113	-.0036	-.7461	.0041	-.0287	.718	-.0758					
-10	12.28	.125	.0596	-.0247	-.2728	.0598	.0264	.050	-.40	.30	.30	.30	.1334	.0011	-.0016	-.2800	.0107	.0086	1.003	-.0495					
-10	31.36	.32	.1020	-.0535	-.6704	.1320	.0299	.350	-.95	1.28	1.10	1.318	.3418	-.0019	-.0042	-.6838	.0163	-.0124	.908	-.0363					
-10	48.89	.800	.1664	-.0971	-.6776	.1288	.0176	.656	2.18	2.40	2.28	.8328	-.0058	-.0047	-.6895	.0080	-.0230	.748	-.0432						
-18	12.25	.125	.0405	-.0385	-.4695	.0822	.0299	.050	-.80	-.80	-.80	.1361	0	-.0001	-.2287	.0164	-.0018	1.617	-.0128						
-18	31.36	.32	.1017	-.0953	-.6354	.1850	.0456	.325	1.00	1.45	1.22	.8450	-.0027	-.0022	-.6228	.0173	-.0130	.896	-.0378						
-18	48.89	.800	.1692	-.1447	-.5861	.1725	.0546	.750	2.28	2.70	2.48	.8443	-.0081	-.0040	-.6130	.0231	-.0014	.756	-.0026						
10	0	12.25	.125	.0581	-.0036	-.2992	.0068	.080	.25	.25	.25	.25	.1307	-.0024	-.0032	-.3048	.0100	.0032	1.472	-.0176					
10	0	31.36	.32	.0878	-.0285	-.6932	.0018	.1984	.250	1.08	1.03	1.08	.3324	-.0126	-.0109	-.7186	.0239	.0676	.790	-.2054					
10	0	48.89	.80	.1493	-.0282	-.7445	.0018	.1478	.850	2.00	2.00	2.00	.6225	-.0100	-.0018	-.7889	.0047	.0149	.774	-.0288					
5	12.25	.125	.0599	.0053	-.5050	-.0141	.0440	.085	.40	.20	.50	.1313	-.0021	-.0007	-.5112	.0106	-.0083	1.100	-.0404						
5	31.36	.32	.0271	.0035	-.7198	-.0581	.1816	.200	1.05	1.05	.98	.8218	-.0741	-.0191	-.7427	.0299	.0304	.828	-.0378						
5	48.89	.80	.1557	.0106	-.5380	-.0534	.1214	.625	2.10	1.95	2.03	.8226	-.0104	-.0082	-.6471	.0056	-.0046	.681	-.0093						
10	12.25	.125	.0436	.0141	-.2669	-.0352	.0264	.025	.48	0	.23	.1332	.0001	-.0017	-.2899	.0096	-.0118	1.845	-.0866						
10	31.36	.32	.1068	.0282	-.7480	-.1197	.1672	.200	1.00	.80	.80	.3382	-.0037	-.0126	-.7720	.0314	.0701	.896	-.0378						
10	48.89	.80	.1673	.0847	-.8448	-.1408	.0845	.525	1.85	1.58	1.70	.8300	-.0093	-.0093	-.8604	-.0042	-.0169	.810	-.0318						
18	12.25	.125	.0446	.0237	-.8816	-.0616	.0848	.050	.68	-.40	1.047	-.0009	-.0039	-.2891	-.0039	-.2891	-.0039	1.138	-.0280						
18	31.36	.32	.1179	.0562	-.7040	-.1848	-.1408	.228	1.00	.80	.80	.3468	-.0018	-.0121	-.7278	.0269	.0727	1.064	-.2102						
18	48.89	.80	.1769	.1041	-.8448	-.2112	.0816	.500	2.70	1.80	2.00	.8404	-.0080	-.0071	-.8722	-.0016	-.0166	.693	-.0307						
-5	12.25	.125	.0585	-.0193	-.2968	.0333	.0666	.076	.80	.40	.50	.1316	-.0018	-.0012	-.2608	.0056	.0031	1.280	-.0236						
-5	31.36	.32	.0840	-.0494	-.6072	-.0681	.1147	.325	1.10	1.20	1.15	.3343	-.0121	-.0060	-.6405	.0323	.0219	.943	-.2480						
-5	48.89	.80	.1419	-.0724	-.6824	-.0665	.1481	.680	2.20	2.30	2.25	.8247	-.0097	-.0008	-.6511	.0059	.0124	.773	-.0256						
-10	12.25	.125	.0572	-.0316	-.2883	.0598	.0783	.076	.10	.45	.28	.1342	.0014	-.0014	-.3007	.0122	.0080	.271	-.0278						
-10	31.36	.32	.0833	-.0630	-.6438	-.1091	.1155	.455	1.60	1.55	1.83	.3408	-.0072	-.0082	-.6868	.0368	.0793	.832	-.2327						
-10	48.89	.80	.1394	-.1258	-.5039	-.0950	.1558	.778	2.50	2.90	2.78	.8334	-.0058	-.0049	-.6376	.0177	.0356	.728	-.0350						
-15	12.25	.125	.0404	-.0404	-.4285	.0840	.0858	.128	.80	.70	.45	.1373	.0059	-.0039	-.2879	.0196	.0111	1.007	-.0608						
-15	31.36	.32	.0793	-.1158	-.4393	.1330	.2155	.550	1.85	2.20	2.03	.3492	-.0056	-.0102	-.4972	.0406	.0864	.778	-.2474						
-15	48.89	.80	.1370	-.1712	-.5150	.1021	.1250	.925	3.10	3.55	3.35	.6480	-.0021	-.0036	-.3511	.0283	.0335	.708	-.0614						
20	0	12.25	.125	.0662	-.0088	-.2885	.0068	.1155	.075	.40	.20	.50	.1303	-.0034	-.0041	-.2856	.0137	.0126	1.693	-.1044					
20	0	31.36	.32	.0632	-.0316	-.6863	.0018	.2780	.278	1.10	1.00	1.05	.3318	-.0143	-.0012	-.7101	.0116	.0299	.819	-.0901					
20	0	48.89	.80	.1377	-.0494	-.7216	-.0018	.6062	.850	2.10	2.00	2.05	.8207	-.0154	-.0007	-.7022	.0109	.0396	.780	-.0769					
5	12.25	.125	.0386	0	-.2200	-.0140	.0840	.078	.65	-.85	-.85	.1306	-.0041	-.0018	-.2823	.0070	-.0117	1.038	-.0684						
5	31.36	.32	.0941	-.0018	-.7018	-.0613	.4573	.288	1.00	.80	.80	.3333	-.0142	-.0015	-.7497	.0078	.0206	.824	-.0416						
5	48.89	.80	.1538	-.0035	-.6290	-.0787	.5115	.475	1.80	1.80	1.70	.8228	-.0161	-.0037	-.4882	.0083	.0261	.765	-.0814						
10	12.25	.125	.0438	.0035	-.5150	-.0380	.0875	.080	.45	-.50	.50	.1325	-.0008	-.0048	-.2881	.0181	-.0134	1.747	-.1011						
10	31.36	.32	.1057	.0193	-.7280	-.1190	.2205	.200	1.20	.80	1.00	-.3374	.0107	-.0044	-.7499	.0277	-.0030	.718	-.0089						
10	48.89	.80	.1705	.0282	-.8240	-.1637	.2974	.400	1.82	1.47	1.65	.8289	-.0113	-.0071	-.8963	.0040	.0119	.890	-.0322						
18	12.25	.125	.0443	.0156	-.2783	-.0395	.0788	.050	.80	-.80	.80	.1384	-.0042	-.0047	-.2960	.0187	-.0017	1.979	-.0127						
18	31.36	.32	.1204	.0474	-.7178	-.1855	.2083	.200	.80	.30	.85	-.8461	-.0047	-.0037	-.7697	.0077	.0101	1.450	-.0393						
18	48.89	.80	.1881	.0653	-.9874	-.2562	.2662	.350	1.70	1.80	1.45	.6380	-.0077	-.0140	-.10812	-.0009	-.0143	.721	-.0266						
-5	12.25	.125	.0244	-.0246	-.2800	.0315	.100	.25	.40	.45	.33	.1320	.0001	-.0002	-.2787	-.0144	-.0737	1.803	-.5606						
-5	31.36	.32	-.0622	-.0632	-.6790	.0328	.2625	.400	1.50	1.40	1.35	.3364	-.0045	-.0019	-.7896	-.0043	-.0025	.616	-.0074						
-5	48.89	.80	.1348	-.0993	-.4224	.0610	.2898	.728	2.40	2.40	2.40	.8265	-.0030	-.0025	-.8014	.0041	.1048	.823	-.1991						
-10	12.25	.125	.0340	-.0333	-.2278	.0543	.1243	.150	.40	.80	.80	.1337	.0025	-.0036											

TABLE I.- Continued
 TABULATION OF TEST DATA AND RESULTS

(a) $\beta = 0^\circ$; $\tau = 24^\circ$



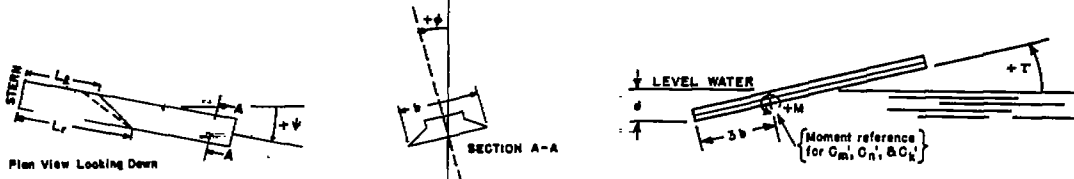
$C_L = 14.00$

TEST PARAMETERS		WIND AXIS							BODY AXIS																						
ψ	ϕ	C_{L_1}	C_{D_1}	$C_{C_{D_1}}$	C_{m_1}	C_{n_1}	C_{k_1}	d/b	L_T	L_2	λ	C_{L_1}'	C_{D_1}'	$C_{C_{D_1}}'$	C_{m_1}'	C_{n_1}'	C_{k_1}'	C_{L_2}'	C_{D_2}'	$C_{C_{D_2}}'$	C_{m_2}'	C_{n_2}'	C_{k_2}'	C_{L_3}'	C_{D_3}'	$C_{C_{D_3}}'$	C_{m_3}'	C_{n_3}'	C_{k_3}'		
0	0	12.25	.125	.0491	-.0035	-.3508	.0070	-.0141	.075	0.20	0.20	1.542	-.0080	-.0035	-.3508	-.0007	-.0157	1.555	-.1170												
0	0	31.35	.32	.1341	-.0035	-.3453	.0105	-.0245	.100	.70	.68	.3480	-.0077	-.0035	-.3453	-.0004	-.0287	.327	-.0770												
0	5	48.89	.50	.2065	-.0063	-1.1085	.0105	-.0352	.425	1.35	1.35	.6408	-.0147	-.0063	-1.1085	-.0046	-.0255	.704	-.0475												
5	5	12.25	.125	.0512	-.0071	-.3274	-.0106	-.0405	.075	.25	.10	.18	.1551	-.0041	-.0047	-.2254	-.0025	-.0227	3.121	-.2420											
5	5	31.35	.32	.1260	-.0098	-.3610	-.0012	-.0520	.250	.75	.80	.68	.3449	-.0121	-.0005	-.3594	-.0035	-.0225	.725	-.0245											
5	5	48.89	.50	.2076	-.0408	-1.1085	-.0757	-.0845	.450	1.40	1.30	1.35	.6427	-.0137	-.0087	-1.1155	-.0055	-.0454	.959	-.0722											
-10	10	12.25	.125	.0544	-.0028	-.3290	.0095	-.0345	.075	0	.45	.18	.1582	-.0011	-.0015	-.3553	-.0025	-.0215	3.189	-.0074											
-10	10	31.35	.32	.1450	-.0067	-.3955	-.1415	-.0253	.175	.80	.80	.70	.3475	-.0023	-.0047	-.3501	-.0024	-.0275	1.035	-.0752											
-10	10	48.89	.50	.2111	-.0085	-1.0472	.1795	-.0615	.475	1.35	1.80	1.45	.6515	-.0105	-.0031	-1.0541	-.0043	-.0157	.724	-.0503											
-15	15	12.25	.125	.0600	-.0051	-.3153	.0875	-.0315	.100	0	.45	.23	.1450	-.0040	-.0020	-.3245	-.0055	-.0045	3.113	-.0475											
-15	15	31.35	.32	.1374	-.0080	-.3015	.2045	-.1065	.300	.80	1.00	.80	.3505	-.0045	-.0003	-.3359	-.0122	-.0143	.859	-.0397											
-15	15	48.89	.50	.2118	-.1515	-1.0032	.2592	-.1054	.350	1.80	1.80	1.70	.5837	-.0095	-.0061	-1.0405	-.0070	-.0073	.675	-.0120											
10	0	12.25	.125	.0455	-.0105	-.3500	.0085	-.0225	.075	.20	.20	.20	.1332	-.0062	-.0024	-.3535	-.0044	-.0120	1.720	-.0900											
10	0	31.35	.32	.1274	-.0045	-.3925	.0015	-.1275	.350	.70	.70	.70	.3452	-.0021	-.0025	-.3505	-.0025	-.0115	.951	-.0355											
10	0	48.89	.50	.2012	-.0405	-1.0947	0	-.0255	.450	1.40	1.35	1.35	.6425	-.0109	-.0050	-1.1135	-.0055	-.0115	.650	-.0215											
5	12.25	.125	.0357	.0035	-.3055	-.0140	.0455	.075	.30	.20	.25	.1554	-.0031	-.0009	-.3095	-.0104	-.0055	2.920	-.0257												
5	5	31.35	.32	.1274	0	-.3550	-.0715	-.0955	.350	.80	.80	.70	.3445	-.0155	-.0075	-.3454	-.0132	-.0132	1.114	-.0119											
5	5	48.89	.50	.2079	.0071	-1.1245	-.0845	-.1405	.425	1.35	1.30	1.25	.6425	-.0175	-.0041	-1.1354	-.0003	-.0174	.707	-.0321											
10	12.25	.125	.0441	.0140	-.3290	-.0332	.0140	.050	.40	.40	.20	.1415	-.0047	-.0004	-.3295	-.0055	-.0055	3.345	-.1845												
10	10	31.35	.32	.1455	.0252	-.3190	-.1245	-.0455	.225	.80	.80	.70	.3531	-.0055	-.0102	-.3455	-.0099	-.0400	.924	-.1133											
10	10	48.89	.50	.2195	.0454	-1.1194	-.1790	-.0845	.450	1.40	1.20	1.30	.6494	-.0155	-.0025	-1.1355	-.0054	-.0500	.717	-.0545											
15	12.25	.125	.0705	.0221	-.2115	-.0555	0	.050	.45	.40	.40	.23	.1465	-.0085	-.0022	-.3177	-.0005	-.0224	3.622	-.1525											
15	15	31.35	.32	.1322	.0737	-.3555	-.1890	-.0210	.225	.85	.85	.60	.73	.3519	-.0047	-.0054	-.3580	-.0043	-.0417	.755	-.1152										
15	15	48.89	.50	.2344	.0935	-1.0550	-.2522	-.0634	.375	1.40	1.15	1.25	.6515	-.0075	-.0109	-1.0957	-.0052	-.0049	.815	-.0087											
-5	12.25	.125	.0355	-.0123	-.3190	.0280	.0645	.075	.20	.40	.30	.1295	-.0161	-.0055	-.3220	-.0131	-.0237	1.557	-.1524												
-5	5	31.35	.32	.1285	-.0544	-.3050	.0893	-.1400	.300	.80	.80	.80	.3495	-.0059	-.0005	-.3495	-.0090	-.0225	.823	-.0243											
-5	5	48.89	.50	.1935	-.0547	-1.0173	.0952	-.2334	.475	1.40	1.45	1.45	.6454	-.0102	-.0012	-1.0477	-.0115	-.0157	.757	-.0287											
-10	12.25	.125	.0515	-.0359	-.3195	.0680	-.0925	.100	.20	.40	.30	.1332	-.0153	-.0075	-.3470	-.0054	-.0133	1.557	-.0575												
-10	10	31.35	.32	.1295	-.0642	-.3515	-.1225	-.1545	.300	.80	1.00	.90	.3525	-.0012	-.0010	-.3525	-.0057	-.0214	.858	-.0714											
-10	10	48.89	.50	.1917	-.1324	-.3147	.1565	-.2505	.575	1.60	1.70	1.60	.6525	-.0065	-.0015	-.3573	-.0124	-.0250	.775	-.0470											
-15	12.25	.125	.0457	-.0475	-.3555	.0925	-.1105	.125	.15	.50	.33	.1420	-.0081	-.0025	-.3377	-.0023	-.0123	1.829	-.0908												
-15	15	31.35	.32	.1278	-.1155	-.3525	.1820	-.2275	.375	1.00	1.20	1.10	.3543	-.0032	-.0023	-.3415	-.0192	-.0224	.877	-.0315											
-15	15	48.89	.50	.1889	-.1535	-.3043	.2077	-.2235	.700	1.80	2.10	1.95	.6423	-.0043	-.0018	-.3507	-.0015	-.0254	.785	-.0165											
0	12.25	.125	.0459	-.0177	-.3454	.0063	.1355	.075	.25	.20	.23	.1345	-.0051	-.0005	-.3454	-.0117	-.0254	2.543	-.1502												
0	5	31.35	.32	.1295	-.0459	-.3550	-.0015	-.2555	.150	.80	.65	.65	.3525	-.0054	-.0004	-.3525	-.0054	-.0005	.807	-.0014											
0	5	48.89	.50	.1935	-.0724	-1.0205	-.0070	-.3990	.455	1.40	1.45	1.40	.6409	-.0144	-.0015	-1.0947	-.0030	-.0539	.683	-.0442											
5	12.25	.125	.0540	-.0035	-.3520	-.0135	.1105	.075	.30	.20	.15	.1351	-.0034	-.0003	-.3520	-.0112	-.0084	1.920	-.0617												
5	5	31.35	.32	.1354	-.0123	-.3015	-.0545	.2455	.225	.80	.60	.70	.3457	-.0115	-.0035	-.3457	-.0024	-.0105	.819	-.0312											
5	5	48.89	.50	.2090	-.0229	-1.0580	-.0933	-.3731	.400	1.35	1.15	1.25	.6422	-.0155	-.0027	-1.1255	-.0054	-.0253	.742	-.0522											
10	12.25	.125	.0741	.0071	-.2155	-.0370	.0845	.075	.40	--	.80	.1445	-.0105	-.0070	-.3495	-.0121	-.0114	2.417	-.0787												
10	10	31.35	.32	.1295	-.0459	-.3550	-.0015	-.2555	.150	.80	.65	.65	.3525	-.0054	-.0004	-.3525	-.0054	-.0005	.807	-.0014											
10	10	48.89	.50	.2227	.0105	-1.1405	-.1535	-.3414	.150	1.35	1.05	1.20	.6472	-.0155	-.0090	-1.2052	-.0022	-.0133	.645	-.0543											
15	12.25	.125	.0770	.0105	-.3045	-.0634	.0880	.080	.40	--	.30	.1457	-.0120	-.0017	-.3229	-.0175	-.0052	2.453	-.0354												
15	15	31.35	.32	.1324	.0585	-.3184	-.1915	-.1813	.175	.80	.40	.80	.3509	-.0029	-.0015	-.3595	-.0025	-.0221	1.050	-.0312											
15	15	48.89	.50	.2457	.0582	-1.1722	-.3734	-.2575	.300	1.20	.80	1.00	.6505	-.0095	-.0052	-1.2352	-.0001	-.0211	.795	-.0375											
-5	12.25	.125	.0455	-.0229	-.3539	-.0545	.1584	.100	.20	.30	.25	.1353	-.0037	-.0022	-.3255	-.0059	-.0254	2.340	-.4911												
-5	5	31.35	.32	.1211	-.0705	-.3710	-.0581	-.3184	.325	1.00	1.00	1.00	.3493	-.0041	-.0055	-.3705	-.0055	-.0275	.725	-.2104											
-5	5	48.89	.50	.1950	-.1135	-.3755	-.0704	-.4205	.575	1.40	1.80	1.40	.6480	-.0075	-.0035	-.3725	-.0154	-.0554	.751	-.1073											
-10	12.25	.125	.0522	-.0459	-.3515	.0615	.1554	.125	.30	.40	.30	.1																			

TABLE I.- Continued

TABULATION OF TEST DATA AND RESULTS

(e) $\beta = 0^\circ$; $\tau = 30^\circ$

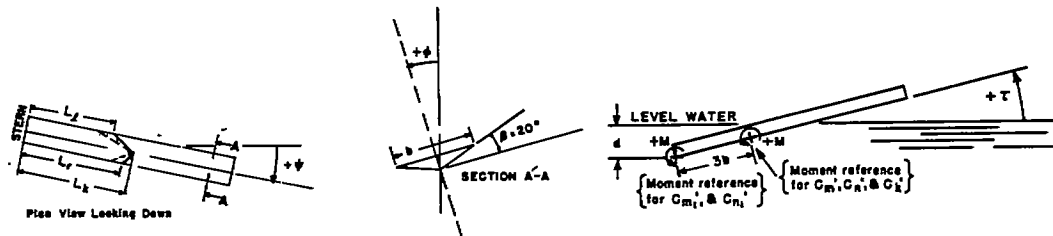


$C_v = 16.00$

TEST PARAMETERS			WIND AXIS							BODY AXIS													
ψ	ϕ	C_a	C_{L_0}	C_{D_0}	C_{L_1}	C_{D_1}	C_{L_2}	C_{D_2}	C_m	C_n	C_x	d/b	L_r	L_z	λ	C_{L_1}'	C_{D_1}'	C_{L_2}'	C_{D_2}'	C_m'	C_n'	C_x'	C_y'
0	0	17.61	.18	.0903	-.0035	-.5717	.0169	-.0089	.100	0.20	0.30	0.28	.0010	-.0118	-.0035	-.5717	.0093	-.0187	.624	-.0781			
0	0	31.36	.32	.1819	-.0036	-.9449	.0189	-.0233	.178	.80	.60	.60	.0010	-.0198	-.0036	-.9499	.0021	-.0281	.712	-.0788			
0	0	46.89	.50	.2680	-.0071	-1.3182	.0035	.0211	.400	1.00	1.00	1.00	.0020	-.0266	-.0071	-1.3318	.0109	.0165	.986	.0284			
5	17.61	.18	.0987	.0189	-.0811	-.0405	.100	.30	.20	.28	.28	.28	.0044	-.0071	-.0019	-.4603	.0088	-.0456	2.082	-.2231			
5	46.89	.50	.2680	.0456	-1.3283	-.0888	-.1103	.378	1.08	1.00	1.05	.8588	-.0266	-.0038	-1.3245	-.0158	-.1394	.632	-.2458				
-10	17.61	.18	.0999	-.0588	-.5333	-.0480	.0178	.100	.40	.40	.30	.8088	-.0035	-.0026	-.8400	-.0099	-.0288	1.410	-.1376				
-10	31.36	.32	.1768	-.0712	-.6987	.1442	.0889	.200	.40	.65	.85	.8717	-.0080	-.0068	-.9127	-.0007	-.0150	1.028	-.0404				
-10	46.89	.50	.2727	-.1053	-1.2723	.0330	.0948	.425	1.00	1.15	1.08	.6790	-.0138	-.0048	-1.2917	-.0013	-.0187	.712	-.0340				
-18	17.61	.18	.1028	-.0647	-.8061	.1232	.0616	.126	.10	.40	.25	.8149	-.0001	.0009	-.8235	.0021	-.0083	2.256	-.0568				
-18	31.36	.32	.1720	-.1189	-.9169	.0089	.0974	.225	.40	.80	.60	.8810	-.0110	-.0188	-.9451	-.0155	-.0201	.668	-.0228				
-18	46.89	.50	.2878	-.1890	-1.1690	.2888	.1805	.478	1.05	1.38	1.20	.6883	-.0183	-.0059	-1.2134	.0117	-.0141	.781	-.0240				
0	17.61	.18	.0972	-.0177	-.5850	.0070	.0704	.100	.40	.40	.20	.8094	-.0130	-.0023	-.8391	-.0087	-.0839	1.060	-.1193				
0	31.36	.32	.1899	-.0371	-.8293	0	-.1284	.200	.88	.88	.88	.8891	-.0180	-.0088	-.9427	-.0027	-.0077	.861	-.0214				
0	46.89	.50	.2824	-.0389	-1.2793	-.0035	.1170	.378	1.18	1.10	1.15	.8907	-.0289	-.0085	-1.2976	-.0085	-.0078	.607	-.0010				
5	17.61	.18	.0925	-.0088	-.8466	-.0817	.0887	.075	.50	.10	.40	.8021	-.0098	-.0105	-.8466	-.0021	-.0332	1.470	-.1643				
5	31.36	.32	.1803	0	-.9328	-.0598	.1074	.200	.80	.40	.45	.8871	-.0233	-.0024	-.9407	-.0024	-.0188	.818	-.0526				
5	46.89	.50	.2616	-.0018	-1.1688	-.0945	.1840	.278	1.00	1.00	1.00	.8638	-.0248	-.0058	-1.1708	-.0044	-.0046	.923	-.0082				
10	17.61	.18	.0966	-.0088	-.8129	-.0886	.0317	.078	.88	.10	.25	.8080	-.0073	-.0100	-.8192	.0018	-.0180	2.030	-.0780				
10	31.36	.32	.1726	-.0338	-.9604	-.1250	.0681	.175	.60	.40	.30	.8647	-.0178	-.0004	-.8599	.0046	-.0309	.734	-.0647				
10	46.89	.50	.2661	-.0481	-1.3213	-.1906	.0823	.378	1.10	1.00	1.05	.8677	-.0304	-.0041	-1.3371	-.0076	-.0381	.814	-.0683				
15	17.61	.18	.1048	-.0318	-.8182	-.1038	.0083	.075	.40	0	.20	.8106	-.0054	-.0062	-.8222	.0065	-.0206	1.800	-.0978				
15	31.36	.32	.1832	-.0600	-.9263	-.1984	.0088	.178	.78	.40	.60	.8733	-.0128	-.0028	-.9659	.0013	-.0356	.787	-.0934				
15	46.89	.50	.2887	-.0948	-1.3125	-.2818	.0281	.378	1.20	1.00	1.10	.8832	-.0206	-.0028	-1.3423	.0034	-.0325	.635	-.0587				
8	17.61	.18	.0900	-.0383	-.8446	.0405	.1182	.100	.18	.20	.18	.8042	-.0079	-.0015	-.8096	.0049	-.0046	1.150	-.0220				
-8	31.36	.32	.1853	-.0629	-.8869	.0704	.1848	.225	.70	.60	.65	.8608	-.0180	-.0041	-.8882	-.0008	-.0078	.828	-.0216				
-8	46.89	.50	.2457	-.1053	-1.1988	.0988	.2485	.400	1.10	1.25	1.23	.8683	-.0248	-.0117	-1.2277	-.0084	-.0148	.876	-.0261				
-10	17.61	.18	.0893	-.0600	-.8460	.0810	.1390	.125	.80	.40	.30	.8095	-.0048	-.0073	-.8100	.0021	-.0083	1.887	-.0283				
-10	31.36	.32	.1689	-.1009	-.8319	.1328	.2443	.280	.60	.78	.68	.8710	-.0093	-.0076	-.8769	.0110	-.0188	.935	-.0456				
-10	46.89	.50	.2464	-.1447	-1.1200	.1760	.3115	.328	1.15	1.25	1.20	.8766	-.0181	-.0003	-1.1787	.0046	-.0092	.790	-.0610				
-18	17.61	.18	.0858	-.0777	-.8465	.1179	.1707	.160	.38	.55	.48	.8138	-.0061	-.0085	-.8083	.0148	-.0158	1.384	-.0786				
-18	31.36	.32	.1822	-.1341	-.7744	.2005	.2788	.225	.60	.90	.78	.8780	-.0047	-.0080	-.8447	.0290	-.0189	1.006	-.0422				
-18	46.89	.50	.2478	-.2067	-1.0500	.2834	.3678	.878	1.80	1.00	1.45	.8943	-.0079	-.0049	-1.1408	.0148	-.0288	.748	-.0488				
0	17.61	.18	.0816	-.0388	-.8405	.0018	.1742	.100	.58	.20	.28	.8008	-.0122	-.0086	-.8111	.0012	-.0018	1.825	-.0075				
0	31.36	.32	.1846	-.0547	-.8378	0	.2821	.200	.60	.80	.60	.8591	-.0180	-.0015	-.8974	.0021	-.0140	.858	-.0360				
0	46.89	.50	.2422	-.0918	-1.1616	-.0070	.4282	.450	1.10	1.08	1.08	.8628	-.0287	-.0034	-1.2414	.0012	-.0180	.754	-.0264				
5	17.61	.18	.0821	-.0212	-.8480	-.0817	.1795	.075	.35	.20	.28	.8196	-.0145	-.0082	-.8168	.0192	-.0188	1.467	-.0032				
5	31.36	.32	.1689	-.0318	-.8800	-.0634	.2888	.200	.60	.60	.55	.8880	-.0213	-.0068	-.9282	.0112	-.0089	.740	-.0026				
5	46.89	.50	.2603	-.0318	-1.2330	-.1003	.3781	.378	1.05	1.00	1.03	.8688	-.0389	.0071	-1.2911	-.0098	-.0111	.670	-.0199				
10	17.61	.18	.0946	-.0106	-.8069	-.0681	.1867	.078	.40	0	.40	.8080	-.0099	-.0151	-.8253	.0080	-.0148	2.085	-.0714				
10	31.36	.32	.1854	-.0019	-.9064	-.1258	.2270	.178	.68	.40	.58	.8894	-.0288	-.0041	-.8498	-.0008	-.0189	.704	-.0470				
10	46.89	.50	.2602	-.0018	-1.2901	.1866	.3344	.350	1.05	.88	.85	.8823	-.0388	-.0071	-1.3458	.0087	-.0187	.859	-.0297				
15	17.61	.18	.0648	-.0212	-.8280	-.0915	.1128	.080	.40	0	.20	.8187	-.0316	-.0047	-.8466	.0287	-.0193	.185	-.0161				
15	31.36	.32	.1878	-.0355	-.9152	-.2006	.1848	.180	.70	.40	.65	.8722	-.0171	-.0006	-.9548	.0028	-.0204	.794	-.0548				
15	46.89	.50	.2858	-.0441	-1.2672	-.1884	.2693	.278	1.08	.80	.94	.8785	-.0324	-.0109	-1.2996	.1066	-.0758	.789	-.1277				
-8	17.61	.18	.0833	-.0689	-.8488	.0387	.2024	.125	.30	.30	.30	.8021	-.0065	.0067	-.8001	.0071	.0490	1.813	-.2877				
-8	31.36	.32	.1478	-.0883	-.7832	-.0384	.2643	.200	.90	.70	.60	.8432	-.0135	-.0007	-.8603	.0166	.0928	.981	-.2649				
-8	46.89	.50	.2418	-.1412	-1.0736	-.1003	.3139	.560	1.20	1.20	1.20	.8728	-.0117	-.0002	-1.1778	-.1321	.1604	.787	-.2826				
-10	17.61	.18	.0776	-.0777	-.8777	.0810	.2283	.178	.40	.60	.48	.8106	-.0041	-.0108	-.8489	.0213	.0972	1.498	-.4018				
-10	31.36	.32	.1383	-.1200	-.7869	.1302	.2837	.160	.78	.80	.78	.8685	-.0119	-.0015	-.8312	.0248	.1681	.963	-.4389				
-10	46.89	.50	.2259	-.1783	-.9968	.1614	.3204	.680	1.40	1.58	1.48	.8767	-.0134	.0100	-1.1292	.0046	.1958	.704	-.3395				
-15	17.61	.18	.0784	-.0847	-.8907	.1279	.2808	.200	.40	.60	.60	.8180	-.0062	.0004	-.8816	.346	.1852	1.486	-.7321				
-15	31.36	.32	.1359	-.1518	-.8829	.1798	.4083	.428	1.00	1.10	1.06	.8793	-.0064	.0021	-.8744	.0204	.2198	.812	-.5798				
-15	46.89	.50	.2090	-.2456	-.8448	.2182	.6129	.778	1.88	1.80	1.88	.8941	-.0078	-.0036	-1.0106	.0255	.2771	.691	-.4664				

TABLE I.- Continued
 TABULATION OF TEST DATA AND RESULTS

(f) $\beta = 20^\circ$; $\tau = 6^\circ$

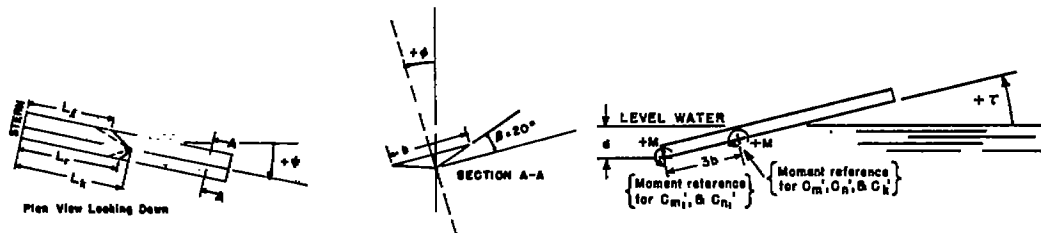


TEST PARAMETERS			WIND AXIS										BODY AXIS														
ψ	ϕ	C_L	$C_{L\alpha}$	C_{D0}	$C_{D\alpha}$	$C_{D\beta}$	$C_{D\tau}$	$C_{D\beta\tau}$	$C_{D\beta\beta}$	$C_{D\tau\tau}$	$C_{D\beta\tau\beta}$	$C_{D\beta\tau\tau}$	$C_{D\beta\beta\tau}$	$C_{D\beta\tau\beta\tau}$	$C_{D\beta\beta\tau\beta}$	$C_{D\beta\tau\beta\tau\beta}$	$C_{D\beta\beta\tau\beta\tau}$	$C_{D\beta\tau\beta\tau\beta\tau}$	$C_{D\beta\beta\tau\beta\tau\beta}$	$C_{D\beta\tau\beta\tau\beta\tau\beta}$	$C_{D\beta\beta\tau\beta\tau\beta\tau}$	$C_{D\beta\tau\beta\tau\beta\tau\beta\tau}$	$C_{D\beta\beta\tau\beta\tau\beta\tau\beta}$	$C_{D\beta\tau\beta\tau\beta\tau\beta\tau\beta}$	$C_{D\beta\beta\tau\beta\tau\beta\tau\beta\tau}$		
$C_v = 7.10$																											
0	0	6.18	.246	.0368	0	.2694	0	0	.725	4.23	6.23	7.20	6.74	.2475	-.0107	0	.2896	0	0	1.0121	0						
15	15		.245	.0367	.0411	.2074	-.0472	0	.773	7.16	5.95	7.40	6.78	.2517	-.0308	-.0243	.2096	-.0337	-.0050	1.0647	-.1064						
10	15		.245	.0365	-.0445	.2734	-.0274	.0242	.828	6.40	7.35	7.80	7.38	.2558	-.0336	.0117	.2704	-.0479	-.0389	1.0372	.0830						
20	15		.245	.0312	.0422	0	-.0274	.0684	.875	4.60	3.40	4.80	4.48	.2423	-.0103	.0227	-.0167	-.0165	.0639	.7702	.0515						
10	15		.245	.0444	.0822	.0342	-.0137	.0542	.873	4.85	3.80	5.10	4.71	.2497	-.0121	.0289	-.0174	-.0140	.0450	.7995	.0637						
$C_v = 10.00$																											
0	0	12.25	.245	.0400	-.0138	.6544	-.0173	-.0245	--	7.60	7.50	6.80	6.00	.2478	-.0142	-.0139	.2548	-.0134	-.0261	1.2788	-.0278						
15	15		.248	.0262	.0449	.6024	-.0346	0	1.47	4.70	7.35	6.85	6.41	.2526	-.0223	-.0211	.2081	-.0435	-.0101	1.3859	-.1271						
10	15		.245	.0475	-.0854	.2314	.0279	.0178	.828	5.75	4.50	5.00	5.56	.2454	-.0289	.0291	.2288	-.0269	-.0548	1.0280	.0584						
20	15		.245	.0873	.1220	.1208	-.0273	-.0345	.800	5.24	4.10	5.60	5.09	.2721	-.0098	.0597	.1848	-.0171	-.0167	.8411	.1820						
10	15		.245	.0987	.1277	-.0173	-.1035	-.0845	.450	4.10	3.0	4.40	3.98	.2501	-.0232	.0841	-.0162	-.1117	-.0787	.8821	.1403						
20	15		.245	.0867	.1380	-.0245	-.1206	-.1035	.450	3.95	2.80	4.20	3.79	.2501	-.0285	.0899	-.0312	-.1278	-.0588	.8091	.1619						
$C_v = 11.70$																											
0	0	12.25	.180	.0471	0	.2587	.0061	0	.780	6.85	5.90	6.20	6.39	.1424	.0227	0	.2657	.0051	-.0025	.7971	.0051						
10	15		.180	.0437	.0	.2506	.0263	.450	3.85	2.90	4.15	3.69	1.943	.0130	.0205	-.0389	.0645	.0108	.0460	.1208							
20	15		.180	.0894	.0889	-.1771	-.1514	.1012	--	2.70	1.60	3.0	2.69	.2073	-.0545	-.0854	-.0903	.0502	.5914	.3969							
$C_v = 12.20$																											
10	15	18.20	.245	.0545	.0833	.1617	.0231	.0116	--	6.10	4.80	6.40	5.93	.2431	.0134	.0245	.1589	-.0145	.0369	.8482	.0590						
20	15		.245	.0908	.1222	-.0247	-.0936	.0924	.425	4.00	2.90	4.20	3.83	.2794	-.0140	-.0888	-.0866	-.0718	.0849	.7332	.1662						
$C_v = 14.00$																											
0	0	12.25	.128	.0198	0	-.0178	.0140	-.0088	.450	2.90	3.00	4.00	3.48	.1264	.0064	0	-.0175	.0130	-.0102	.3617	.0130						
15	15		.128	.0185	0	-.2112	.0088	0	.400	2.60	2.50	3.40	2.98	.1283	.0053	0	-.2112	.0068	-.0009	1.1777	.0068						
10	15		.128	.0228	.0178	.0525	0	-.0175	.40	4.20	3.00	4.00	4.36	.1270	.0108	-.0159	.0502	-.0164	0	.4313	-.0631						
15	15		.128	.0189	.0177	-.0294	-.0089	-.0176	.45	3.65	2.40	4.00	3.51	.1268	.0087	-.0186	-.0282	-.0034	-.0156	1.1501	-.0502						
10	0	12.25	.128	.0326	-.0226	.0613	.0178	.0178	.55	3.40	4.70	5.00	4.83	.1233	.0184	.0110	.0845	.0245	.0188	.4421	.0878						
15	15		.128	.0237	-.0247	.0088	-.0248	.0088	.45	2.80	4.00	4.20	3.78	.1289	.0105	.0090	.0015	.0268	.0047	.3886	.0358						
20	15		.128	.0372	.0404	.1225	.0158	.0140	.65	4.60	4.90	5.60	5.05	.1274	.0164	.0463	.1182	.0134	.0332	.8004	.1583						
10	0	12.25	.125	.0314	.0388	.0528	-.0141	.0440	.56	3.60	3.60	4.60	4.10	.1269	.0110	.0437	.0444	-.0085	.0337	.4251	.1226						
15	15		.125	.0287	.0404	-.1463	-.0785	.0350	.30	2.10	.98	2.40	1.98	.1274	.0061	.0463	.1182	.0194	.0154	.2172	.0028						
10	15		.125	.0247	.0389	-.1672	-.0704	.0362	.20	1.90	1.80	2.10	1.80	.1283	.0044	.0437	.0444	-.0085	.0130	.2158	.0025						
20	15		.125	.0274	.0441	.3280	.0175	.0264	.70	5.50	5.90	6.15	5.88	.1123	.0561	.0692	.8089	.0607	.0635	.0438	.3483						
10	0	17.60	.125	.0396	.0579	-.1908	-.1228	.0963	--	1.50	.30	1.70	1.20	.1292	.0033	.0327	-.2309	-.0022	.0379	.1217	.0379						
15	15		.125	.0396	.0618	-.1948	-.1320	.0988	.15	1.65	1.00	1.80	1.64	.1402	.0028	.0385	-.2330	-.0705	.0414	.1978	.0380						
20	15		.125	.0189	-.0106	.2124	.0177	0	--	6.20	5.20	6.18	5.68	.1807	-.0030	-.0106	.3124	.0176	-.0019	.7845	-.0142						
10	0	17.60	.120	.0333	.0070	.1928	.0178	-.0088	.70	5.35	6.00	6.18	5.68	.1824	.0145	-.0089	.1832	-.0004	-.0108	.7434	-.0271						
15	15		.120	.0381	.0140	.2276	.0263	.0053	.70	5.85	6.15	6.40	5.98	.1828	.0181	-.0179	.2887	-.0132	.0025	.7756	-.0669						
20	15		.120	.0400	.0289	.2975	.0350	-.0133	.75	6.50	6.50	6.80	6.43	.1947	.0210	-.0186	.2960	-.0448	-.0066	.8501	-.1004						
10	0	17.60	.120	.0899	-.0139	.2124	.0177	0	.75	5.20	6.20	6.18	5.68	.1827	.0109	.0020	.2101	.0281	-.0019	.7822	.0221						
15	15		.120	.0382	-.0316	.2638	-.0088	.0088	.80	5.60	6.20	6.70	6.25	.1858	.0172	.0006	.2854	.0364	.0097	.8078	.0382						
20	15		.120	.0152	-.0389	.3415	-.0263	.0225	.75	5.78	6.00	6.25	6.06	.1878	.0321	.0121	.3388	.0684	.0199	.8986	.1017						
10	0	17.60	.120	.0392	.0228	.2266	.0284	.0098	--	5.88	5.85	6.60	6.06	.1828	.0176	.0274	.2261	.0293	.0358	.7765	.1116						
15	15		.120	.0406	.0477	.0264	-.0123	0	.55	4.55	3.30	4.40	4.36	.1947	.0568	.0045	.0223	-.0184	.0058	.8094	-.0058						
20	15		.120	.0547	.0600	.4782	.1144	.0086	.85	7.80	7.80	8.30	7.70	.1854	.0244	.0086	.4563	.1233	.0797	1.0178	.3281						
10	0	17.60	.120	.0448	.0565	-.0284	-.0317	.0440	.50	5.90	3.10	4.40	3.96	.1908	.0183	.0307	-.0579	-.0212	.0418	.8545	.0769						
15	15		.120	.0311	.0871	-.0988	-.0651	-.0382	.40	3.30	2.20	3.60	3.18	.1832	.0001	.0222	-.1143	-.0345	.0248	.6652	.0321						
20	15		.120	.0805	.0741	-.1848	-.1144	.0792	.378	2.80	1.30	2.90	2.43	.1864	.0394	.0414	-.2209	-.1472	.0245	.8785	-.0330						
10	0	24.0	.120	.0766	.1130	.0352	-.0848	.0792	.475	3.68	3.20	4.40	3.96	.2027	.0143	.0297	-.0071	-.0749	.0948	.8010	.2212						
15	15		.120	.0581	.0214	-.1178	-.0865	.0860	--	2.40	1.00																

TABLE I.- Continued

TABULATION OF TEST DATA AND RESULTS

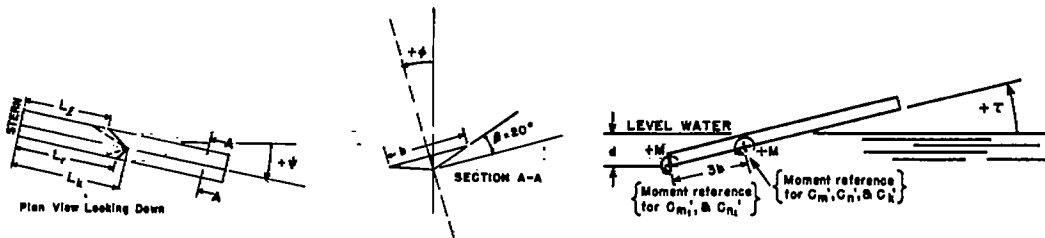
(g) $\beta = 20^\circ$; $\tau = 12^\circ$



TEST PARAMETERS			WIND AXIS						BODY AXIS																																																																																																																																																																																																																																																																																																									
ψ	ϕ	C_a	C_{L_0}	C_{D_0}	C_{C_0}	C_m	C_n	C_x	C_y	C_z	C_{L_1}	C_{L_2}	C_{L_3}	C_{L_4}	C_{L_5}	C_{L_6}	C_{L_7}	C_{L_8}	C_{L_9}	$C_{L_{10}}$	$C_{L_{11}}$	$C_{L_{12}}$	$C_{L_{13}}$	$C_{L_{14}}$	$C_{L_{15}}$	$C_{L_{16}}$	$C_{L_{17}}$	$C_{L_{18}}$	$C_{L_{19}}$	$C_{L_{20}}$	$C_{L_{21}}$	$C_{L_{22}}$	$C_{L_{23}}$	$C_{L_{24}}$	$C_{L_{25}}$	$C_{L_{26}}$	$C_{L_{27}}$	$C_{L_{28}}$	$C_{L_{29}}$	$C_{L_{30}}$	$C_{L_{31}}$	$C_{L_{32}}$	$C_{L_{33}}$	$C_{L_{34}}$	$C_{L_{35}}$	$C_{L_{36}}$	$C_{L_{37}}$	$C_{L_{38}}$	$C_{L_{39}}$	$C_{L_{40}}$	$C_{L_{41}}$	$C_{L_{42}}$	$C_{L_{43}}$	$C_{L_{44}}$	$C_{L_{45}}$	$C_{L_{46}}$	$C_{L_{47}}$	$C_{L_{48}}$	$C_{L_{49}}$	$C_{L_{50}}$	$C_{L_{51}}$	$C_{L_{52}}$	$C_{L_{53}}$	$C_{L_{54}}$	$C_{L_{55}}$	$C_{L_{56}}$	$C_{L_{57}}$	$C_{L_{58}}$	$C_{L_{59}}$	$C_{L_{60}}$	$C_{L_{61}}$	$C_{L_{62}}$	$C_{L_{63}}$	$C_{L_{64}}$	$C_{L_{65}}$	$C_{L_{66}}$	$C_{L_{67}}$	$C_{L_{68}}$	$C_{L_{69}}$	$C_{L_{70}}$	$C_{L_{71}}$	$C_{L_{72}}$	$C_{L_{73}}$	$C_{L_{74}}$	$C_{L_{75}}$	$C_{L_{76}}$	$C_{L_{77}}$	$C_{L_{78}}$	$C_{L_{79}}$	$C_{L_{80}}$	$C_{L_{81}}$	$C_{L_{82}}$	$C_{L_{83}}$	$C_{L_{84}}$	$C_{L_{85}}$	$C_{L_{86}}$	$C_{L_{87}}$	$C_{L_{88}}$	$C_{L_{89}}$	$C_{L_{90}}$	$C_{L_{91}}$	$C_{L_{92}}$	$C_{L_{93}}$	$C_{L_{94}}$	$C_{L_{95}}$	$C_{L_{96}}$	$C_{L_{97}}$	$C_{L_{98}}$	$C_{L_{99}}$	$C_{L_{100}}$																																																																																																																																																																																																				
$C_u = 8.00$																																																																																																																																																																																																																																																																																																																		
0	0	12.25	.320	.0791	0	-.2435	-.0221	0	.68	2.70	2.60	2.55	2.50	2.45	.3394	.0104	0	-.2424	.0214	-.0044	.7429	.0214	18	.320	.0818	-.0443	-.1325	-.0176	-.0441	.78	3.45	3.15	3.60	3.41	.3302	.0135	-.0424	-.1344	.0088	-.0395	.8880	-.1190	-15	.320	.0815	-.0797	-.1105	.0617	.0662	.76	3.15	3.75	3.65	3.65	.3394	.0135	.0084	-.1287	-.0430	.0319	.8925	.0862	10	0	.320	.0823	.0264	-.1317	-.0381	.0678	.78	3.20	3.20	3.65	2.43	.3289	.0095	.0405	-.1480	-.0211	.0884	.8417	.0896	16	.320	.0939	.0708	-.3951	-.1317	.0220	.80	2.85	1.95	2.80	2.43	.3401	.0116	-.0078	-.4142	-.0322	-.0158	.8061	-.0894	0	.320	-.1494	.1055	-.2198	-.0439	-.1098	1.00	4.80	4.80	-5.15	4.88	.3341	.0418	.1492	.1488	-.0059	.1896	1.1709	.4417	20	0	.320	.1122	.0879	-.4629	-.2283	-.1756	.40	--	--	--	--	.3488	.0138	.0331	-.6827	-.0627	.0475	.4637	.0172																																																																																																																																																																		
$C_u = 14.00$																																																																																																																																																																																																																																																																																																																		
0	0	12.25	.125	.0240	-.0035	-.2640	.0088	0	.20	.43	.43	.38	.30	.20	-.1275	-.0025	-.0035	-.2640	.0088	-.0018	.1179	-.0018	15	.125	.0240	.0114	-.2376	-.0186	-.0582	.10	1.00	.90	1.10	.80	.1261	-.0024	-.0210	-.2554	.0398	-.0312	.1429	-.0318	-15	.125	.0240	-.0212	-.2376	.0408	.0176	.20	.80	1.00	1.10	.88	.1284	-.0025	.0125	-.2407	-.0387	.0068	.1448	-.0178	10	0	.125	.0274	.0123	-.2450	-.0420	.0225	.18	.45	.80	1.00	.74	.1276	-.0023	.0149	-.2404	-.0382	-.0177	.1318	.0116	-18	.125	.0342	.0212	-.2454	-.0492	.0440	.15	.60	.60	.60	.70	.1311	.0039	.0092	-.2419	-.0382	.0106	.1416	-.0083	20	0	.125	.0312	.0055	-.1485	-.0105	.0613	.38	.95	1.65	1.60	1.68	.1219	.0039	.0912	-.1810	-.0437	.0360	.2147	.2299	0	.125	.0392	.0289	-.2200	-.0848	.1144	.28	.90	.58	1.00	.79	.1279	.0027	.0408	-.2458	-.0785	.0491	.1379	.0459	16	.125	.0445	.0265	-.2376	-.0704	.0968	.18	.70	.20	.80	.60	.1351	.0087	.0058	-.2492	-.0018	.0241	.1561	.0192	0	.320	.0611	-.0124	-.2112	-.0176	-.0088	.65	2.85	2.80	3.40	3.14	.3287	-.0068	-.0124	-.2112	.0184	-.0123	.7659	-.0218	18	.320	.0752	.0494	-.1232	-.0176	-.0582	.78	3.80	3.90	3.90	3.68	.3302	.0070	-.0374	-.1254	.0022	-.0306	.8682	-.1040	10	0	.320	.0780	-.0671	-.0704	.0405	.0085	.80	3.20	3.95	4.00	3.78	.3348	.0070	.0203	-.0787	.0218	.0002	.8287	.0827	16	.320	.0801	.0555	-.1101	-.0387	.0440	.95	3.20	3.20	3.40	3.50	.3277	.0038	.0483	-.1949	-.0387	.0181	.7882	.1092	20	0	.320	.0801	.0847	-.4189	-.1820	.0618	.30	2.28	1.80	2.40	2.39	.3404	-.0026	.0055	-.4394	-.0178	.0156	.8818	-.0017	18	.320	.1484	-.1394	.2552	-.0569	.0650	1.00	4.80	4.80	5.40	5.10	.3318	.0291	.1807	.2054	-.0501	.1802	1.2041	-.2727	20	.320	.1112	.1024	-.4928	-.2288	.1584	.60	2.10	1.88	2.20	1.98	.3510	.0080	.0468	-.6474	-.0463	.0283	.4856	.0541

TABLE I.- Continued
 TABULATION OF TEST DATA AND RESULTS

(i) $\beta = 20^\circ$; $\tau = 24^\circ$



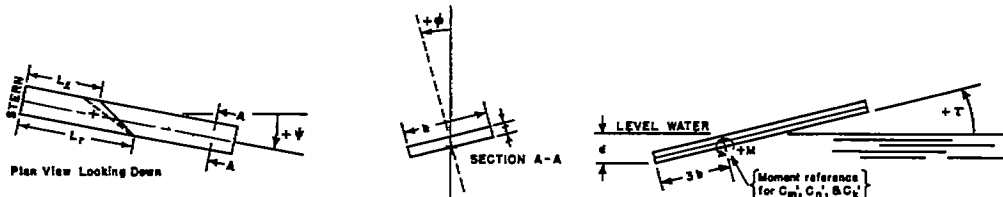
TEST PARAMETERS			WIND AXIS							BODY AXIS													
ψ	ϕ	C_d	C_{L_b}	C_{D_b}	C_{C_b}	C_m	C_n	C_k	d/b	L_c	L_f	L_k	λ	$C_{L_b}^*$	$C_{D_b}^*$	$C_{C_b}^*$	C_m^*	C_n^*	C_k^*	$C_{m_1}^*$	$C_{n_1}^*$	$C_{k_1}^*$	
$C_v = 14.00$																							
0	0	12.28	.128	.0830	0	-.3160	.0140	-.0088	.18	.18	.30	.40	0.26	.1288	-.0024	0	-.3180	.0092	-.0127	.0924	.0092		
15	15		.128	.0481	-.0088	-.2978	.0070	-.0850	.06	.38	0	.40	.29	.1318	-.0049	-.0261	-.2894	.0824	-.0448	.1081	-.0089		
-15	15		.128	.0837	-.0140	-.2888	.0178	-.0285	.10	0	.38	.40	.29	.1380	-.0018	-.0217	-.2889	-.0420	.0189	.1191	-.0161		
10	0		.128	.0893	-.0035	-.2900	-.0193	.0626	.05	.10	.10	.40	.28	.1382	-.0031	-.0048	-.2848	-.0184	.0813	.1293	-.0040		
15	15		.128	.0841	-.0088	-.2978	-.0168	.0285	.18	.30	0	.40	.2A	.1283	-.0036	-.0176	.2830	-.0481	.0773	.6889	-.1109		
-15	15		.128	.0609	-.0088	-.2978	.0035	.0700	.18	0	.40	.40	.30	.1206	-.0037	.0352	-.2974	-.0681	.0144	-.0244	.0366		
0	0		.128	.0872	.0035	-.2828	-.0490	.1138	.18	.20	.20	.88	.34	.1268	-.0034	.0845	-.2838	-.0378	.0356	.1288	.0387		
15	15		.128	.0878	.0070	-.2828	-.0298	-.0700	.20	.40	0	.48	.33	.1372	-.0039	-.0097	-.2710	.0265	-.0698	.1408	.0038		
-15	15		.128	.0491	-.0125	-.2858	-.0228	-.1400	.18	.28	.40	.60	.46	.1287	-.0049	-.0399	-.2789	-.0767	-.0508	.1108	.0450		
0	18	31.36	.320	.1040	-.0088	-.2856	.0178	-.0178	.378	.80	.80	1.08	.93	.3546	-.0052	-.0088	-.2856	-.0089	.0232	.2582	-.0178		
15	18		.320	.1423	.0477	-.2804	-.0918	-.0880	.478	1.10	.96	1.20	1.11	.3606	-.0002	-.0446	-.2864	.0757	-.0292	.3184	-.0601		
-15	18		.320	.1318	-.0618	-.2818	.1832	.0689	.478	.88	1.10	1.20	1.09	.3808	-.0098	.0298	-.2832	-.1498	.0110	.3174	-.0802		
10	0		.320	.1388	-.0035	-.2458	-.0878	.1812	.30	.80	.80	1.08	.93	.3471	-.0071	.0184	-.2850	-.0827	.0256	.2860	.0028		
15	15		.320	.1478	.0459	-.2152	-.1498	.0440	.78	1.00	.80	1.00	.90	.3646	-.0080	-.0217	-.2826	.0878	-.0448	.1380	-.0072		
-15	15		.320	.1341	-.0466	-.2890	.0178	.1682	.86	1.20	1.26	1.26	1.46	.3430	-.0028	-.0698	-.2804	-.1189	.0481	.4246	.0884		
20	0		.320	.1480	.0071	-.2800	-.1220	.2464	.60	1.06	1.08	1.48	1.23	.3808	-.0048	.0576	-.2800	-.1182	.0890	.3608	-.0414		
15	15		.320	.1449	.0898	-.2866	-.2280	.1848	.06	.86	.60	1.00	.86	.3621	-.0007	-.0009	-.2818	-.0262	.0098	.2490	-.0188		
-15	15		.320	.1539	.0124	-.2204	-.1478	.1780	1.10	2.40	2.80	2.70	2.09	.3209	-.0019	-.1828	-.2827	-.1907	.1208	.6890	.2866		

TABLE II.- Continued

TABULATION OF ADDITIONAL TEST DATA AND RESULTS TO ESTABLISH
 MAGNITUDE OF CHINE-EDGE-THICKNESS EFFECTS

$[\beta = 0^\circ; C_V = 14.00]$

(b) $t = 0.182b$



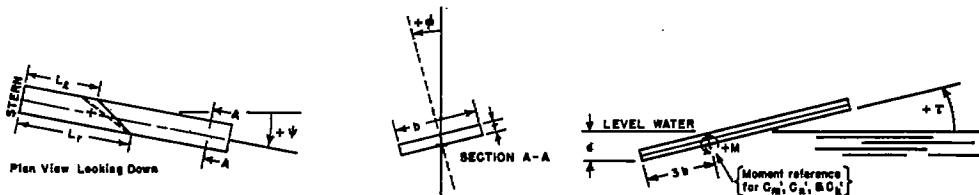
TEST PARAMETERS			WING AXIS							BODY AXIS													
ψ	ϕ	C_A	C_{L_b}	C_{D_b}	C_{C_b}	C_m	C_n	C_y	d/b	L_1	L_2	L_3	λ	C_{L_b}'	C_{D_b}'	C_{C_b}'	C_m'	C_n'	C_y'	C_p'	C_y'		
$Ta = 0^\circ$																							
2	0	17.61	.16	.0281	.0063	.0283	.0123	.0106	.490	3.90	3.80	3.80	.1519	.0276	.0063	.0259	.0134	.0101	.826		-.0656		
	5			.0228	.0176	.0350	.0063	-.0038	.400	3.60	3.20	3.40	.1822	.0219	.0028	.0354	.0020	-.0028	.939		-.0154		
	7			.0232	.0246	.0175	-.0018	-.0018	.400	3.90	3.20	3.60	.1851	.0220	.0031	.0172	-.0040	.0008	.854		-.0244		
	8			.0318	.0263	.0263	0	-.0063	.450	4.40	3.80	4.00	.1943	.0335	.0018	.0262	-.0041	-.0044	.788		-.0259		
	9			.0323	.0509	.1050	0	0	.475	4.50	3.60	4.05	.1881	.0301	.0239	.1037	-.0160	.0036	.877		-.0191		
	10			.0295	.0609	.0175	-.0106	.0088	.475	4.60	3.55	4.08	.1882	.0274	.0195	.0153	-.0123	.0108	.755		-.0658		
	-3			.0228	-.0063	.0700	.0123	0	.425	3.40	3.60	3.50	.1814	.0227	.0050	.0692	.0161	.0011	.966		-.0081		
	-8			.0298	-.0228	.0875	.0313	0	.600	4.20	4.60	4.40	.1833	.0302	-.0060	.0850	.0382	-.0003	.787		.0016		
	-5			.0337	-.0369	.1050	.0158	0	.500	4.20	4.80	4.50	.1851	.0346	-.0197	.1051	.0262	.0020	.790		-.0108		
	-10			.0404	-.0438	.2100	-.0063	.0088	.825	4.88	5.96	5.40	.1890	.0415	-.0100	.2070	.0329	.0166	.759		-.0853		
	-14			.0482	-.0441	.4576	-.0759	-.0033	.725	5.90	6.40	7.00	.1887	.0435	.0033	.4614	.0405	.0153	.718		-.0970		
	-18			.0448	-.0424	.4576	-.0810	0	.725	7.00	—	7.00	.1900	.0481	.0014	.4622	.0482	.0244	.697		-.1184		
3	-10			.0372	-.0369	.2363	-.0053	0	.600	4.80	5.90	6.35	.1864	.0387	-.0026	.2330	.0371	.0119	.794		-.0692		
	-14			.0448	-.0388	—	-.0861	.0229	.725	7.00	5.90	7.80	.1873	.0483	.0082	—	—	—	—		—		
	-8			.0305	-.0228	.0963	.0158	-.0088	.500	4.15	4.60	4.38	.1835	.0317	-.0046	.0950	.0239	-.0057	.806		.0202		
	-10			.0283	-.0298	.1838	-.0063	-.0123	.600	4.85	5.96	5.45	.1851	.0399	.0062	.1823	.0269	.0011	.731		-.0089		
5	0			.0264	-.0036	-.1062	.0108	.0283	.428	3.45	3.45	3.45	.1920	.0283	-.0011	-.1033	.0126	.0177	.704		-.0975		
	2			.0346	-.0071	-.0704	.0063	.0335	.378	3.40	3.20	3.90	.1823	.0335	.0037	-.0702	.0075	-.0032	.793		.0176		
	4			.0265	-.0106	-.0792	.0063	.0063	.350	3.15	2.80	2.88	.1821	.0251	.0002	-.0789	.0068	-.0020	.861		.0110		
	8			.0261	.0141	-.0792	-.0035	.0123	.350	3.20	2.66	2.93	.1853	.0248	.0004	-.0792	.0041	-.0187	.874		.1026		
	10			.0256	.0211	-.1050	-.0070	.0350	.325	3.10	2.40	2.75	.1850	.0233	.0010	-.1074	.0069	.0063	.877		-.1437		
	-2			.0280	.0316	-.1313	-.0245	0	.325	3.20	2.80	2.70	.1845	.0228	.0017	-.1333	-.0025	-.0088	.844		.0477		
	-8			.0306	.0597	-.1225	-.0513	-.0175	.325	3.15	2.00	2.58	.1915	.0249	.0130	-.1255	-.0019	-.0247	.909		.1220		
	-10			.0258	-.0108	.0088	.0141	.0178	.460	3.88	3.93	3.90	.1820	.0265	-.0020	.0067	.0162	.0167	.799		-.0918		
	-12			.0242	-.0140	-.0613	-.0070	.0438	.500	4.05	4.60	4.23	.1820	.0250	.0040	.0890	.0170	.0480	.784		-.2637		
	-10			.0340	-.0176	.1875	-.0088	.0106	.600	4.80	5.96	5.58	.1855	.0350	.0174	.1347	.0213	.0213	.715		-.1370		
	-12			.0516	.0404	-.1225	-.0243	.0175	.325	3.50	2.80	2.70	.1860	.0278	.0799	.1159	-.0488	.0093	.1342		-.0500		
10	0			.0332	.0088	-.1232	-.0141	.0887	.500	2.75	2.75	2.75	.1826	.0308	.0144	-.1281	-.0123	.0181	.835		-.0991		
	2			.0264	.0124	-.1408	-.0158	.0440	.250	2.80	2.40	2.80	.1819	.0228	.0103	-.1467	-.0086	.0204	.877		-.1121		
	5			.0260	.0178	-.1780	-.0140	.0438	.250	2.25	1.90	2.03	.1821	.0222	.0060	-.1804	.0029	.0141	.930		-.0774		
	10			.0332	.0320	-.2301	-.0428	.0443	.200	2.20	1.20	1.70	.1852	.0239	.0047	-.2380	-.0006	.0081	1.008		-.0437		
$Ta = 12^\circ$																							
5	0	31.36	.32	.0688	-.0123	-.4650	-.0106	.0475	.460	2.15	2.10	2.13	.3275	.0016	-.0063	-.4574	.0116	.0061	.792		-.0156		
	15			.0759	.0612	-.4574	-.1179	0	.425	2.40	1.80	2.10	.3588	.0144	-.0002	-.4723	-.0016	-.0145	.765		.0422		
	-5			.0642	-.0383	-.2908	-.1328	.0495	.500	2.20	2.40	2.30	.3283	-.0010	-.0010	-.3612	-.1584	.0461	.639		-.1874		
	-8			.0642	-.0580	-.3432	.0698	.0828	.580	2.40	2.80	2.60	.3307	.0006	-.0012	-.3619	.0144	.0098	.745		-.0226		
	-9			.0554	-.0798	-.2278	.0890	.0428	.600	2.80	3.00	2.80	.3340	.0013	-.0188	-.2454	.0836	.0029	.811		-.0087		
	-10			.0635	-.0622	-.2450	.0810	.0815	.625	2.58	2.15	2.90	.3360	.0024	-.0184	-.2625	.0855	.0199	.768		-.0692		
	-13			.0636	-.0865	-.0828	.0387	.0616	.780	3.40	4.20	3.80	.3378	.0029	.0062	.0069	.0350	.0475	.756		-.1406		
	-10	48.89	.50	.1004	-.1334	—	-.0823	—	1.178	6.26	6.70	5.48	.8281	.0082	-.0333	—	—	—	—		—		
	-10	31.36	.32	.0674	-.0741	-.1813	.0739	.0616	.600	2.80	3.20	3.00	.3333	-.0031	-.0100	-.1950	.0474	.0260	.802		-.0780		
	-10			.0674	-.0655	-.1408	.0610	.0323	.650	3.15	3.40	3.38	.3323	-.0001	-.0008	-.1834	.0316	.0264	.761		-.0794		
	-10			.0697	-.0648	-.2112	.0828	.0845	.600	2.80	3.20	3.00	.3317	.0010	.0019	-.2277	.0245	.0469	.771		-.1284		
	-10			.0614	-.0530	-.1408	.0387	.0628	.880	3.18	3.60	3.38	.3299	-.0008	.0124	-.1817	.0181	.0684	.761		-.0600		
10	5			.0615	-.0194	-.2104	-.0406	.0880	.375	1.80	1.80	1.70	.3280	-.0029	.0028	-.5194	.0063	.0065	.833		-.0198		
	10			.0688	.0458	-.5280	-.0882	.0851	.350	1.85	1.40	1.68	.3294	-.0078	-.0002	-.8389	.0037	-.0021	.859		-.0839		
	-5			.0697	-.0424	-.3820	.0382	.0880	.525	2.40	2.80	2.50	.3282	-.0018	-.0028	-.3640	.0061	.0177	.756		-.0699		
	-7			.0611	-.0391	-.2975	.0280	.0783	.580	2.80	2.80	2.85	.3275	-.0017	.0181	-.3077	-.0068	.0162	.777		-.0496		
	-10			.0653	-.0424	-.2376	.0211	.0868	.650	2.80	3.20	3.00	.3282	.0006	.0270	-.2825	-.0122	.0485	.744		-.1678		
	0			.0611	-.0018	-.4288	-.0248	.1125	.425	1.90	1.80	1.90	.3254	-.0063	.0141	-.4458	-.0242	.0041	.802		-.0126		
	5			.0614	.0085	-.3018	-.0246	.1498	.375	1.80	1.80	1.70	.3257	-.0094	.0022	-.5236	.0094	.0136	.818		-.0599		
	5			.0614	.0104	-.2104	-.0315	.1575	.350	1.70	1.40	1.56	.3258	-.0118	-.0084	-.5738	.0212	.0188	.888		-.0483		
20	5			.0616	.0158	-.2600	-.0465	.2100	.325	1.80	2.30	1.48	.3258	-.0150	.0078	-.6013	.0117	.0195	.792		-.0699		

TABLE II.- Concluded --

TABULATION OF ADDITIONAL TEST DATA AND RESULTS TO ESTABLISH
 MAGNITUDE OF CHINE-EDGE-THICKNESS EFFECTS

$$[\beta = 0^\circ; C_V = 14.00]$$

(b) Concluded.



TEST PARAMETERS			WIND AXIS										BODY AXIS									
ψ	ϕ	C_A	C_{L_b}	C_{D_b}	C_{D_c}	C_m	$C_{m'}$	$C_{m''}$	d/b	L_f	L_f	λ	C_{L_b}'	C_{D_b}'	C_{D_c}'	$C_{m'}$	$C_{m''}$	C_k'	C_p'	C_y'		
$T = 18^\circ$																						
7	-18	51.36	.52	.0904	-.0928	-.5720	.1657	.1445	.450	---	---	---	.3489	-.0037	.0028	-.5118	.0808	.0195	--	-.0656		
8	-16			.0911	-.0847	-.5408	.1320	.1849	.450	1.40	1.80	1.60	.3428	-.0007	.0200	-.5817	-.0281	.0236	.814	-.0688		
10	-10			.0879	-.0777	-.5356	.1109	.1320	.400	1.40	1.80	1.36	.3408	-.0037	-.0031	-.4688	-.0024	-.0153	.945	-.0449		
15	-18			.0819	-.0863	-.5192	.1126	.1948	.500	1.40	1.80	1.66	.3439	-.0041	-.0166	-.3328	-.0172	.0245	.844	-.0712		
0	0			.0919	-.0926	-.5685	.0985	.2640	.375	1.05	1.00	1.05	.3339	-.0060	-.0018	-.7143	.0306	.0763	.856	-.1826		
5	5			.0850	.0038	-.7504	-.0563	.1848	.450	1.00	.80	.80	.3356	-.0128	-.0011	-.7854	.0081	.0074	.818	-.0222		
10	10			.1154	.0600	-.7744	-.1830	.1320	.300	1.05	.60	.82	.3468	-.0077	-.0018	-.8064	.0126	-.0138	.811	-.0671		
15	15			.0885	-.0424	-.6336	.0405	.2263	.328	1.10	1.10	1.10	.3347	-.0071	-.0008	-.6723	.0199	.0385	.801	-.1150		
20	20			.0807	-.0459	-.6248	.0405	.2200	.350	1.20	1.30	1.28	.3368	-.0043	.0084	-.6627	-.0036	.0385	.821	-.1047		
5	-5			.0818	-.0459	-.5984	.0406	.2263	.378	1.20	1.36	1.28	.3388	-.0038	.0209	-.6358	-.0601	.0472	.870	-.1334		
10	-10			.0807	-.0418	-.5596	.0440	.2158	.485	1.40	1.40	1.60	.3378	-.0004	.0237	-.6233	-.0502	.0402	.763	-.1191		
15	-15			.0904	-.0300	-.6245	-.0141	.2728	.328	1.15	1.10	1.13	.3358	-.0083	.0144	-.6300	-.0226	.0362	.850	-.1068		
20	-20			.0835	-.0318	-.5808	-.0088	.2640	.350	1.20	1.30	1.25	.3334	-.0060	.0218	-.6348	-.0464	.0443	.878	-.1338		
5	-5			.0828	-.0528	-.5280	-.0141	.2306	.478	1.60	1.70	1.70	.3311	-.0053	.0256	-.6569	-.1021	.0387	.758	-.1108		
$T = 24^\circ$																						
15	15	51.36	.52	.1391	.0512	-.5448	-.1894	.1179	.300	0.90	0.88	0.78	.3321	-.0195	-.0130	-.8749	.0066	-.0182	.708	-.0460		
5	-5			.1115	-.0653	-.7480	.0866	.2608	.378	.80	.80	.80	.3460	-.0183	-.0062	-.7344	.0171	.0251	.850	-.0785		
10	-10			.0791	-.0741	-.7392	.0899	.2728	.278	.85	1.00	.93	.3350	-.0488	-.0104	-.7924	.0180	.0294	.862	-.0878		
15	-15			.1181	-.0777	-.7040	.0833	.2675	.300	.90	1.08	.98	.3485	-.0102	.0155	-.7681	-.0187	.0618	.846	-.0907		
20	-20			.1200	-.0986	-.6424	.1021	.2781	.400	1.10	1.30	1.20	.3846	-.0009	.0284	-.7065	-.0459	.0820	.846	-.1466		
5	-5			.1165	-.0812	-.7392	.0846	.3045	.350	.80	.80	.80	.3441	-.0142	.0067	-.7898	.0081	.0204	.846	-.0583		
10	-10			.1106	-.0547	-.7040	.0299	.3188	.278	.80	.90	.90	.3422	-.0180	.0184	-.7714	-.0188	.0398	.829	-.1185		
15	-15			.1120	-.0653	-.6800	.0234	.3048	.410	1.00	1.10	1.10	.3486	-.0078	.0237	-.7329	-.0226	.0412	.830	-.1201		
$T = 30^\circ$																						
15	15	51.36	.52	.1228	-.0477	-1.0384	-.2025	.1058	.340	0.70	0.40	0.58	.3587	-.0028	-.0981	-1.0222	.0167	-.0432	.871	-.1204		
5	-5			.1468	-.0988	-.8096	.1126	.3045	.390	.70	.80	.78	.3663	-.0161	-.0087	-.8719	.2077	.0170	.817	-.0465		
10	-10			.1465	-.0971	-.7744	.1285	.3221	.315	.70	.80	.78	.3647	-.0167	.0078	-.8477	.0198	.0316	.801	-.0866		
15	-15			.1425	-.1130	-.7504	.1373	.3221	.340	.85	1.00	.95	.3641	-.0155	.0234	-.8066	-.0308	.0371	.858	-.1019		
20	-20			.1453	-.0868	-.8560	.0865	.3650	.390	.80	.80	.80	.3606	-.0178	-.0071	-.9087	.0318	.0007	.800	-.0019		
5	-5			.1408	-.0650	-.8008	.0899	.3221	.390	.70	.70	.70	.3527	-.0208	.0016	-.8806	.0085	.0280	.778	-.0781		
10	-10			.1447	-.0971	-.7668	.0704	.3585	.340	.85	.90	.88	.3635	-.0138	.0217	-.8372	-.0476	.0300	.792	-.0828		

TABLE III

TEST DATA AND RESULTS FOR SYMMETRICAL PLANING CONDITIONS

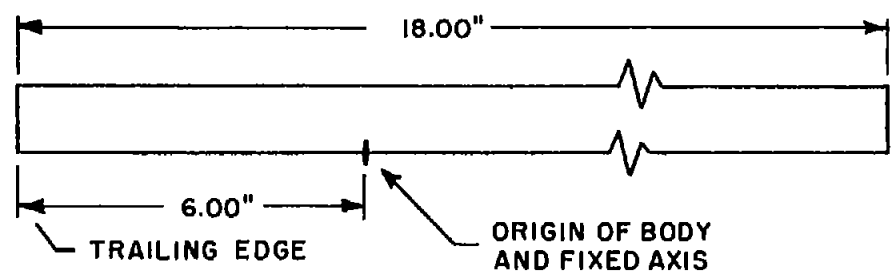
Test parameters			Wind axis						Body axis											
τ , deg	C_v	C_{Δ}	C_{L_b}	C_{D_b}	C_{C_b}	C_m	C_n	C_k	d/b	L_r	L_l	λ	C_{L_b}'	C_{D_b}'	C_{C_b}'	C_m'	C_n'	C_k'	C_p'	C_y'
6	17.50	12.25	0.080	0.0032	0	-0.1680	0.0078	0	0.125	0.80	0.80	0.80	0.0799	-0.0052	0	-0.1680	0.0078	-0.0008	1.121	0.0100
	14.00		.125	.0134	0	-.1654	.0088	0	.175	1.99	2.00	2.00	.1257	.0003	0	-.1654	.0088	-.0009	.842	.0072
	14.00		.125	.0145	-.0053	-.1768	.0053	0	.250	1.80	1.80	1.80	.1258	.0014	-.0053	-.1768	.0053	-.0008	.886	.0064
	11.70		.180	.0319	0	0	.0126	0	.400	4.00	4.00	4.00	.1823	.0129	0	0	.0125	-.0013	.750	.0071
	17.60		.180	.0257	-.0088	.0280	.0131	.0053	.400	4.05	4.05	4.05	.1817	.0067	-.0088	.0280	.0136	.0039	.779	-.0215
	10.00		.245	.0491	0	.4256	.0104	.0104	.750	6.45	6.40	6.43	.2488	.0232	0	.4256	.0114	.0093	.733	-.0374
	10.00		.245	.0527	0	.5709	.0173	0	.700	7.40	7.39	7.40	.2492	.0268	0	.5709	.0172	-.0018	.745	.0072
	12.20	18.20	.245	.0473	0	.4474	.0186	.0210	.625	6.55	6.55	6.55	.2486	.0214	0	.4474	.0207	.0189	.733	-.0760
	14.00	24.00	.245	.0385	-.0049	.4288	.0088	0	.750	6.40	6.40	6.40	.2477	.0127	-.0049	.4288	.0088	-.0009	.739	.0056
	15.60	29.90	.245	.0320	-.0014	.4031	.0139	.0070	.400	6.15	6.00	6.08	.2470	.0062	-.0014	.4031	.0146	.0055	.762	-.0223
	17.10	35.8	.245	.0436	0	.5948	.0110	0	.075	6.60	6.40	6.50	.2482	.0178	0	.5948	.0109	-.0012	.830	.0048
12	14.00	12.25	.125	.0215	0	-.3150	.0053	0	.100	.40	.40	.40	.1267	-.0050	0	-.3150	.0052	-.0011	1.285	.0087
	8.85	12.25	.320	.0782	0	-.3951	.0220	.0220	.400	2.20	2.20	2.20	.3293	.0100	0	-.3951	.0170	-.0261	.818	.0793
	14.00	31.36	.320	.0667	0	-.4347	.0176	-.0018	.375	2.10	2.10	2.10	.3269	-.0013	0	-.4347	.0169	-.0054	.795	.0165
18	17.50	12.25	.080	.0329	0	-----	.0112	0	.025	.30	.30	.30	.0863	.0063	0	-----	.0112	-.0035	-----	.0406
	14.00	31.36	.320	.0852	0	-.7368	.0131	-.0088	.350	1.00	1.00	1.00	.3306	-.0179	0	-.7368	.0098	-.0124	.771	.0375
	7.78	12.25	.405	.1377	0	-.7695	.0285	0	.350	1.60	1.60	1.60	.4278	.0058	0	-.7695	.0285	-.0088	.751	.0206
	7.00	12.25	.500	.1665	-.0073	-.6897	.0363	0	.700	2.25	2.30	2.28	.5270	.0038	-.0073	-.6897	.0363	-.0112	.742	.0213
24	14.00	12.25	.125	.0526	0	-.3520	.0088	0	.003	.15	.15	.15	.1356	-.0027	0	-.3520	.0080	-.0056	.571	.0265
	14.00	31.36	.320	.1199	-.0035	-.8488	.0053	-.0088	.250	.65	.65	.65	.3411	-.0207	-.0035	-.8488	.0012	-.0102	.788	.0299
30	14.00	12.25	.125	.0664	0	-.3872	.0088	0	.050	.35	.35	.35	.1415	-.0050	0	-.3872	.0076	-.0044	.754	.0311
	12.20	18.20	.245	.1453	0	-.7610	.0139	-.0069	.100	.40	.40	.40	.2849	.0033	0	-.7610	.0085	-.0130	.823	.0456
	14.00	31.36	.320	.1672	0	-.9699	.0053	-.0177	.225	.55	.55	.55	.3607	-.0152	0	-.9699	-.0043	-.0180	.566	.0499
	7.78	12.25	.405	.2269	-.0057	-1.1400	.0285	0	.275	.95	.95	.95	.4642	-.0060	-.0057	-1.1400	.0247	-.0143	.573	.0308
	7.00	12.25	.500	.2802	-.0071	-1.2460	0	-.0352	.400	1.10	1.20	1.15	.5731	-.0073	-.0071	-1.2460	-.0176	-.0305	.718	.0532

TABLE IV
 SUMMARY OF EFFECTS OF YAW AND ROLL ANGLE ON HYDRODYNAMIC
 BEHAVIOR OF A PLANING SURFACE^a

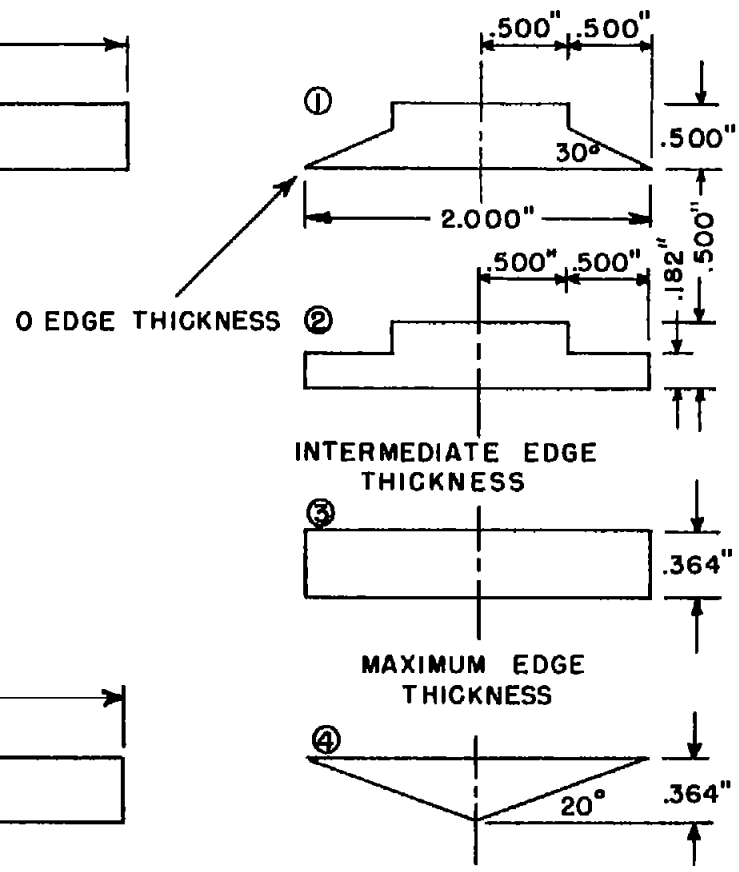
[In all cases yaw angle is positive]

Variable	β , deg	Yaw, no roll	Yaw, positive roll	Yaw, negative roll	Positive roll, no yaw
Mean wetted-length- beam ratio	0	-	-	+	+
	20	+	-	+	+
Side-force coefficient (wind axis)	0	-	+	-	+
	20	+	+	-	+
Drag coefficient (wind axis)	0	-	+	-	+
	20	+	+	N	N
Pitching-moment coefficient (body axis)	0	-	-	+	+
	20	+	-	+	+
Rolling-moment coefficient (body axis)	0	N	N	N	N
	20	+	N	+	-
Yawing-moment coefficient (body axis)	0	N	N	N	N
	20	+	N	+	-

^aFor a given lift coefficient and moderate trim angle, the tabulation indicates qualitatively whether unsymmetrical planing conditions cause an increase (+) a decrease (-) or an insignificant change (N) in wetted length, forces, and moments which exist for symmetrical planing case. In this table, increase means to become more positive, decrease means to become less positive.



(a) Flat plates ①, ②, and ③.



(b) 20° dead-rise model ④.

Figure 1.- Prismatic planing surfaces used in tests.

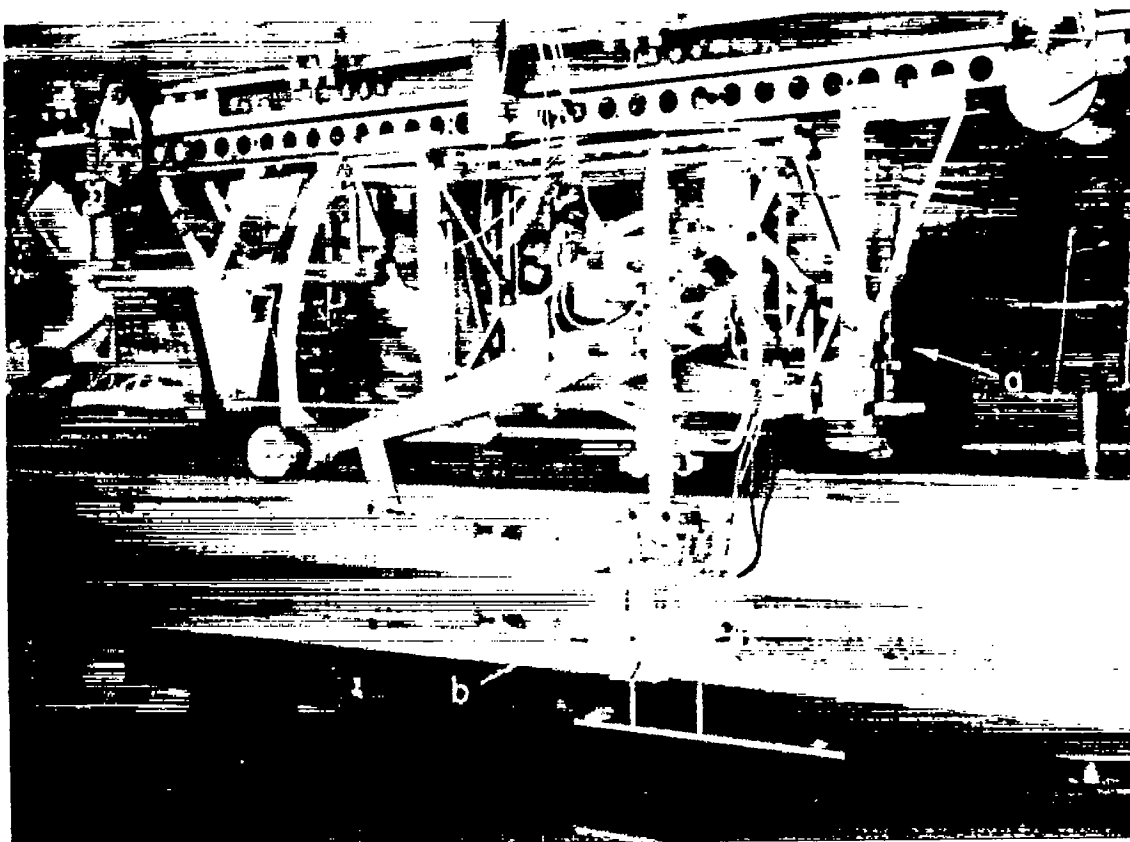


Figure 2.- Test setup. (a) indicates tank no. 3 "lift-drag" apparatus;
(b) indicates four-component balance with attached 0° dead-rise model.

L-58-218

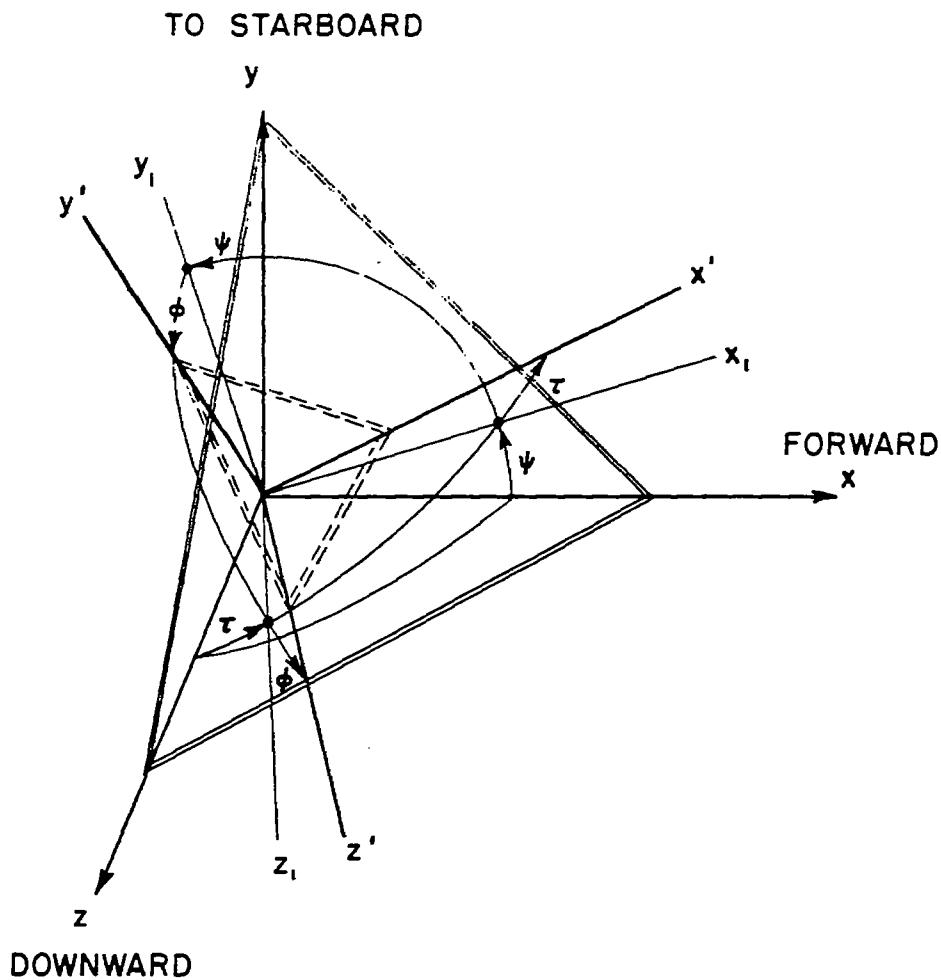


Figure 3.- Orientation of body axes relative to fixed axes in terms of τ , ψ , and ϕ . Viewed from below x,y plane. τ , trim angle; ψ , yaw angle; ϕ , roll angle.

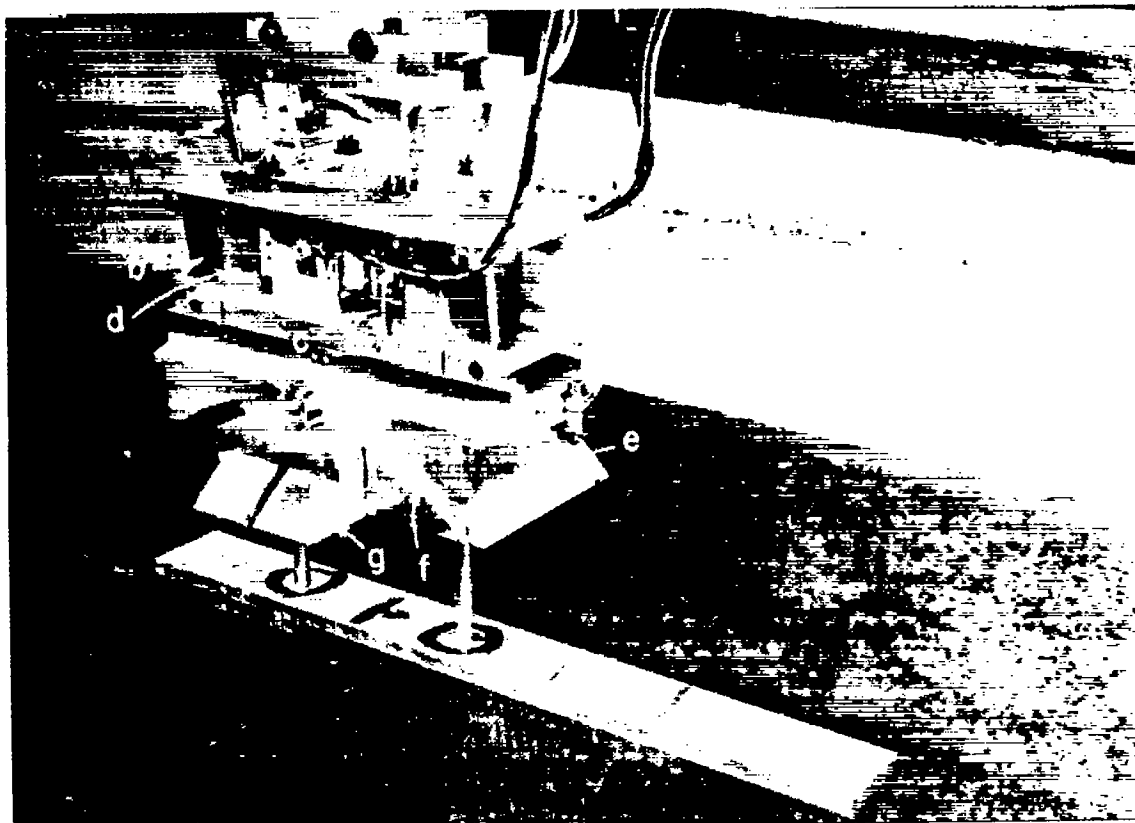


Figure 4.- Four-component balance. (a) indicates pitch springs (note Schaevitz unit); (b) indicates roll springs; (c) indicates yaw springs; (d) indicates side-force springs; (e) indicates yaw scale; (f) indicates pitch scale; and (g) indicates roll scale.

L-58-219

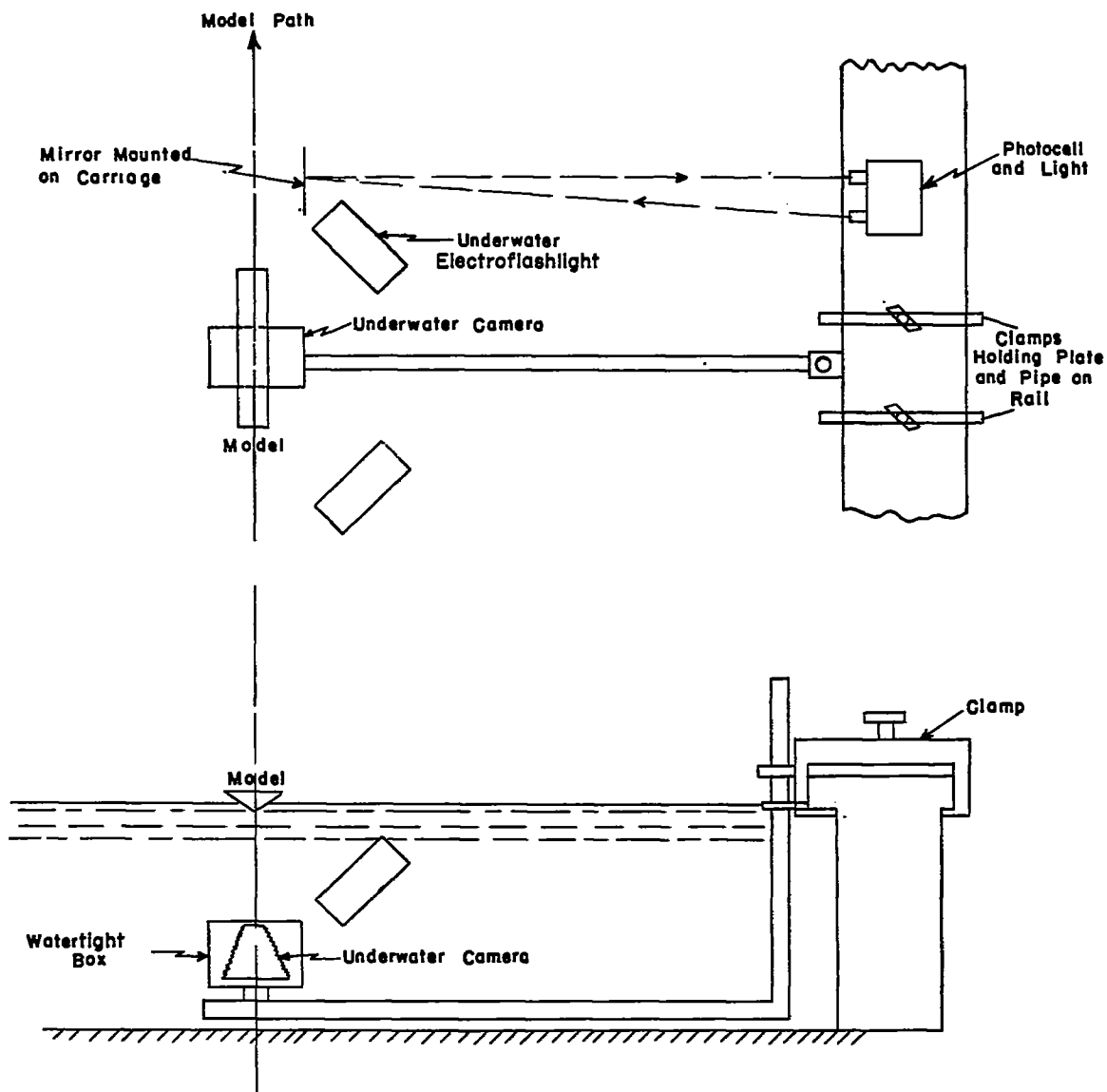


Figure 5.- Setup for lighting and photographing of underwater areas of model.

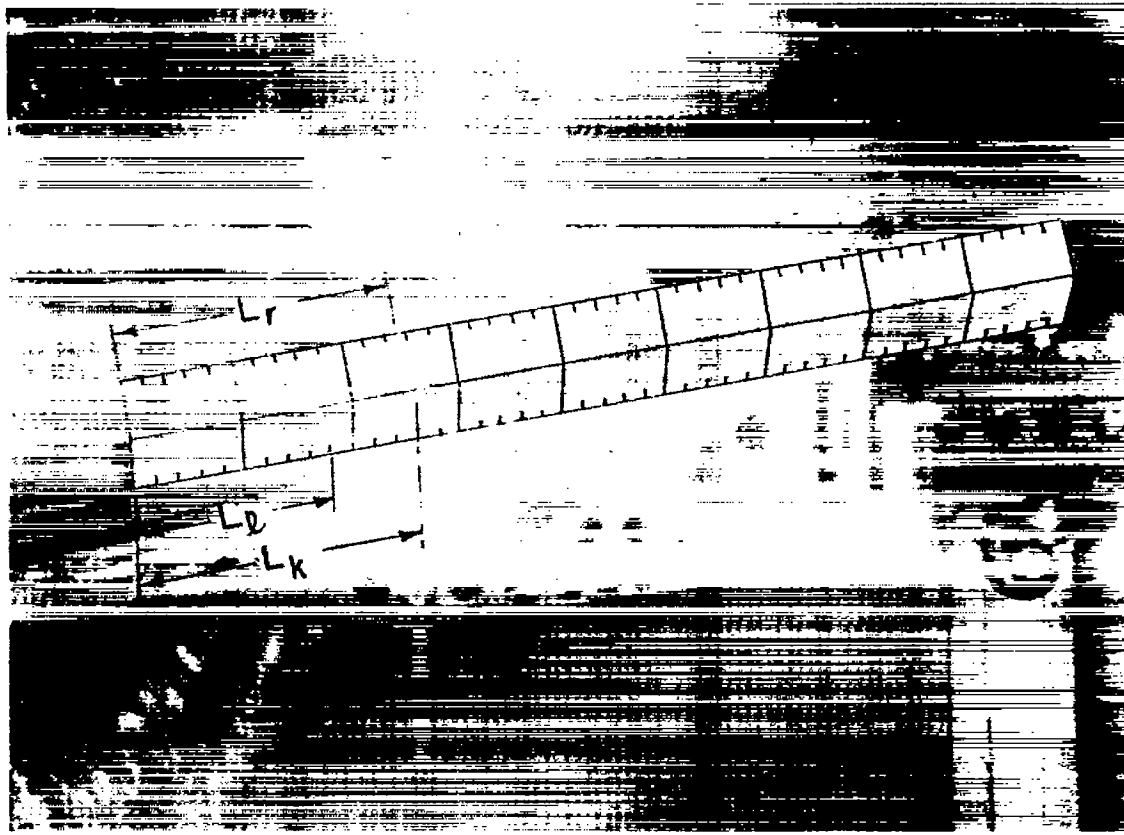
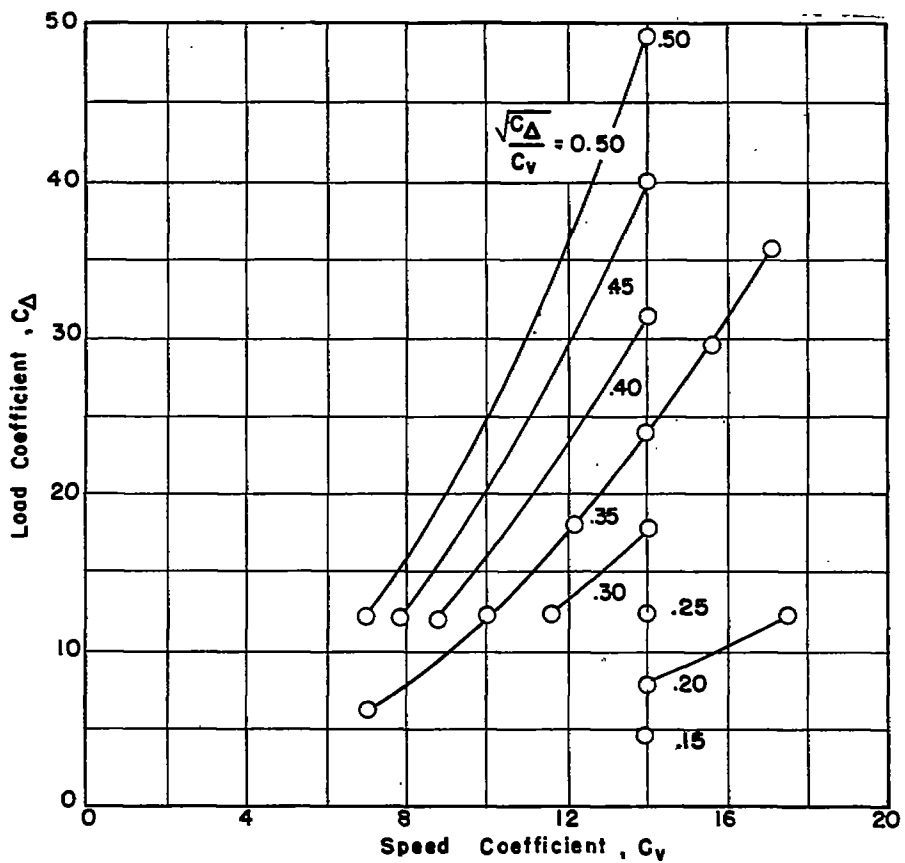
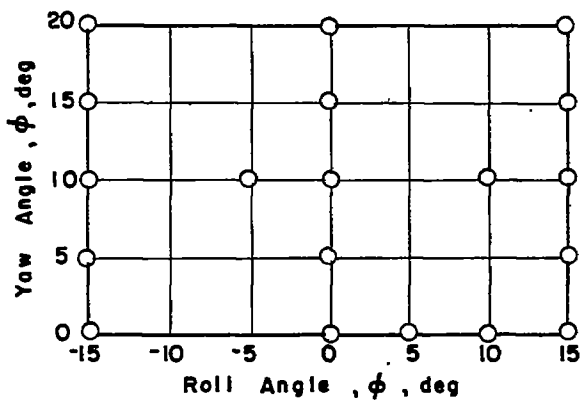


Figure 6.- Enlarged typical underwater photograph of wetted bottom area.
 $\beta = 20^\circ$; $\tau = 12^\circ$; $\psi = 10^\circ$; $\phi = 15^\circ$; $C_\Delta = 31.36$; and $C_V = 14.0$.

L-58-220



(a) Load-speed schedule.



(b) Yaw-roll schedule.

Figure 7.- Outline of basic test program.

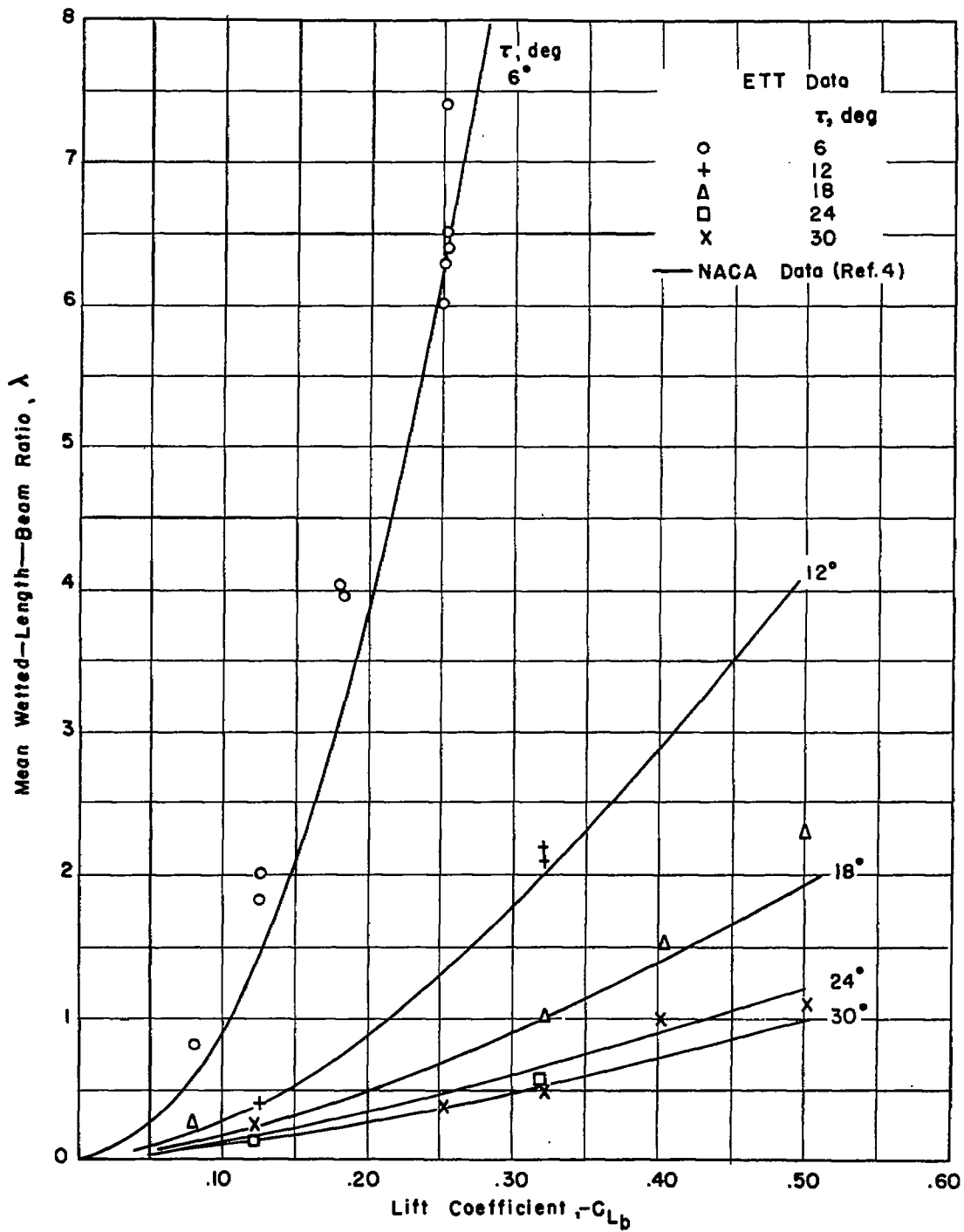


Figure 8.- Comparison of flat-plate high-speed lift data obtained in symmetrical planing tests at NACA and ETT.

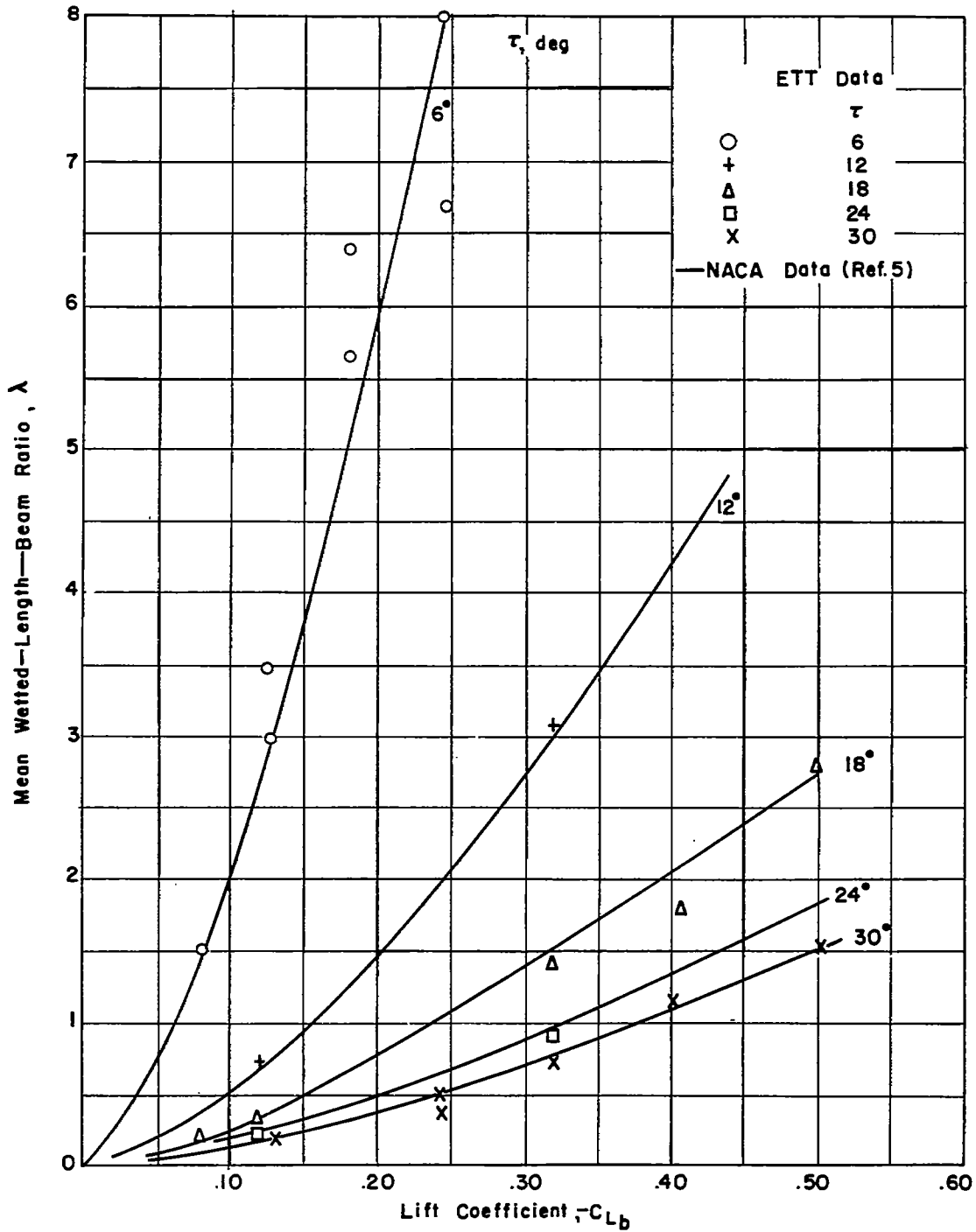
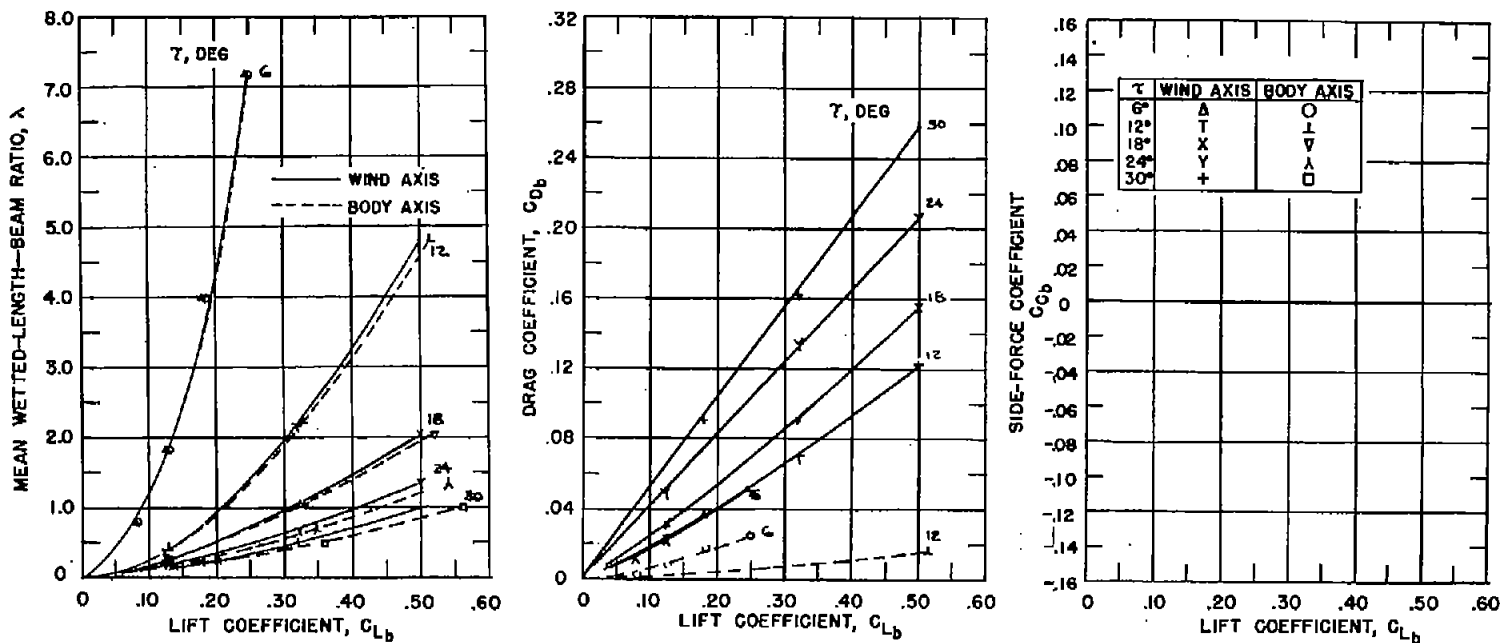
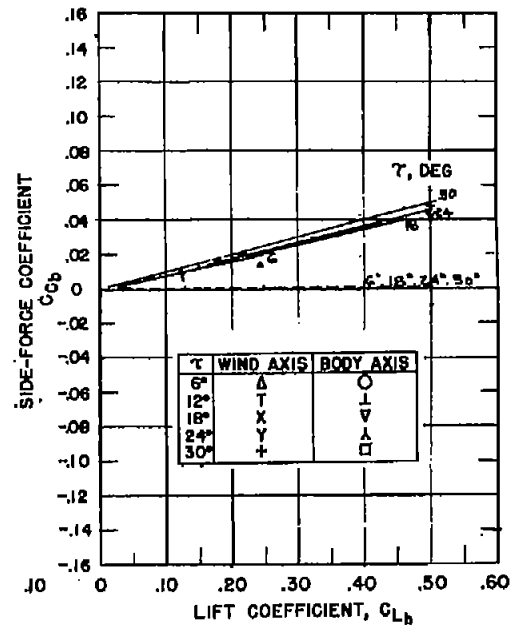
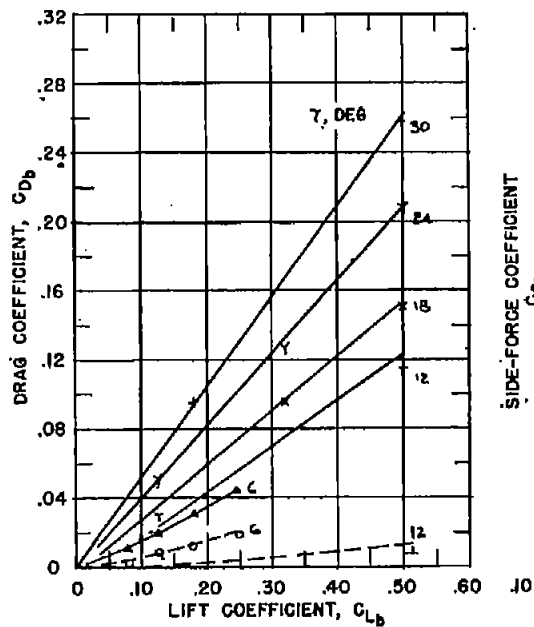
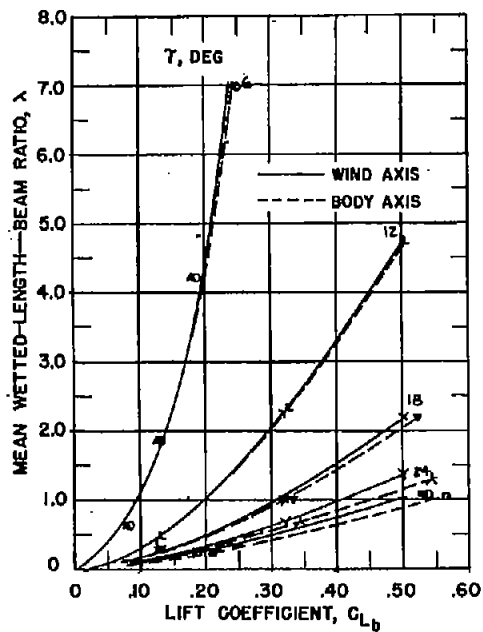


Figure 9.- Comparison of high-speed lift data obtained in symmetrical planing tests at NACA and ETT for 20° dead-rise surface.



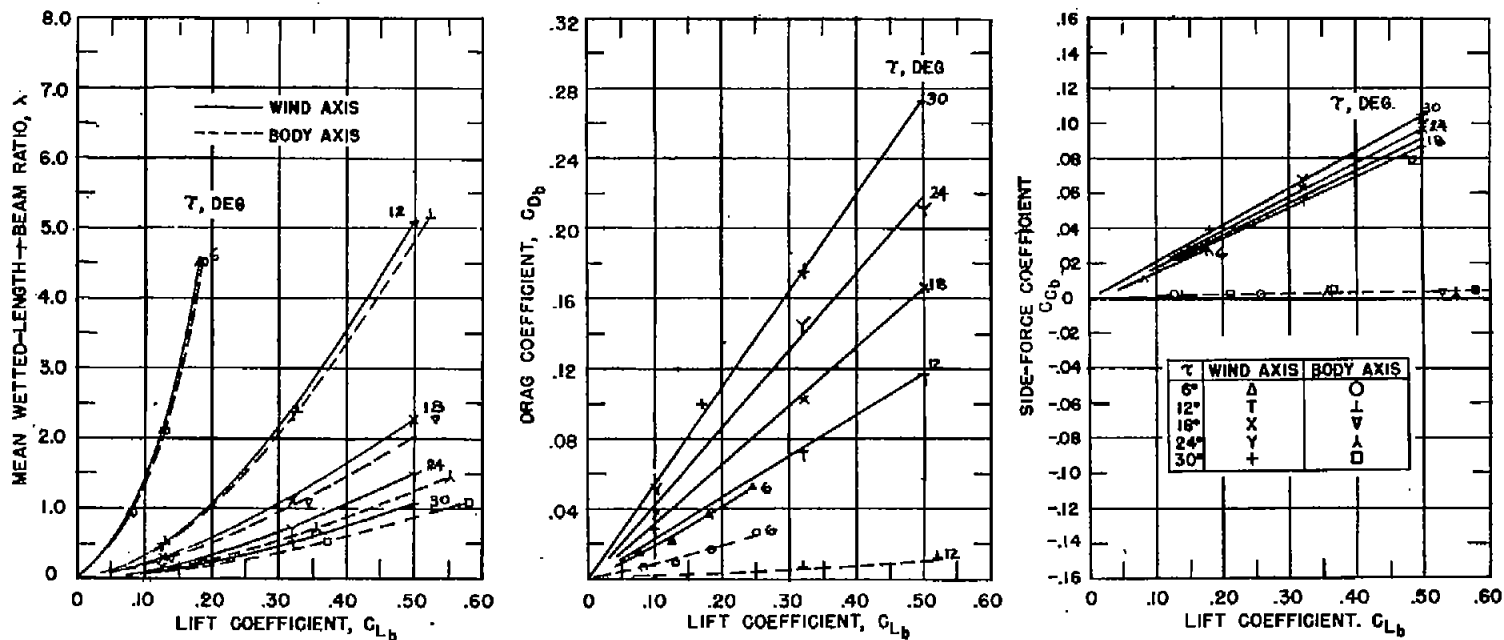
(a) $\phi = 0^\circ$.

Figure 10.- Lift, drag, and side-force coefficients for $\beta = 0^\circ$. $\psi = 0^\circ$.



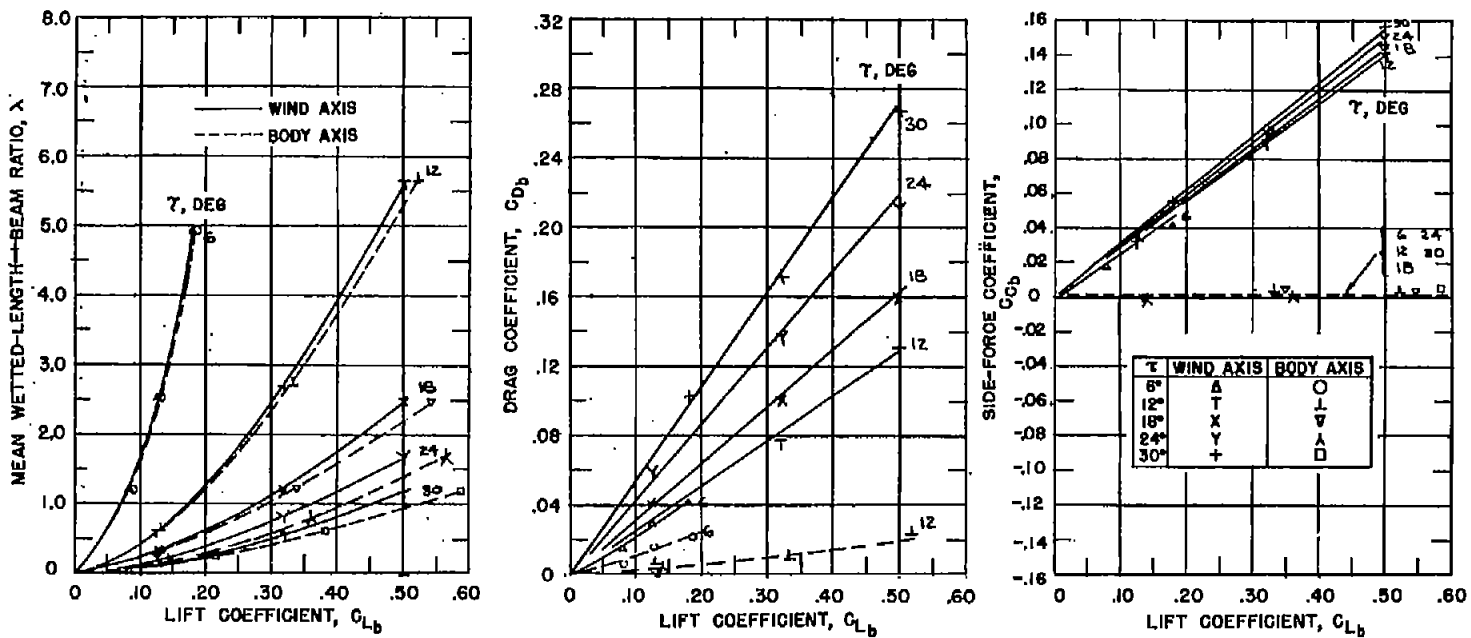
(b) $\phi = 5^\circ$.

Figure 10.- Continued.



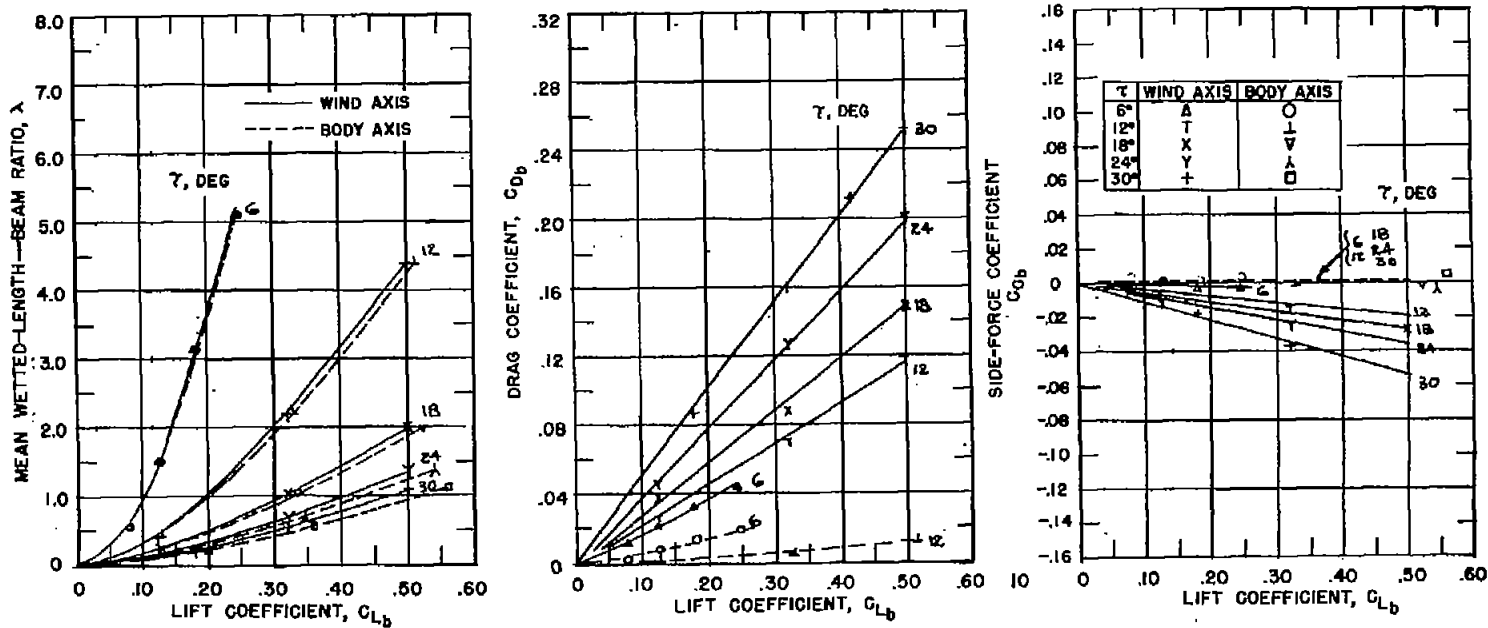
(c) $\phi = 10^\circ$.

Figure 10.- Continued.



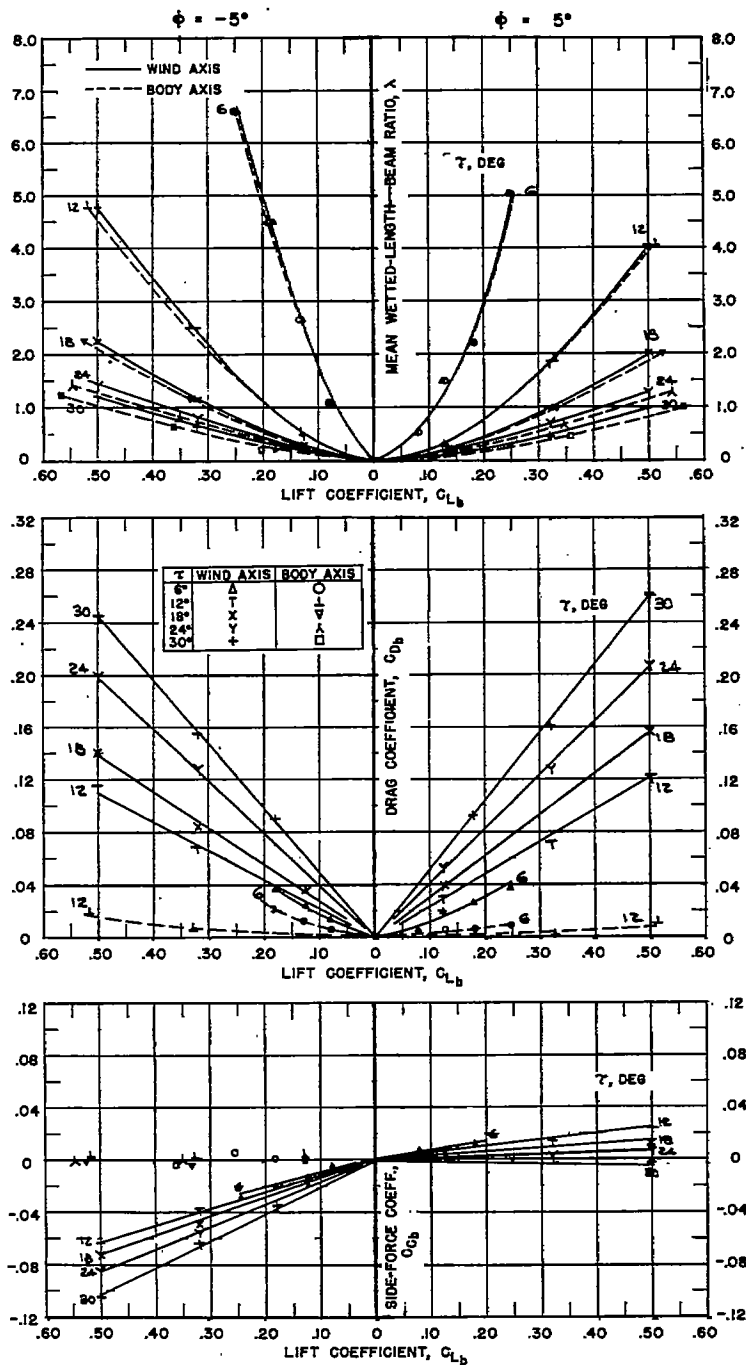
(d) $\phi = 15^\circ$.

Figure 10.- Concluded.



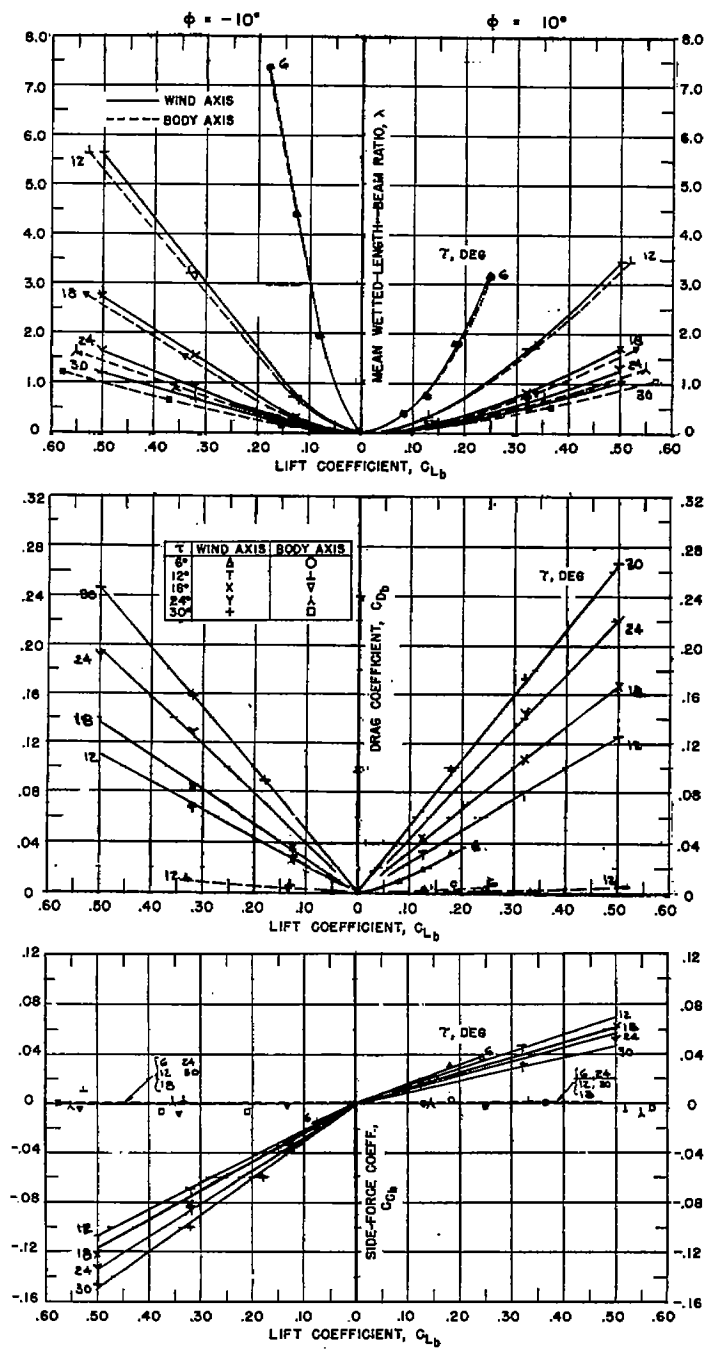
(a) $\phi = 0^\circ$.

Figure 11.- Lift, drag, and side-force coefficients for $\beta = 0^\circ$. $\psi = 10^\circ$.



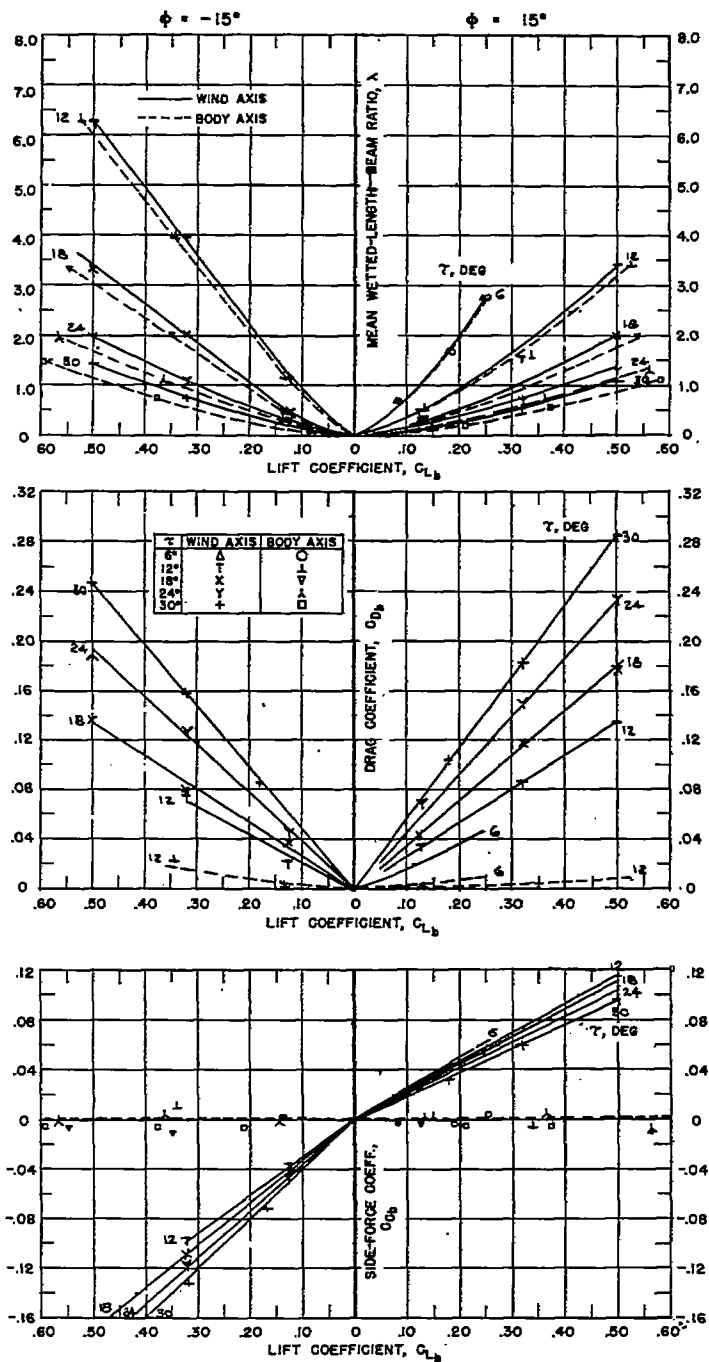
(b) $\phi = -5^\circ$ and 5° .

Figure 11.- Continued.



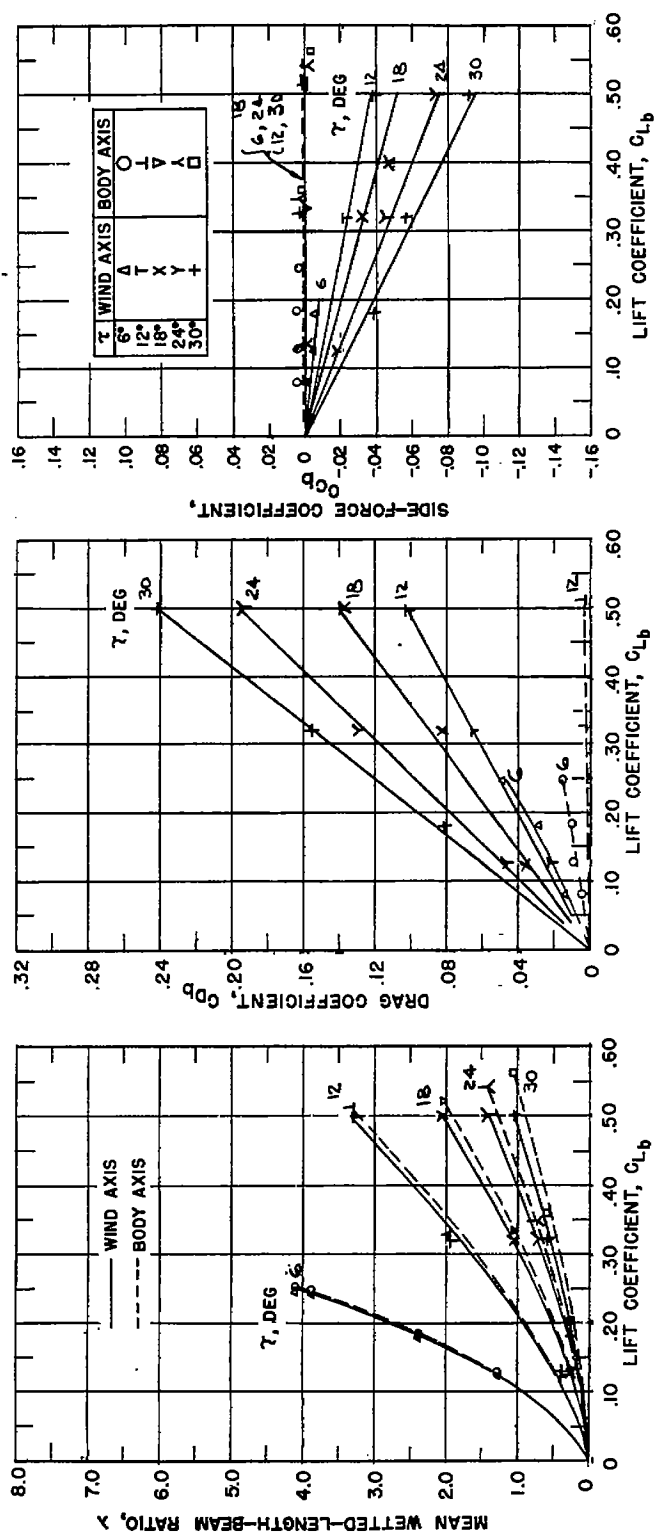
(c) $\phi = -10^\circ$ and 10° .

Figure 11.- Continued.



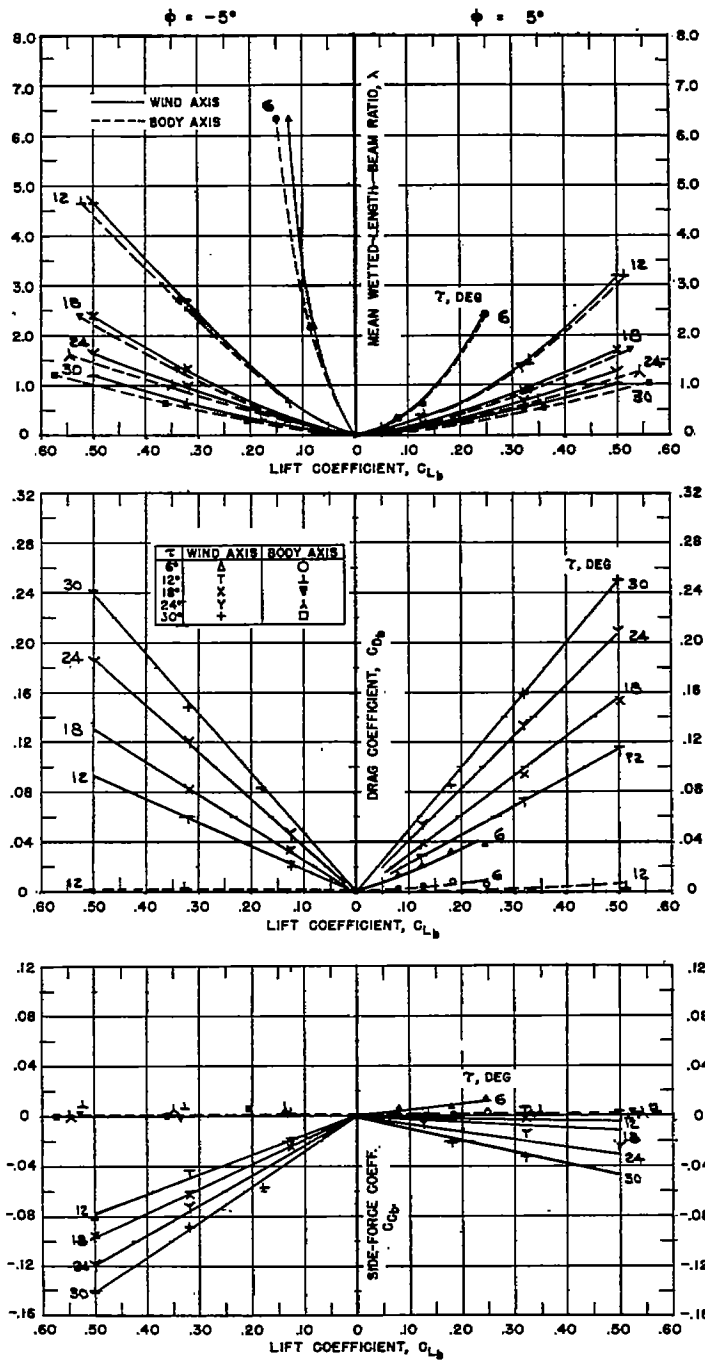
(d) $\phi = -15^\circ$ and 15° .

Figure 11.- Concluded.



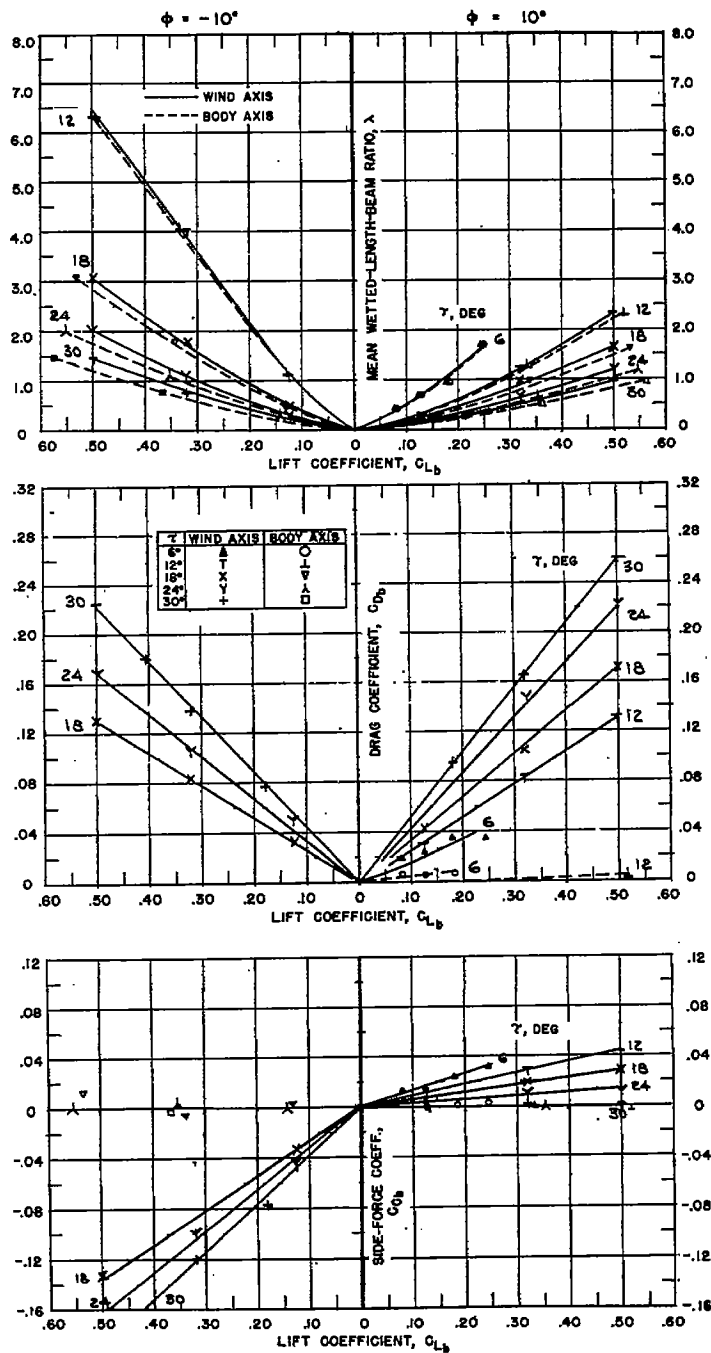
(a) $\phi = 0^\circ$.

Figure 12.- Lift, drag, and side-force coefficients for $\beta = 0^\circ$. $\psi = 20^\circ$.



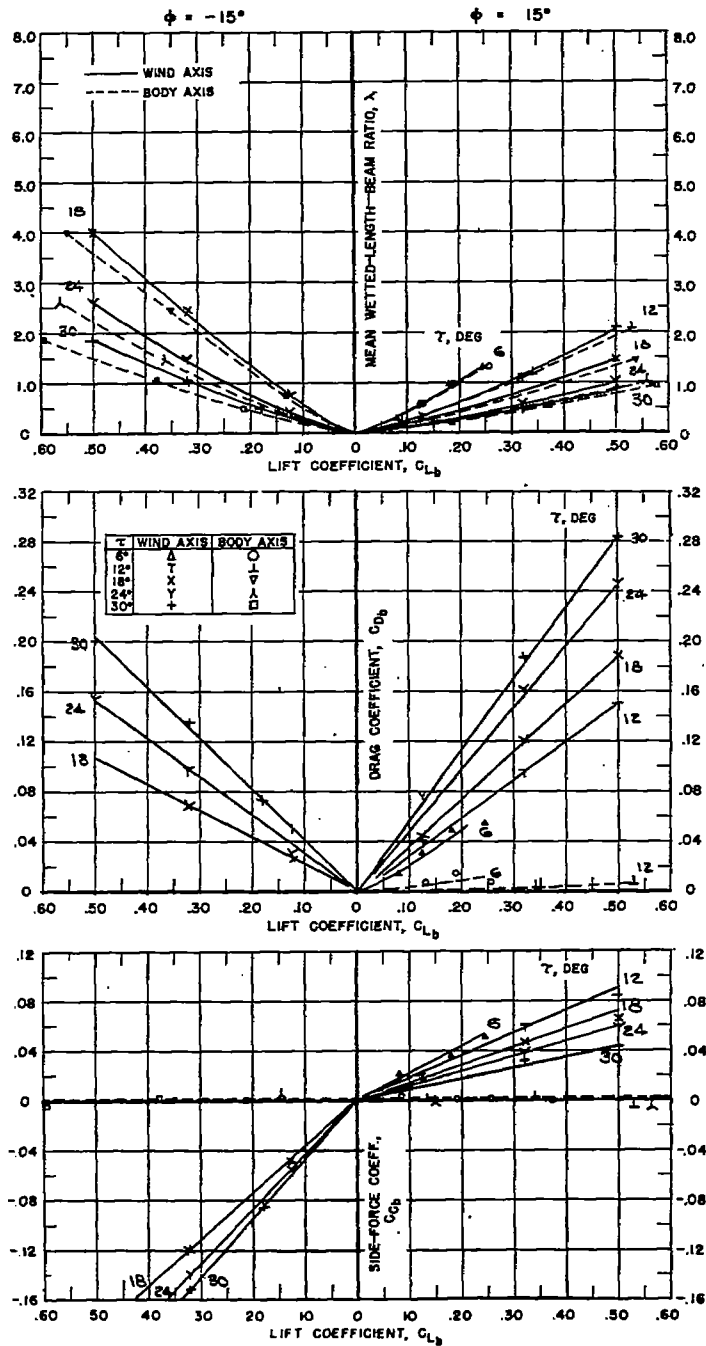
(b) $\phi = -5^\circ$ and 5° .

Figure 12.- Continued.



(c) $\phi = -10^\circ$ and 10° .

Figure 12.- Continued.



(d) $\phi = -15^\circ$ and 15° .

Figure 12.- Concluded.

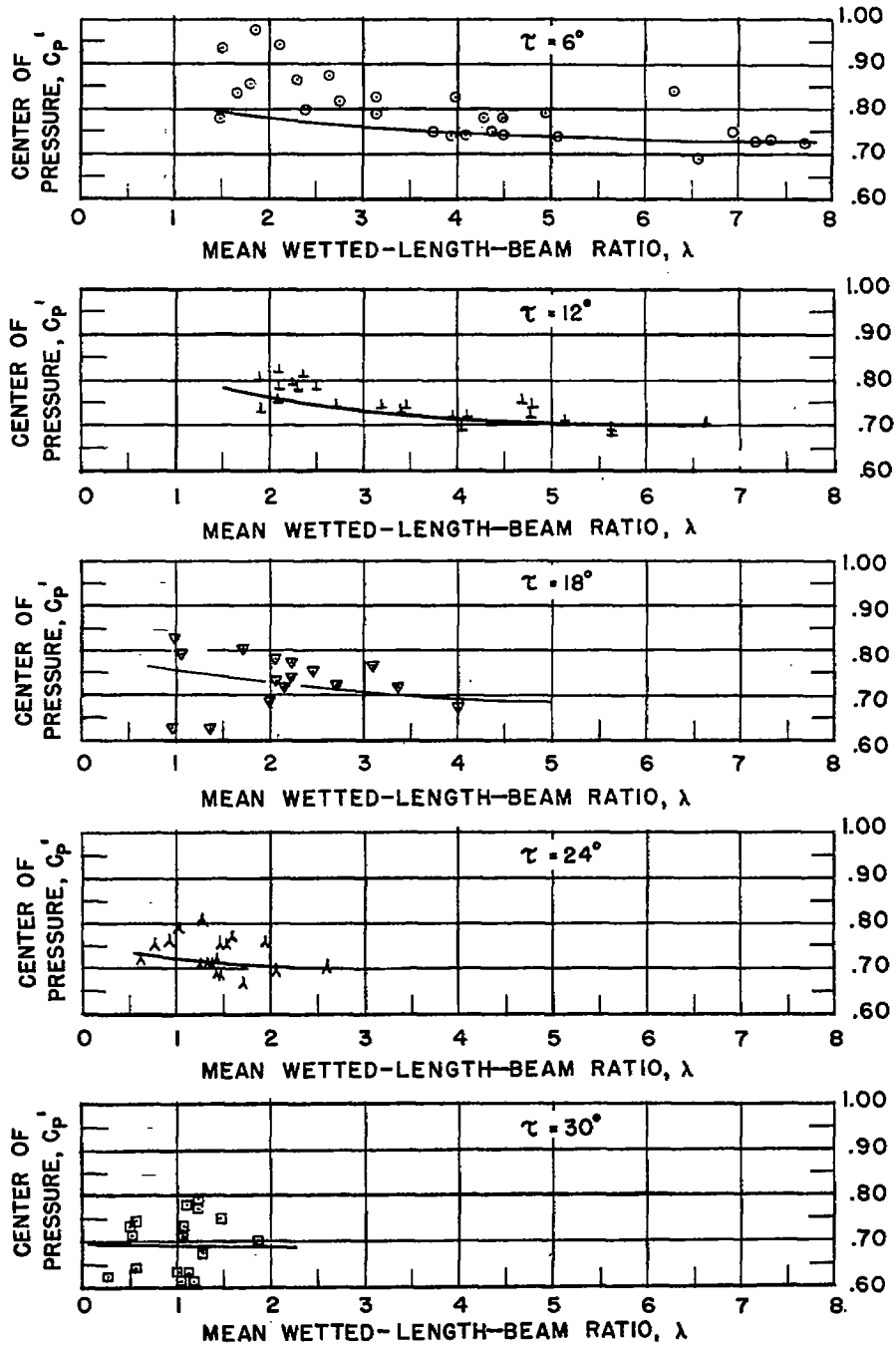
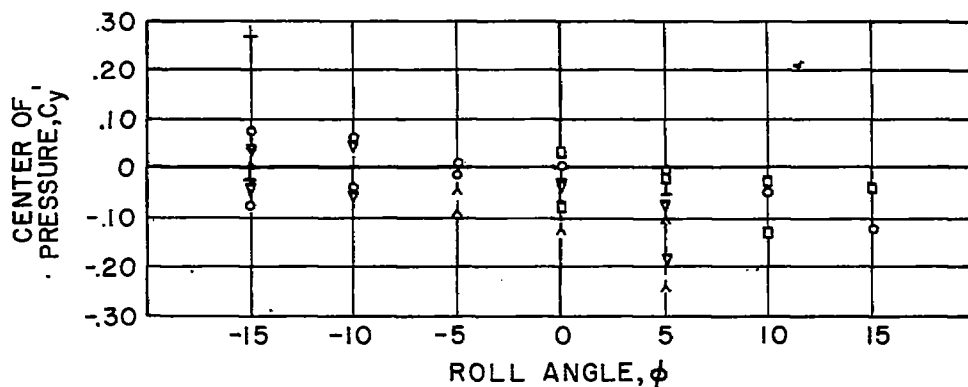
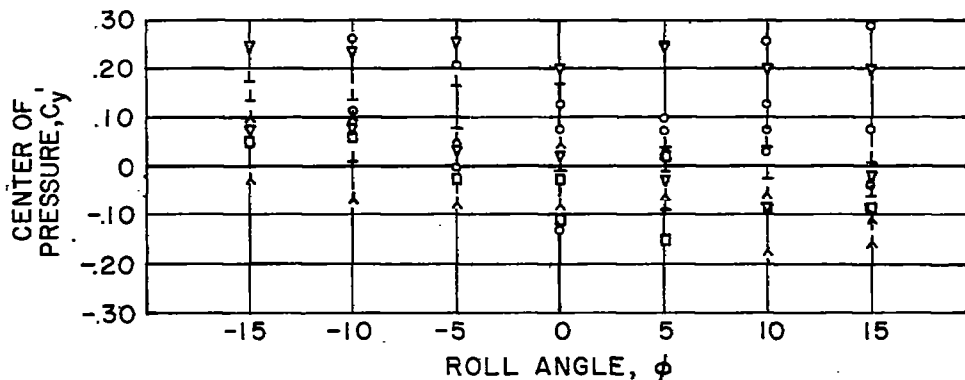


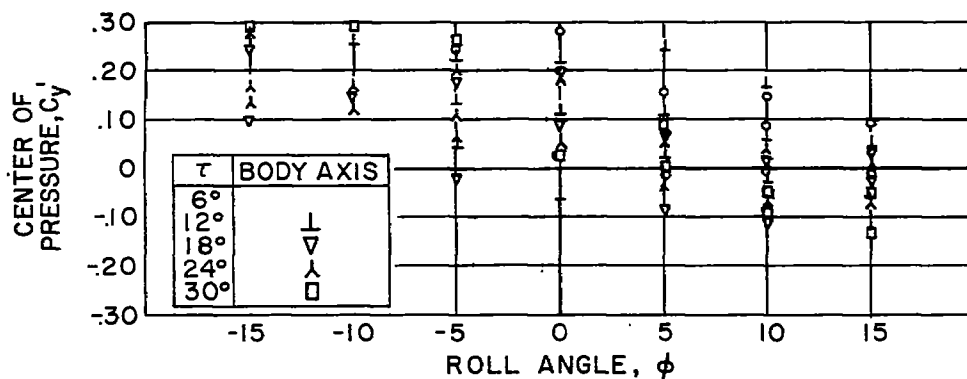
Figure 13.- Variation of longitudinal center of pressure with mean wetted-length-beam ratio for all combinations of roll and yaw angle. $\beta = 0^\circ$.



(a) $\psi = 0^\circ$.

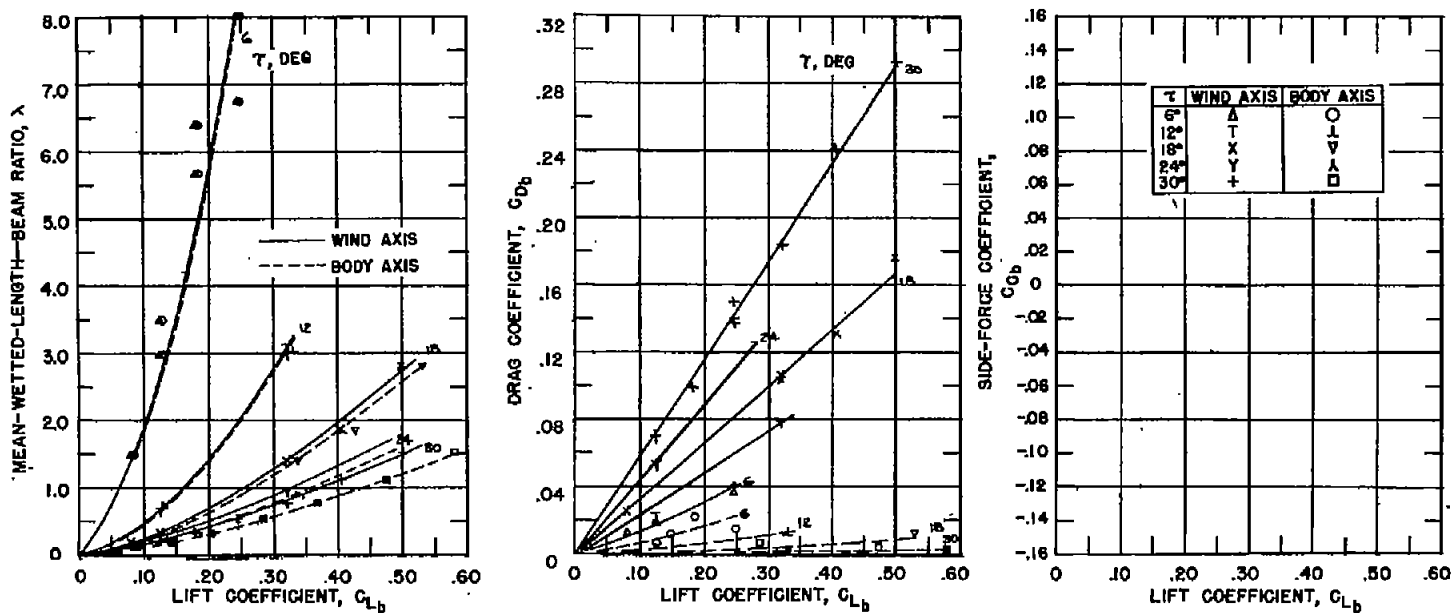


(b) $\psi = 10^\circ$.



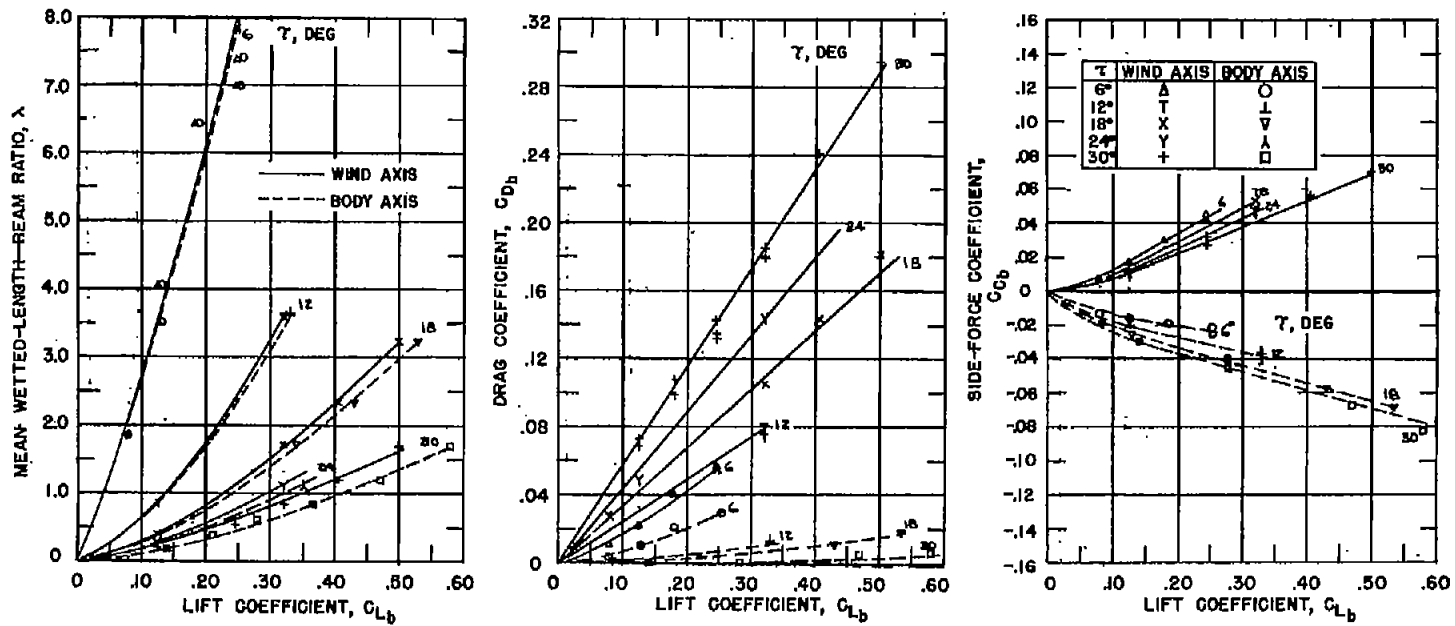
(c) $\psi = 20^\circ$.

Figure 14.- Variation of lateral center of pressure with roll angle.
 $\beta = 0^\circ$.



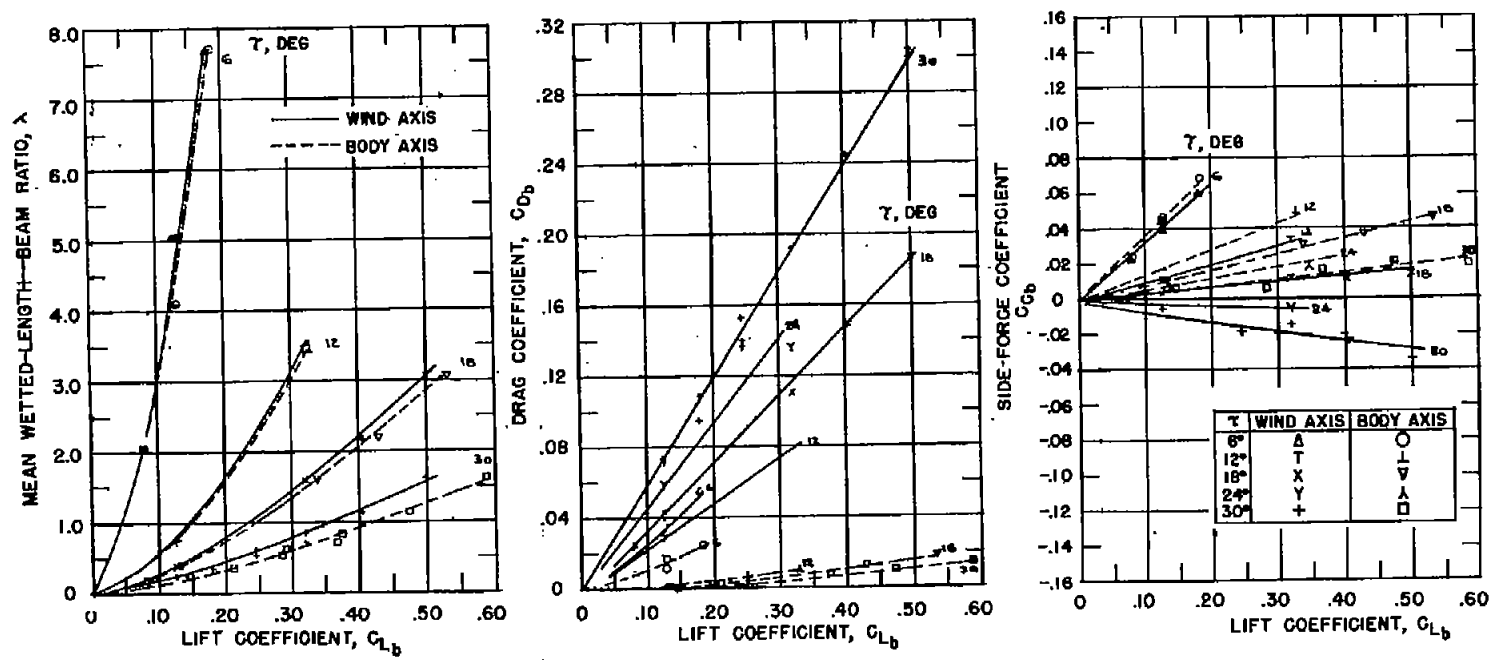
(a) $\phi = 0^\circ$.

Figure 15.- Lift, drag, and side-force coefficients for $\beta = 20^\circ$. $\psi = 0^\circ$.



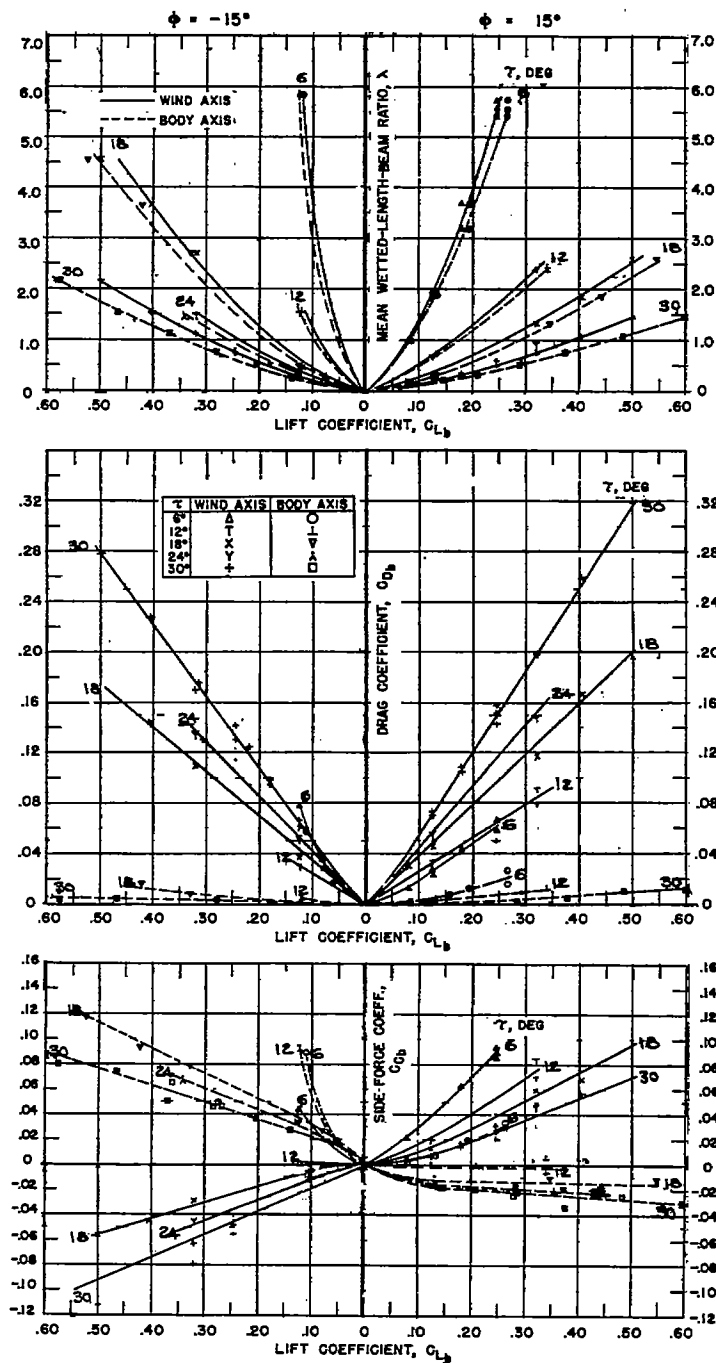
(b) $\phi = 15^\circ$.

Figure 15.- Concluded.



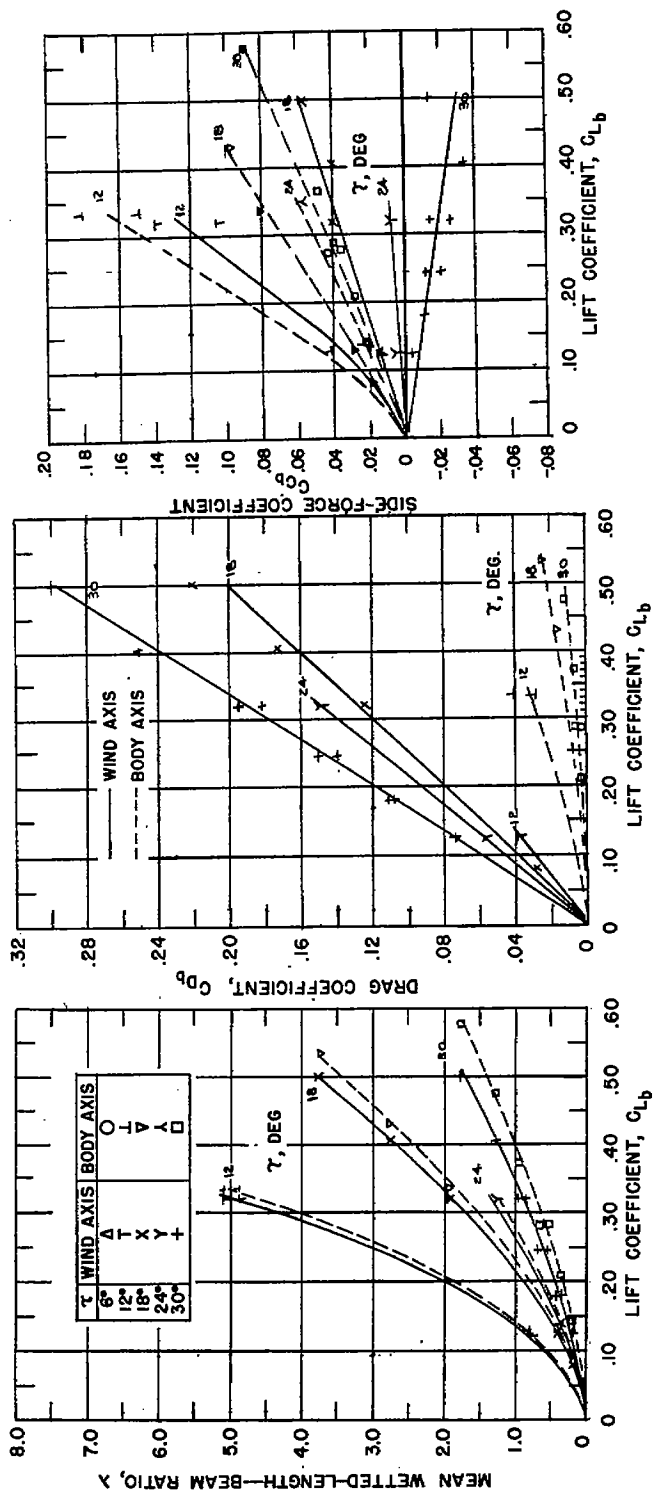
(a) $\phi = 0^\circ$.

Figure 16.- Lift, drag, and side-force coefficients for $\beta = 20^\circ$. $\psi = 10^\circ$.



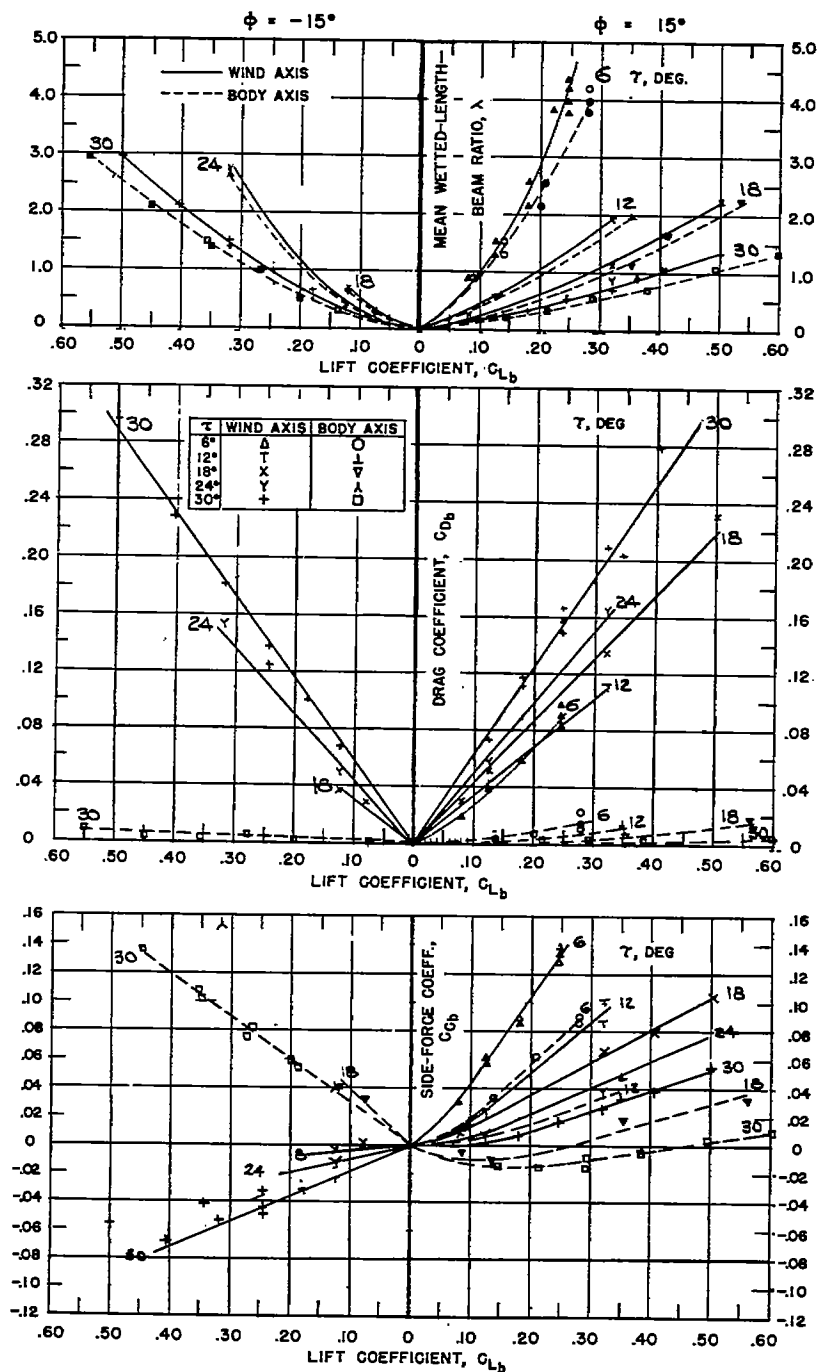
(b) $\phi = -15^\circ$ and 15° .

Figure 16.- Concluded.



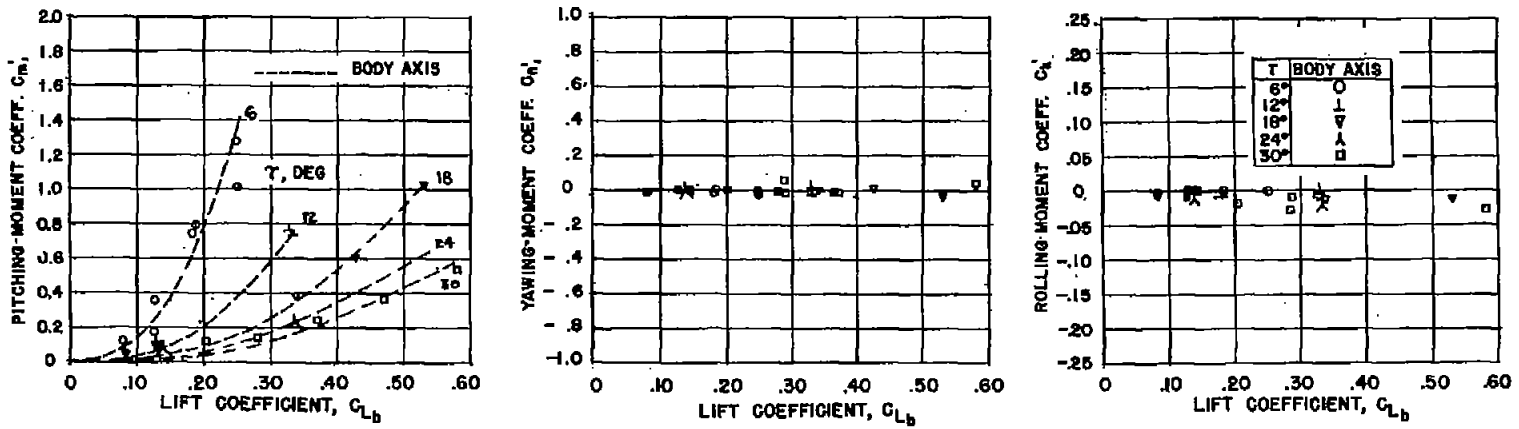
(a) $\phi = 0^\circ$.

Figure 17.- Lift, drag, and side-force coefficients for $\beta = 20^\circ$. $\psi = 20^\circ$.



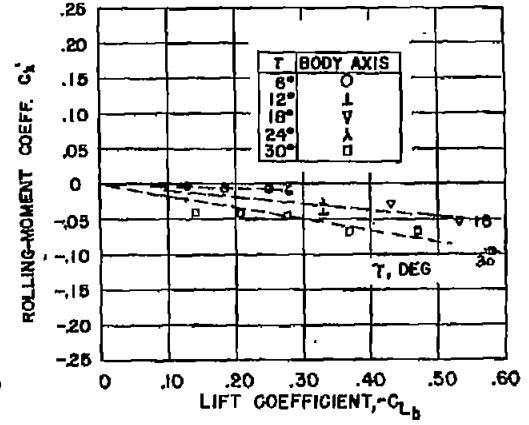
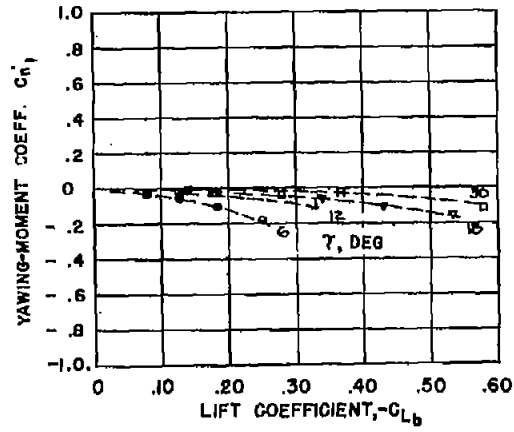
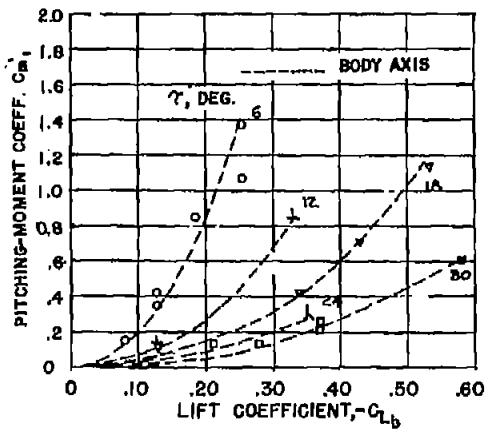
(b) $\phi = -15^\circ$ and 15° .

Figure 17.- Concluded.



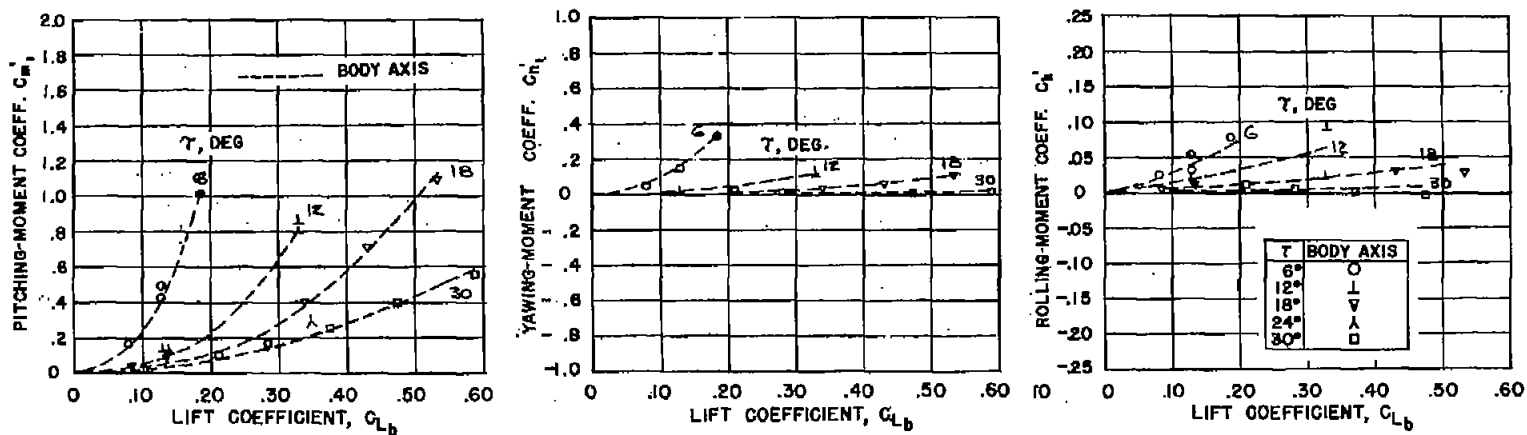
(a) $\phi = 0^\circ$.

Figure 18.- Pitching-, yawing-, and rolling-moment coefficients for $\beta = 20^\circ$. $\psi = 0^\circ$.



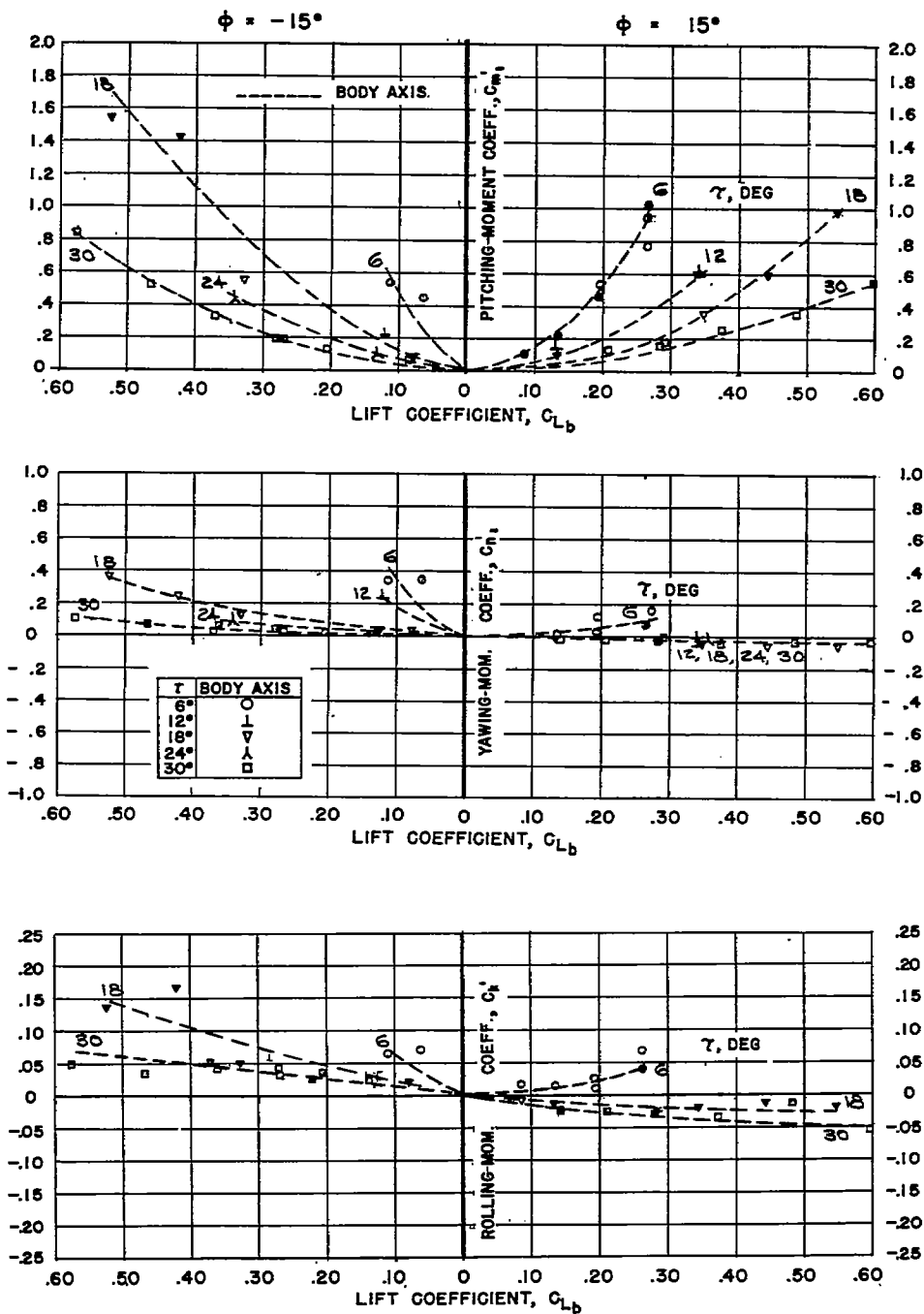
(b) $\phi = 15^\circ$.

Figure 18.- Concluded.



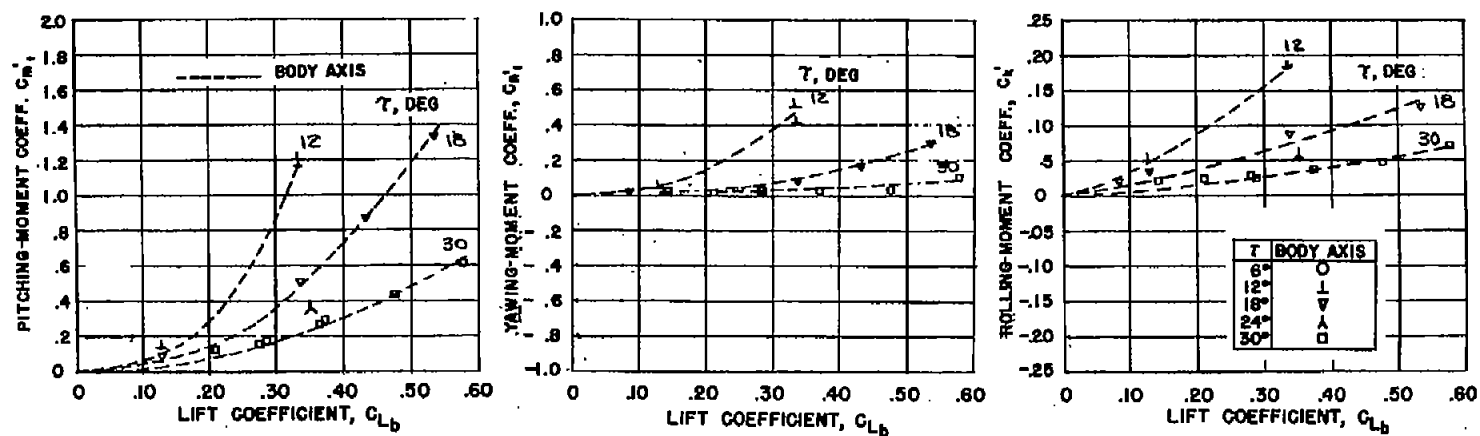
(a) $\phi = 0^\circ$.

Figure 19.- Pitching-, yawing-, and rolling-moment coefficients for $\beta = 20^\circ$. $\psi = 10^\circ$.



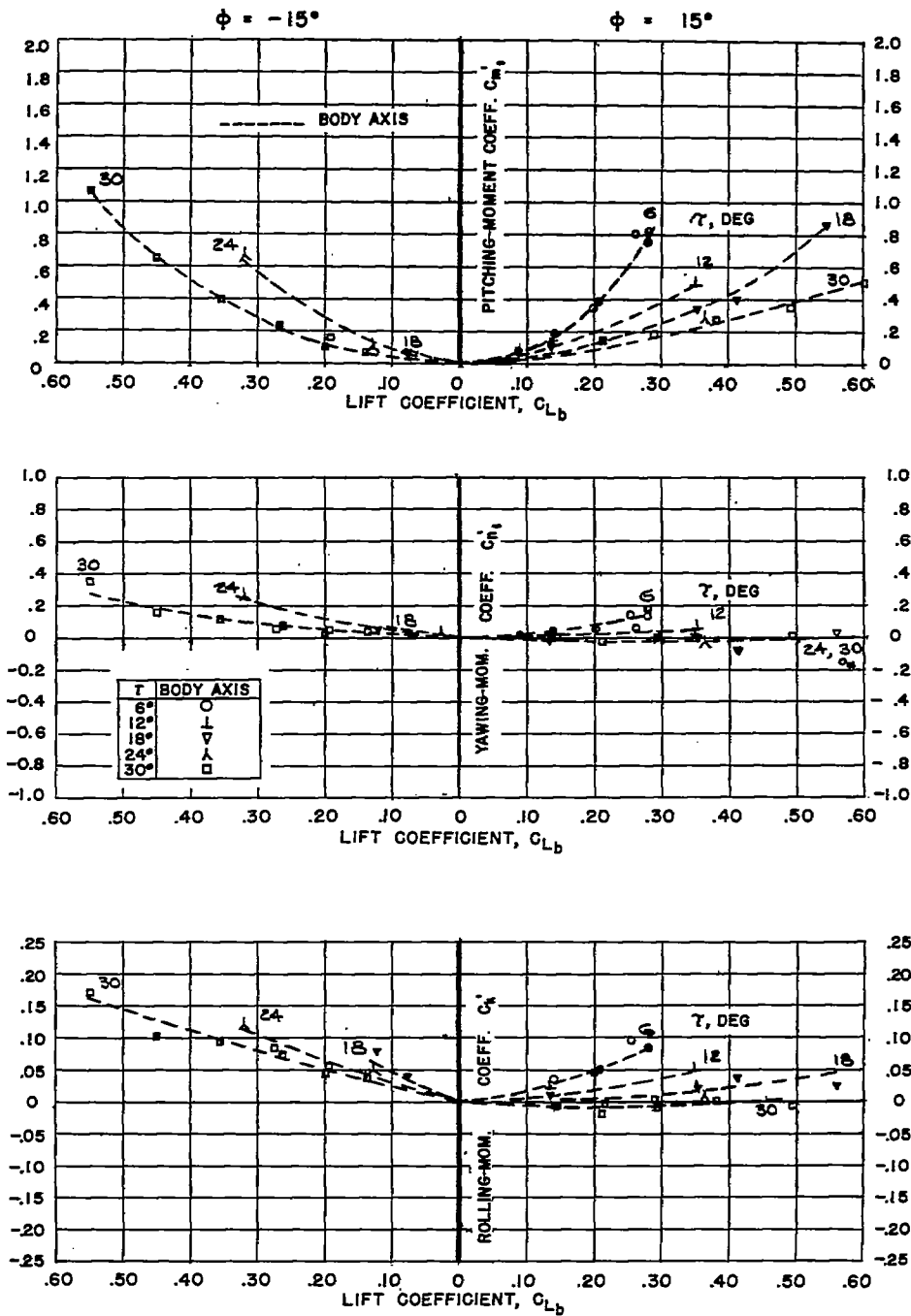
(b) $\phi = -15^\circ$ and 15° .

Figure 19.- Concluded.



(a) $\phi = 0^\circ$.

Figure 20.- Pitching-, yawing-, and rolling-moment coefficients for $\beta = 20^\circ$. $\psi = 20^\circ$.



(b) $\phi = -15^\circ$ and 15° .

Figure 20.- Concluded.

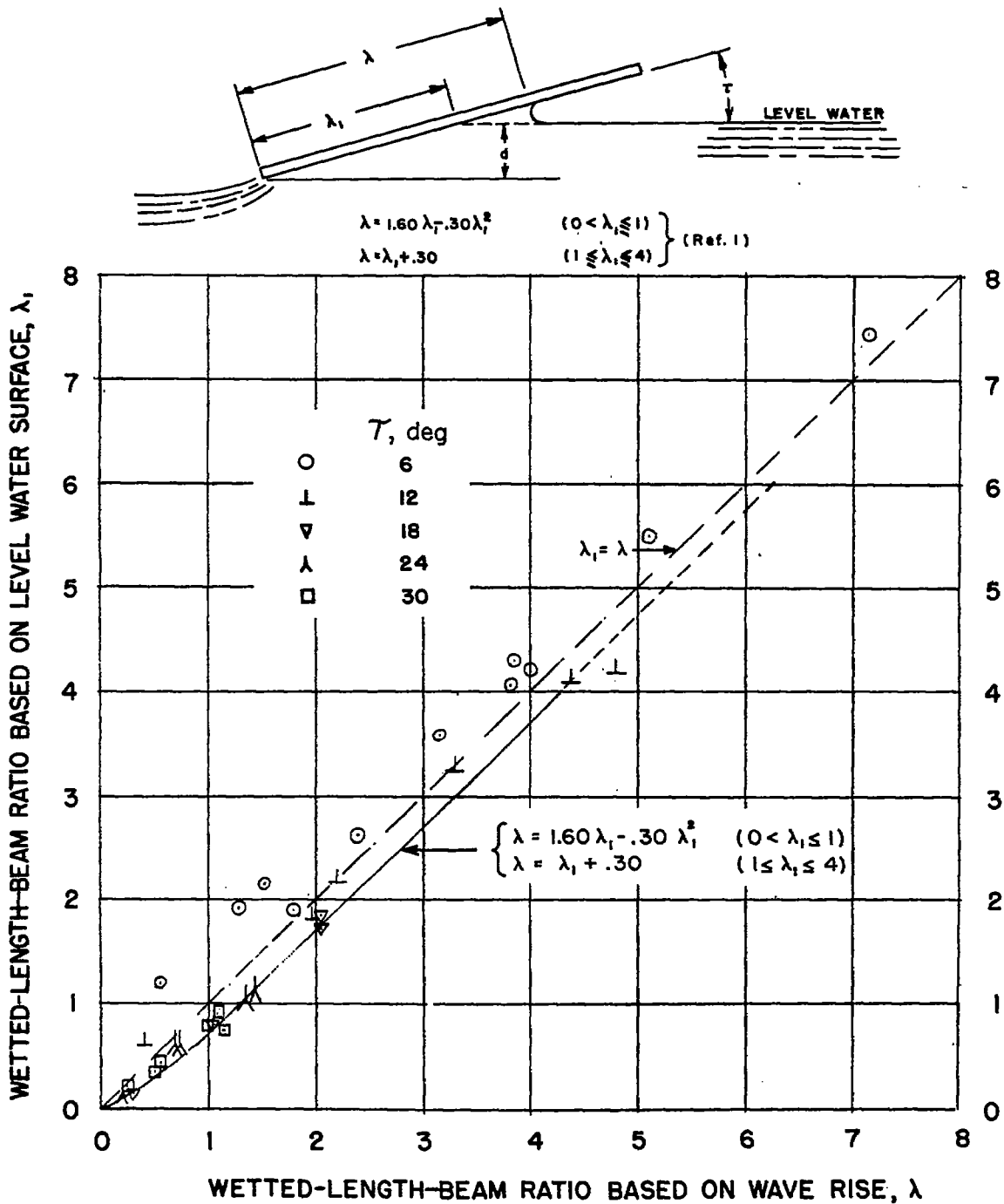


Figure 21.- Wave-rise variation for $\beta = 0^\circ$, $\phi = 0^\circ$, and all test yaw angles.

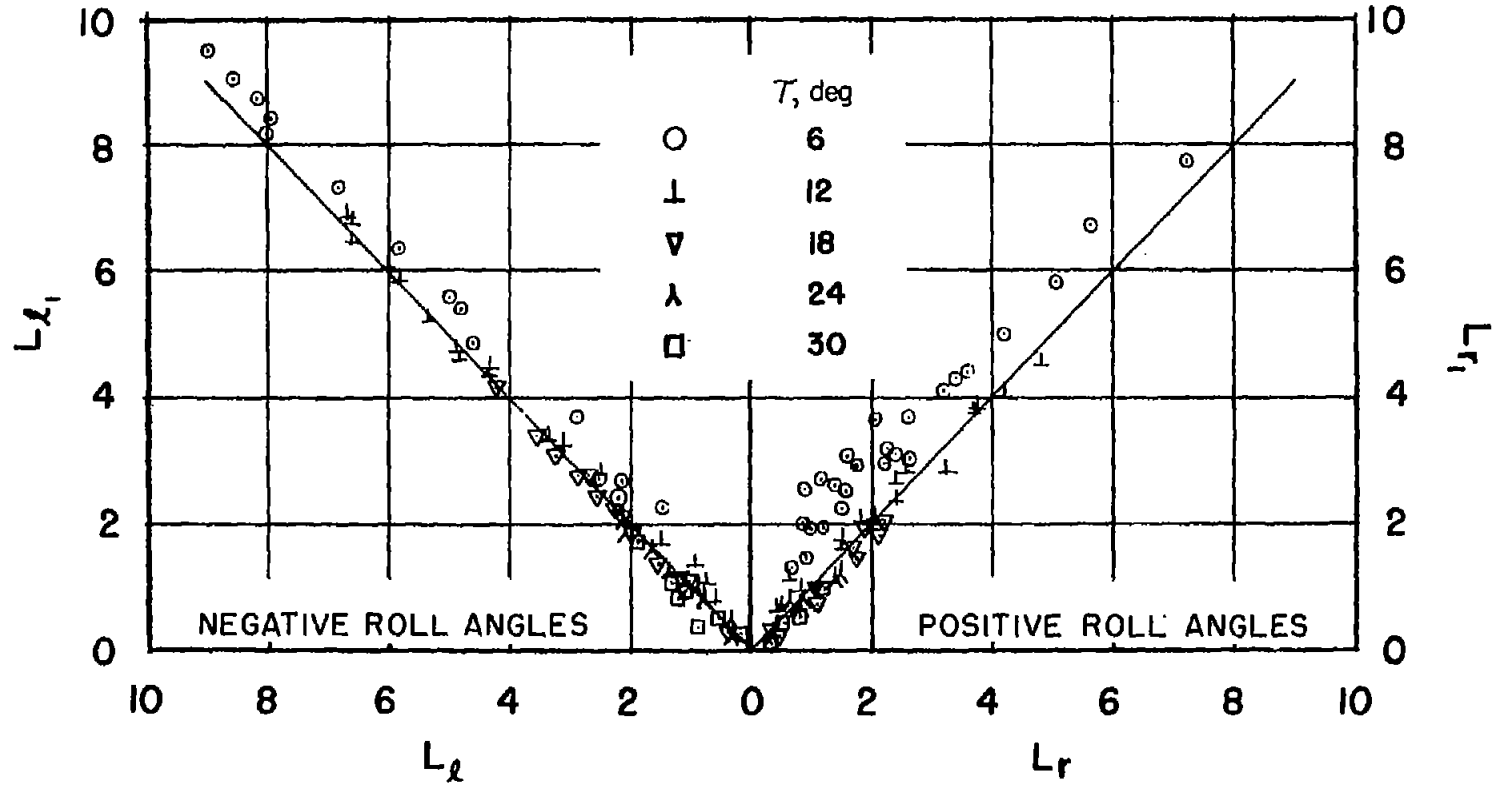


Figure 22.- Comparison of computed and observed wetted-length-beam ratio for rolled-down chine edge (for all combinations of trim, roll, and yaw angle). $\beta = 0^\circ$.

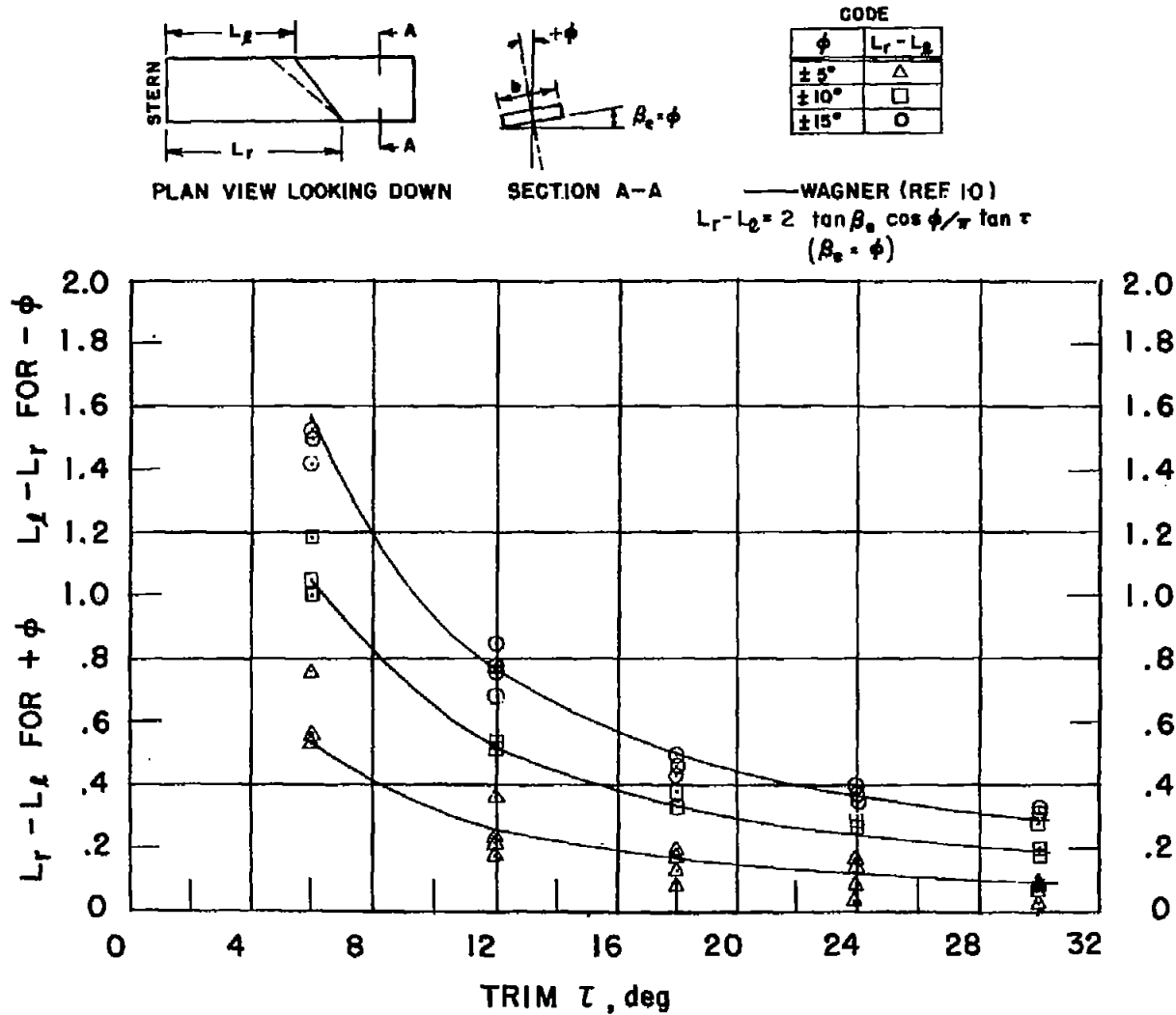


Figure 23.- Variation of $L_r - L_2$ for ϕ and $L_2 - L_r$ for $-\phi$ with trim and roll angles for all test yaw angles of 0° dead-rise surface.

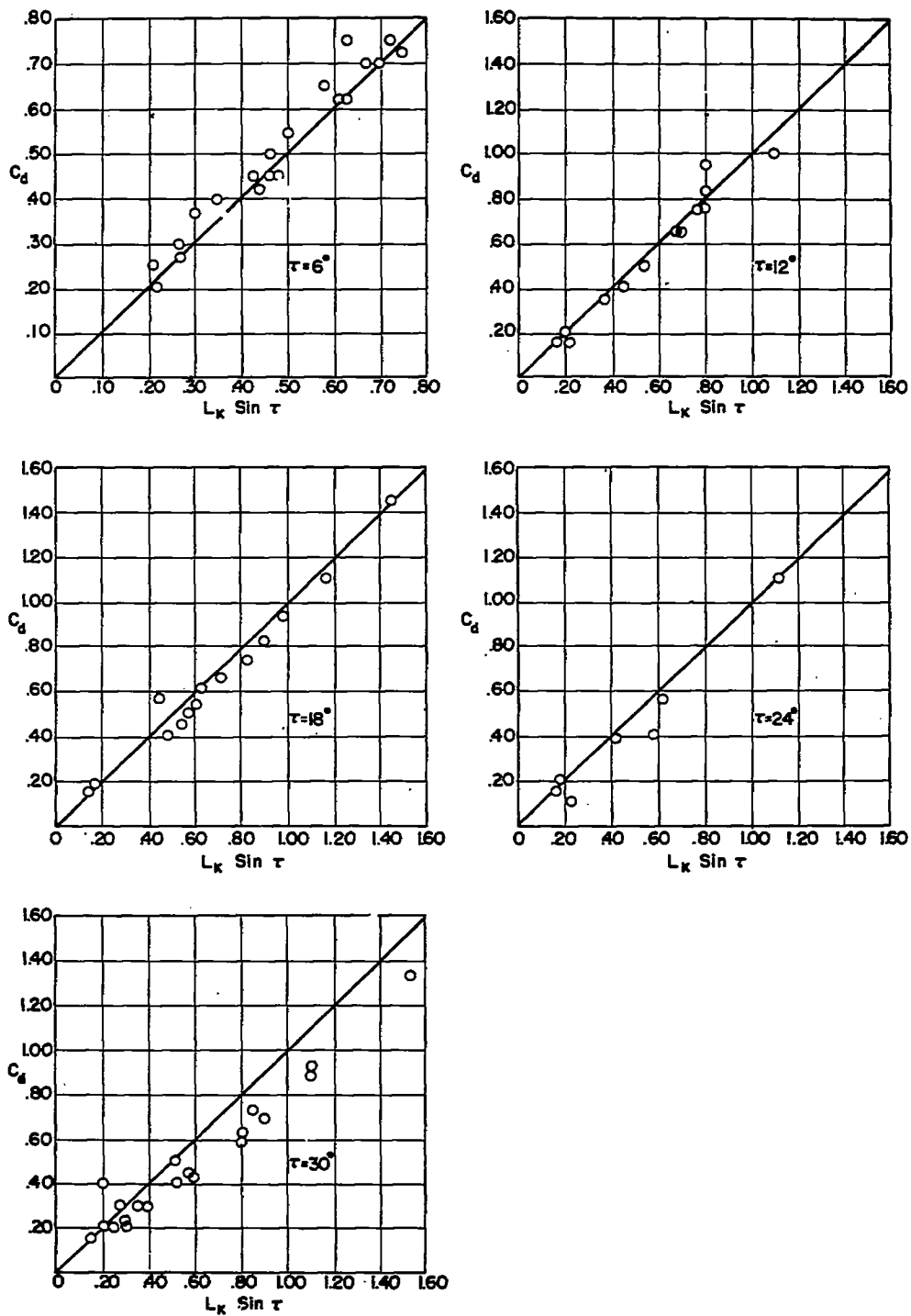
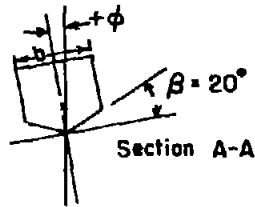
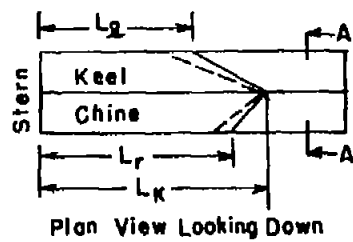


Figure 24.- Comparison of experimental draft with computed draft for 20° dead-rise model at all test values of roll and yaw.



Code

$L_K - L_r$	ϕ	$L_K - L_2$
○	0°	●
△	±5°	▲
□	±10°	■
◇	±15°	◆

— Wagner (Ref 10)

$$L_K - L_C = \tan \beta_e / \pi \tan \tau$$

$$\beta_e = \beta \pm \phi$$

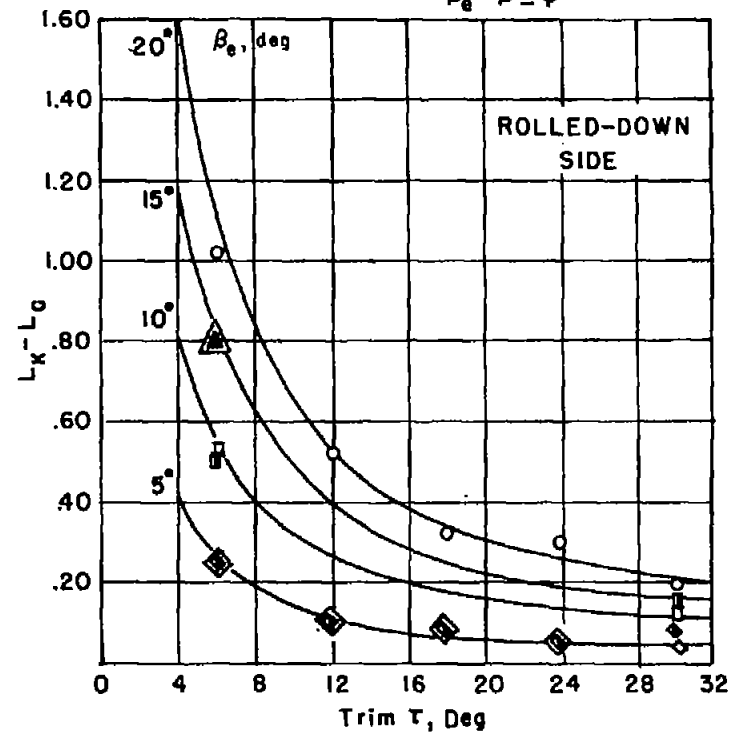
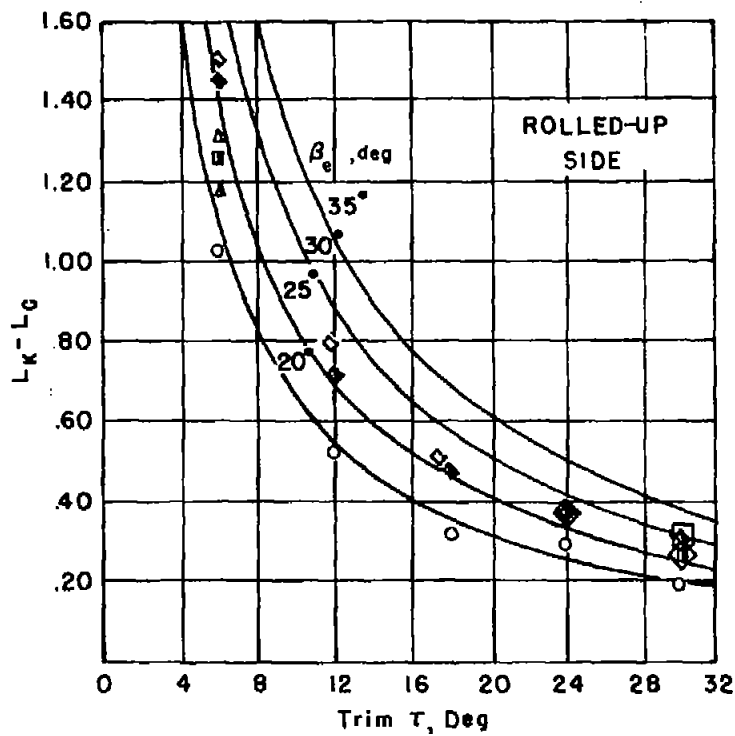
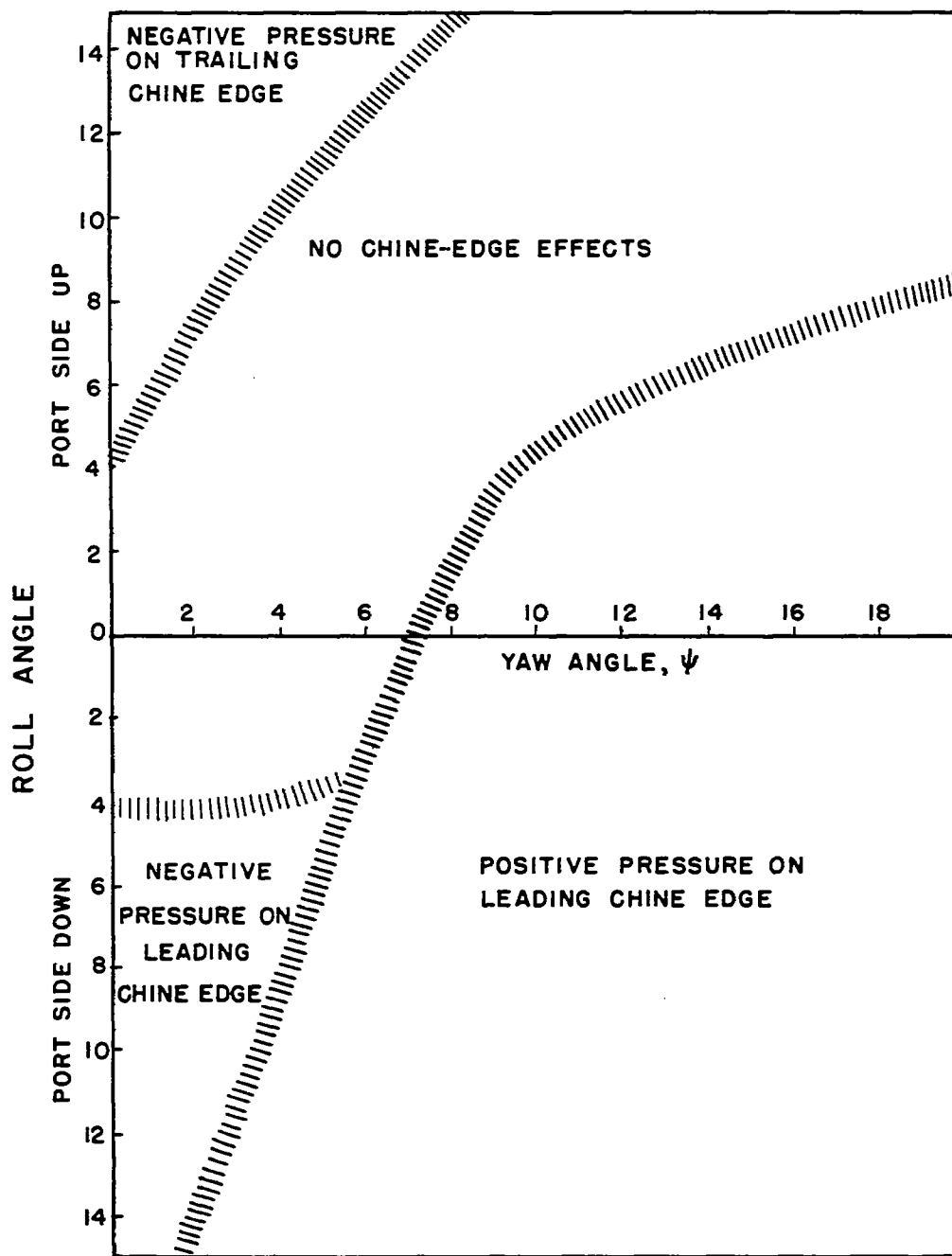
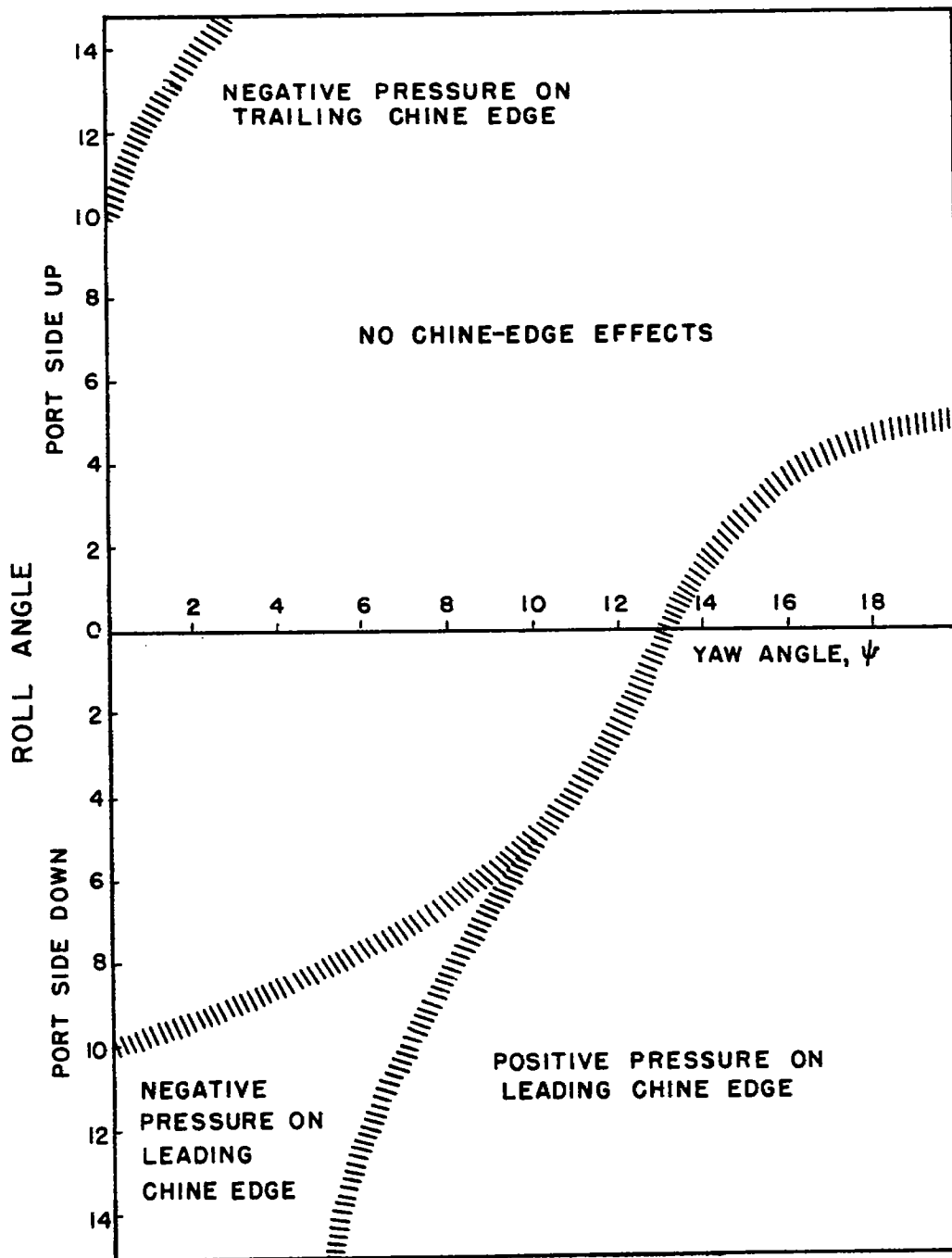


Figure 25.- Variation of $L_K - L_C$ with trim and roll angles for all test yaw angles of 20° dead-rise surface.



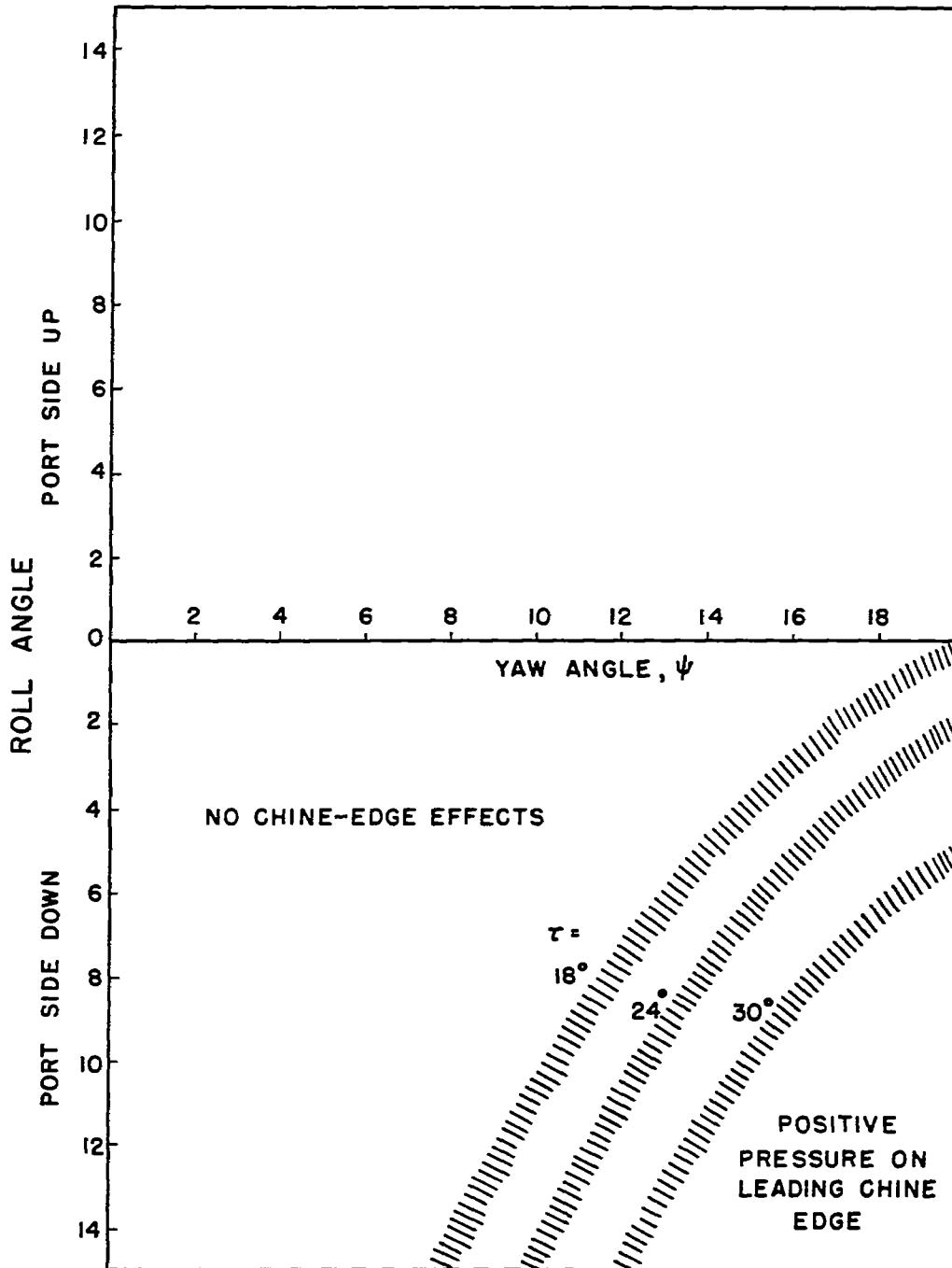
(a) $\tau = 6^\circ$.

Figure 26.- Boundaries for chine-edge wetting in unsymmetrical planing.
 $\beta = 0^\circ$.



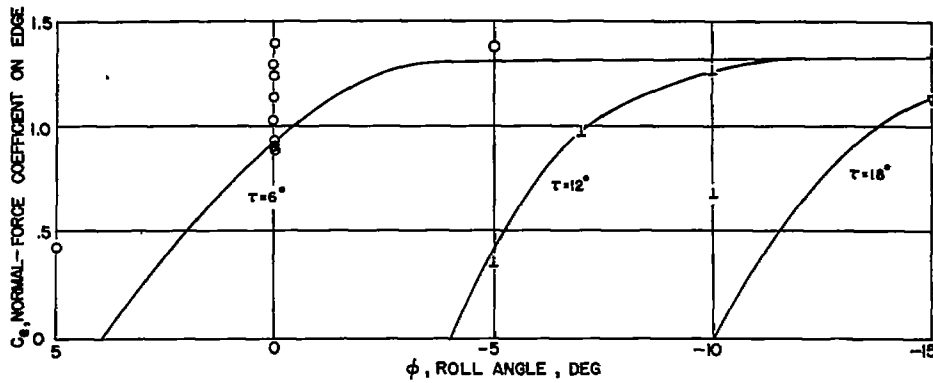
(b) $\tau = 12^\circ$.

Figure 26.- Continued.

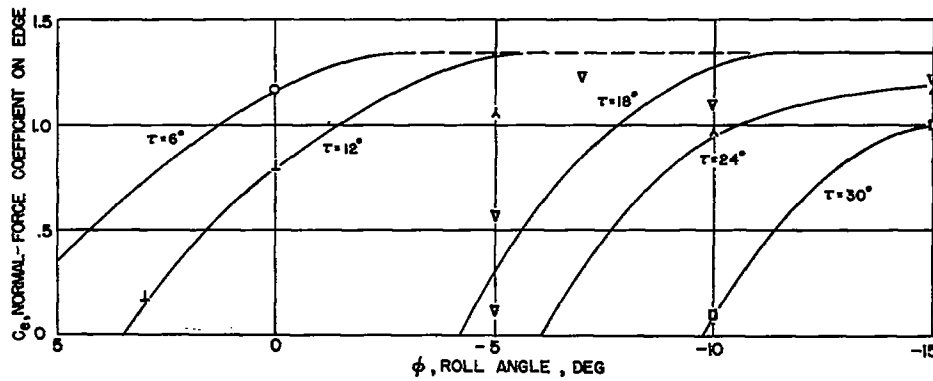


(c) $\tau = 18^\circ, 24^\circ, \text{ and } 30^\circ$.

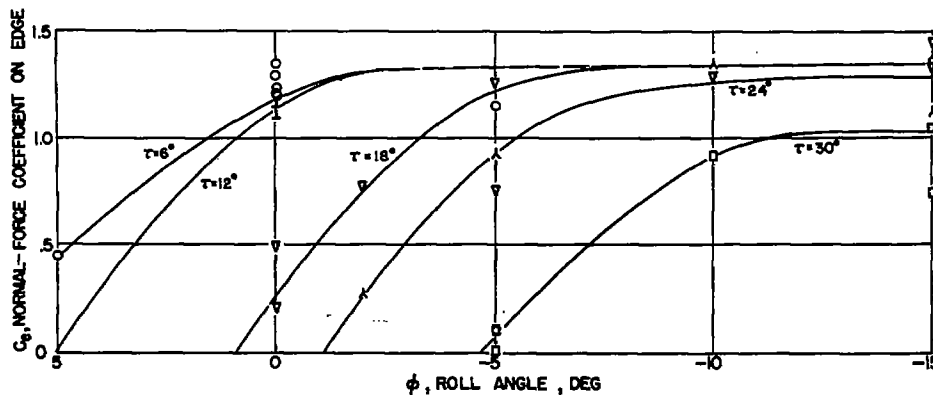
Figure 26.- Concluded.



(a) $\psi = 10^\circ$.

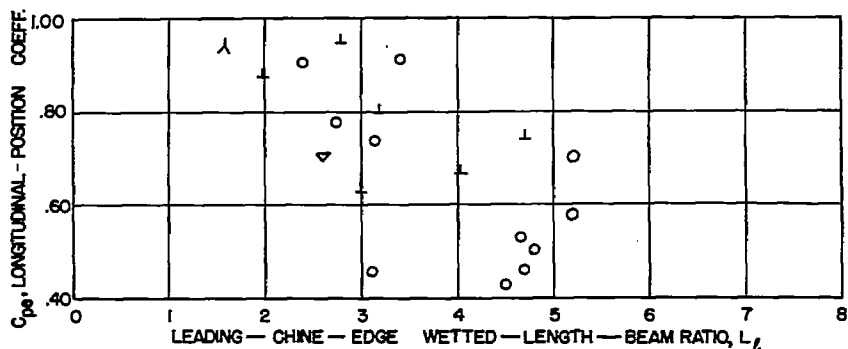


(b) $\psi = 15^\circ$.

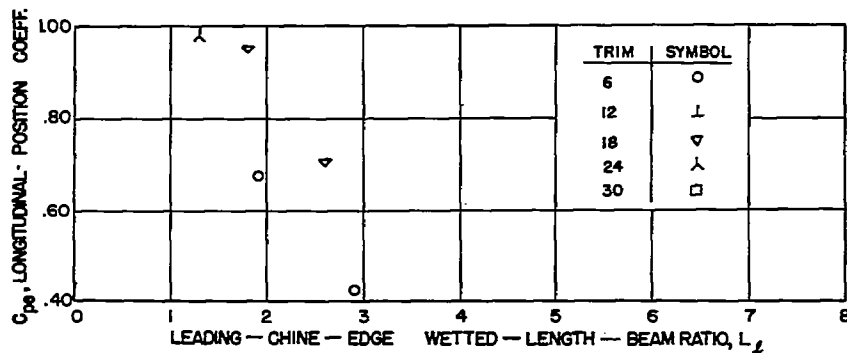


(c) $\psi = 20^\circ$.

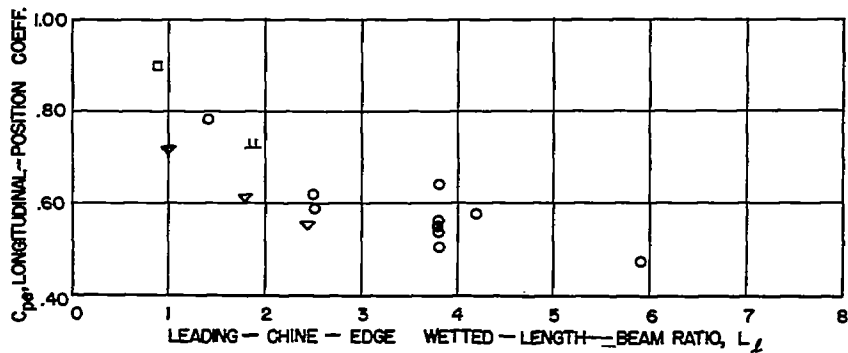
Figure 27.- Normal-force coefficients on leading chine edge of flat planing surface. Data are for edge thicknesses of 0.091b and 0.182b.



(a) $\psi = 10^\circ$.



(b) $\psi = 15^\circ$.



(c) $\psi = 20^\circ$.

Figure 28.- Longitudinal position of normal force coefficients on leading chine edge for flat planing surface. Data are for edge thicknesses of 0.091b and 0.182b.